

Aus dem
Comprehensive Pneumology Center
Institut für Experimentelle Pneumologie
Leitung: Dr. Ali Önder Yildirim
&
der Abteilung „Lung Repair and Regeneration“
Institut der Ludwig-Maximilians-Universität München
Leitung: Prof. Dr. Dr. M. Königshoff

Anti-fibrotic effects of Nintedanib and Pirfenidone on alveolar epithelial cell function in *ex-vivo* 3D-Lung Tissue Cultures

Dissertation
zum Erwerb des Doktorgrades der Medizin
an der Medizinischen Fakultät der
Ludwig-Maximilians-Universität zu München



vorgelegt von

Lara Buhl

aus Hildesheim

2021

Mit Genehmigung der medizinischen Fakultät
der Universität München

Berichterstatter:	Prof. Dr. Dr. Melanie Königshoff
Mitberichterstatter:	Prof. Dr. med. Claus Neurohr Prof. Dr. med. Jürgen Behr apl. Prof. Dr. Matthias Griese
Mitbetreuung durch den promovierten Mitarbeiter:	Dr. rer. nat. Mareike Lehmann
Dekan:	Prof. Dr. med. Thomas Gudermann
Tag der mündlichen Prüfung:	20.10.2021

TABLE OF CONTENTS

TABLE OF CONTENTS	V
ABBREVIATIONS	VIII
1. ZUSAMMENFASSUNG	1
2. SUMMARY	2
3. INTRODUCTION	3
3.1 Interstitial lung diseases	3
3.2 Epidemiology	3
3.3 Clinical presentation and diagnosis	3
3.4 Histopathological features	5
3.5 Pathophysiological features	5
3.5.1 Deregulated pathways	8
3.5.2 Aging	9
3.5.3 Genetics	10
3.5.4 Epigenetic reprogramming.....	12
3.6 Pharmacotherapy	13
3.6.1 Pirfenidone	13
3.6.1.1 Pharmacokinetics.....	14
3.6.1.2 Mode of action.....	15
3.6.2 Nintedanib.....	17
3.6.2.1 Pharmacokinetics.....	18
3.6.2.2 Mode of action.....	19
3.7 Aims of the study	21
4. MATERIALS AND METHODS	22
4.1 Materials	22
4.1.1 Laboratory Equipment	22
4.1.2 Software	23
4.1.3 Chemicals and reagents	23
4.1.4 Consumables	25
4.1.5 Buffers, solutions and media.....	26
4.1.6 Kits.....	27
4.1.7 Antibodies	27
4.1.8 Primers	29
4.2 Methods	30
4.2.1 Human tissue.....	30

4.2.2 Animal experiments	30
4.2.3 Primary murine alveolar type II cell isolation and culture	31
4.2.4 Murine <i>ex-vivo</i> 3D-Lung tissue culture.....	32
4.2.5 Human <i>ex-vivo</i> 3D-Lung tissue cultures	32
4.2.6 Fibrotic cocktail	33
4.2.7 RNA isolation.....	33
4.2.8 cDNA Synthesis.....	34
4.2.9 Quantitative PCR	34
4.2.10 Immunofluorescence	35
4.2.11 Immunoblotting	36
4.2.12 Enzyme-linked immunosorbent assay (ELISA).....	36
4.2.13 WST-1 based cell toxicity assay	36
4.2.14 Fluorescence-activated cell sorting (FACS)	37
4.2.15 Statistical analysis	37
5. RESULTS.....	38
5.1 Murine <i>ex-vivo</i> 3D-Lung Tissue Cultures (3D-LTCs).....	38
5.1.1 Characterization of murine <i>ex-vivo</i> 3D-LTCs as fibrosis model	38
5.1.2 Nintedanib and Pirfenidone dose-dependently inhibit fibrotic marker expression in murine <i>ex-vivo</i> 3D-LTCs	40
5.1.3 Double treatment with Nintedanib and Pirfenidone shows an additive effect in downregulating fibrotic marker expression in fibrotic murine <i>ex-vivo</i> 3D-LTCs.....	42
5.1.4 Nintedanib and Pirfenidone differentially affect epithelial cell function in murine <i>ex-vivo</i> 3D-LTCs	43
5.2 Primary murine alveolar type II (pmAT II) cell monoculture	46
5.2.1 Nintedanib and Pirfenidone inhibit fibrotic marker expression in pmAT II cells.....	46
5.2.2 Nintedanib and Pirfenidone differentially affect epithelial cell marker expression in pmAT II cells	48
5.3 Human <i>ex-vivo</i> 3D-LTCs	52
5.3.1 Nintedanib and Pirfenidone don't significantly inhibit fibrotic marker expression in human <i>ex-vivo</i> 3D-LTCs	52
5.3.2 Nintedanib and Pirfenidone differentially influence epithelial cell function in human <i>ex-vivo</i> 3D-LTCs upon TGF- β treatment	55
5.3.3 Nintedanib and Pirfenidone affecting epithelial cell function in human <i>ex-vivo</i> 3D-LTCs subjected to the Fibrotic Cocktail.....	57
6. DISCUSSION	59
6.1 The applicability of <i>ex-vivo</i> 3D-LTCs for pre-clinical drug testing	60
6.2 Investigating the effect of Nintedanib and Pirfenidone on pro-fibrotic marker expression in murine and human <i>ex-vivo</i> 3D-LTCs	63
6.2.1 Nintedanib and Pirfenidone inhibit fibrotic marker expression in murine <i>ex-vivo</i> 3D-LTCs	63
6.2.2 Double treatment with Nintedanib and Pirfenidone show a synergistic effect in downregulating pro-fibrotic marker expression in murine <i>ex-vivo</i> 3D-LTCs.....	64
6.2.3 The anti-fibrotic action of Nintedanib and Pirfenidone in human <i>ex-vivo</i> 3D-LTCs	65

6.3 Differential effects of Nintedanib and Pirfenidone on epithelial cell phenotype and function in pmAT II cell culture and ex-vivo 3D-LTCs	66
6.3.1 Nintedanib and Pirfenidone inhibit TGF- β induced EMT in alveolar epithelial cells	67
6.3.2 Nintedanib and Pirfenidone differentially affect alveolar epithelial cell phenotype	68
6.3.3 Nintedanib and Pirfenidone interfere with an aberrant epithelial-mesenchymal-crosstalk by decreasing Wisp1 secretion	69
6.4 Conclusions	70
6.5 Future perspective.....	71
7. SUPPLEMENT	73
8. REFERENCES	79
8.1. Bibliography	79
8.2 List of Figures	91
8.3 List of Tables.....	94
9. ACKNOWLEDGEMENTS	95
10. APPENDIX	96
10.1 Abstracts and publications.....	96
10.1.1 Abstracts	96
10.1.2 Publications.....	96
10.2 Eidesstattliche Erklärung	97

ABBREVIATIONS

α SMA/Acta2	Alpha smooth muscle actin
AT I	Alveolar epithelial cell type I
AT II	Alveolar epithelial cell type II
Bach1	BTB and CNC homology 1
BALF	Bronchoalveolar lavage fluids
BLEO	Bleomycin
BSA	Bovine serum albumin
°C	Degree Celsius
Δ Ct	Delta cycle of threshold
cDNA	Complementary DNA
COL1A1	Collagen I
COPD	Chronic obstructive pulmonary disease
CTGF	Connective tissue growth factor
3D-LTCs	3D-Lung tissue cultures
Da	Dalton
DAPI	4',6-diamidino-2-phenylindole
DLCO	Diffusing capacity for carbon monoxide
DNA	Deoxyribonucleic acid
dNTP	Deoxyribonucleoside triphosphate
DPLD	Diffuse parenchymal lung disease
DPP9	Dipeptidyl Peptidase 9
DSP	Desmoplakin
ECAD	E-Cadherin

ECM	Extracellular matrix
EMT	Epithelial-mesenchymal-transition
ERK	Extracellular-signal Regulated Kinases
FACS	Fluorescence-activated cell sorting
FC	Fibrotic cocktail
FCS	Fetal calf serum
FGF	Fibroblast growth factor
FN1	Fibronectin
FVC	Forced vital capacity
fw	Forward
g	gram
GLI1	Glioma-associated oncogene
h	hour
HDAC	Histone deacetylase
HOPX	Homeodomain only protein X
HPRT	Hypoxanthine-guanine-phosphoribosyltransferase
HRCT	High-resolution computed tomography
HSP	Heat shock protein
IL	Interleukin
ILD	Interstitial lung diseases
IPF	Idiopathic pulmonary fibrosis
K	Kilo
L	Liter
LPA	Lysophosphatidic acid
miRNA	microRNA

mm	millimeters
MMP	Matrix-metalloprotease
MUC5B	Mucin 5B
mRNA	Messenger RNA
Nkx2.1	NK2 homeobox 1
Nrf-2	Nuclear factor erythroid 2–related factor 2
PARN	Poly(A)-specific ribonuclease
PDGF	Platelet derived growth factor
PmAT II	Primary murine alveolar epithelial cell type II
PTCH1	Protein-Patched-Homolog 1
qPCR	Quantitative polymerase chain reaction
RNA	Ribonucleic acid
ROS	Reactive oxidant species
RTEL	Regulator of telomere length
rv	reverse
SASP	Senescence-associated secretory phenotype
SDS	Sodium dodecyl sulfate
SEM	Standard error of the mean
SHH	Sonic Hedgehog
SMAD	Sma/Mothers against decapentaplegic
SPA/SFTPA	Surfactant protein A
(pro-)SPC/SFTPC	(pro-) Surfactant protein C
T1 α	Podoplanin
TBS(T)	Tris buffered saline (with Tween 20)
TERC	Telomerase RNA component

TERT	Telomerase reverse transcriptase
TCR	T-cell receptor
TGF- β	Transforming growth factor beta
TIMP	Tissue inhibitor of metalloproteinases
TNF α	Tumor necrosis factor alpha
TOLLIP	Toll-interacting protein
TRIS	Tris(hydroxymethyl)-aminomethane
UIP	Usual interstitial pneumonia
VEGF	Vascular endothelial growth factor
WISP 1	Wnt-induced signaling protein 1
WST-1	Water soluble tetrazolium salt-1
WNT	Wingless/Integrase-1
ZO1	Zonula occludens 1

1. ZUSAMMENFASSUNG

Die Idiopathische Pulmonale Fibrose (IPF) ist eine progredient verlaufende Lungenparenchymerkrankung unbekannter Ursache. Sie geht mit einer deutlich reduzierten Lebenserwartung einher. Die bisher einzigen pharmakologischen Therapieoptionen sind Nintedanib und Pirfenidon, welche den Krankheitsverlauf verlangsamen, jedoch nicht aufhalten. Die Voraussetzung für die Entwicklung neuer therapeutischer Optionen ist ein tieferes Verständnis des antifibrotischen Wirkprinzips beider Medikamente. Insbesondere deren Effekt auf Alveolarepithel Typ (AT) II Zellen, welche eine Schlüsselrolle in der Pathogenese von IPF einnehmen, wurde bisher kaum untersucht. Das Ziel der hier vorgestellten Studie war es daher, den Effekt von Nintedanib und Pirfenidon auf AT II Zellen in *ex-vivo* Lungenschnitten sowie in der primären murinen AT II Zellkultur zu untersuchen. Als Lungenfibrose-Modelle wurden im Wesentlichen das Bleomycin-Mausmodell sowie der Fibrotische Cocktail (FC), bestehend aus verschiedenen Wachstumsfaktoren, in humanen *ex-vivo* Lungenschnitten verwendet.

Zunächst konnten wir zeigen, dass fibrotische murine sowie humane Lungenschnitte *ex-vivo* entscheidende Charakteristika der pulmonalen Fibrose über den Kulturzeitraum aufwiesen. Wir konnten weiterhin zeigen, dass Nintedanib und Pirfenidon die Gen- und Proteinexpression fibrotischer Marker in murinen *ex-vivo* Lungenschnitten sowie in primärer muriner AT II Zellkultur inhibierten. Nintedanib, nicht jedoch Pirfenidon, stimulierte die Expression von AT II Zellmarkern, insbesondere die des Oberflächenmarkers Surfactant-Protein C (SP-C), sowohl in AT II Zellkultur als auch in murinen und humanen *ex-vivo* Lungenschnitten. Es zeigte sich, dass Nkx2.1 und Hopx, beide essenzielle Transkriptionsfaktoren der AT II-Transdifferenzierung, durch Nintedanib hochreguliert wurden. Interessanterweise konnte der Effekt von Nintedanib auf AT II Zellmarkerexpression, nicht aber auf fibrotische Markerexpression in humanen *ex-vivo* Lungenschnitten, rekapituliert werden.

Zusammenfassend zeigt unsere Studie die Anwendbarkeit von *ex-vivo* Lungenschnitten zur präklinischen Testung antifibrotischer Wirkstoffe am Beispiel von Nintedanib und Pirfenidon. Des Weiteren beobachteten wir unterschiedliche Effekte von Nintedanib und Pirfenidon auf AT II Zellen, die potentiell zur antifibrotischen Wirkung von diesen beitragen.

2. SUMMARY

Idiopathic pulmonary fibrosis (IPF) is a devastating interstitial lung disease of unknown cause with restricted therapeutic options. To date, the only approved drugs known to slow disease progression are Nintedanib and Pirfenidone. However, the life expectancy is still limited with or without treatment. Therefore, novel therapeutic options are needed. In this context, a more in-depth understanding of the mechanism of action of Nintedanib and Pirfenidone might help to identify novel therapeutic targets. Furthermore, the potential effect of these drugs on alveolar epithelial cells with being the key driver of the disease can be of particular interest. Therefore, in this study we aim to delineate the potential anti-fibrotic effects of both Nintedanib and Pirfenidone on alveolar epithelial Type II (AT II) cells using primary murine AT II cell culture as well as *ex-vivo* 3D-Lung Tissue Cultures (3D-LTCs). The Bleomycin-induced lung fibrosis model in mice and the Fibrotic Cocktail (FC), consisting of multiple pro-fibrotic growth factors, in human 3D-LTCs were mainly utilized for this study.

Firstly, we demonstrated profibrotic hallmarks to be recapitulated in both murine and human fibrotic *ex-vivo* 3D-LTCs during culture duration. Nintedanib and Pirfenidone subsequently inhibited fibrotic marker gene and protein expression in murine *ex-vivo* 3D-LTCs and primary murine AT II cell culture. We showed Nintedanib, but not Pirfenidone, to induce AT II cell marker expression, in particular Surfactant Protein-C (SP-C), in both primary murine AT II cell culture and *ex-vivo* 3D-LTCs. Our data further indicated that this effect is partly mediated by *Nkx2.1* and *Hopx*, two transcription factors being crucial for AT II transdifferentiation, both being upregulated upon Nintedanib treatment. Interestingly, we were able to recapitulate the effect of Nintedanib on AT II cell marker, but not on fibrotic marker expression in human *ex-vivo* 3D-LTCs.

In summary, we show murine and human *ex-vivo* 3D-LTCs to be a feasible tool for preclinical drug testing. We further showed differential effects of Nintedanib and Pirfenidone on epithelial cell marker expression possibly contributing to their anti-fibrotic action.

3. INTRODUCTION

3.1 Interstitial lung diseases

Interstitial lung diseases (ILD), also referred to as diffuse parenchymal lung diseases (DPLDs), comprise a heterogeneous group of parenchymal lung diseases of known causes, such as drug toxicity, occupational exposures or connective tissue diseases, and unknown causes. The latter are called idiopathic interstitial pneumonias (IIP) and are subdivided into idiopathic pulmonary fibrosis (IPF) and “other IIPs”. The distinction is made upon the presence/absence of a usual interstitial pneumonia (UIP) pattern. Thus, IPF, is defined as chronic progressive interstitial lung disease of unknown cause, restricted to the lung and associated with the presence of a radiologic or histopathologic UIP pattern (Raghu et al. 2011, 2002)

3.2 Epidemiology

Affected patients are typically elderly men (median age of patients is 65 years) with a smoking history (King, Pardo and Selman 2011, Collard 2010a, Raghu et al. 2011). Known risk factors for developing IPF are cigarette smoking, virus infections, gastroesophageal reflux and environmental exposures such as wood and stone dust. The estimated prevalence of IPF ranges between 10-60 per 100 000 people and incidence 2-3 per 100 000 people which significantly increases with age. In total 3 million patients are affected globally by the disease. The life expectancy of 3-5 years at time of the diagnosis if not treated is comparable to the one of cancer patients or worse (Martinez et al. 2017).

3.3 Clinical presentation and diagnosis

IPF diagnosis must be considered in all elderly exhibiting unexplained progressive dyspnea and dry cough. Finger clubbing and bilateral inspiratory crackles in the basal areas can be found in the physical examination. In end stages of the disease peripheral edema and right heart failure might be evident. To establish the diagnosis of IPF the following criteria must be met: This include

1) the exclusion of other ILDs causes by a detailed medical history and examination, 2) identification of usual interstitial pneumonia (UIP) pattern, including honeycombing, reticular opacities and traction bronchiectasis, using high resolution computed tomography (HRCT) or 3) combination of surgical biopsy and HRCT pattern, if the HRCT features alone are inconclusive (Raghu et al. 2011). Due to the risk of major complications and mortality surgical biopsy must only be performed if histopathological findings possibly alter outcome prediction and/or treatment decisions (Martinez et al. 2017). The definite diagnosis is made in a multidisciplinary approach including clinicians and radiologists based on the 2011 American Thoracic Society, European Respiratory Society, Japanese Respiratory and Latin American Thoracic Association consensus statement (Raghu et al. 2011).

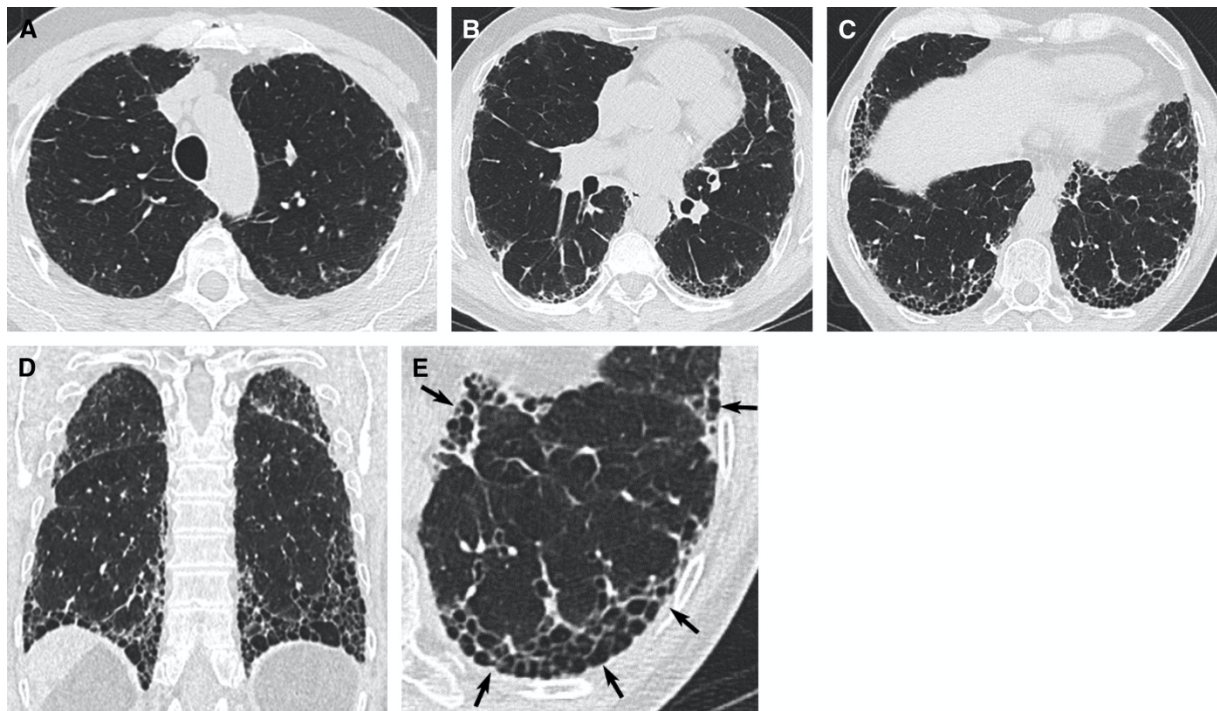


Figure 1: UIP pattern in HRCT. (A-D) Transverse and coronal high-resolution computed tomography (HRCT) depicting usual interstitial pneumonia (UIP) pattern, such as honeycombing and ground-glass opacification. The UIP pattern predominantly manifests in subpleural/basal areas. (E) Magnification of the honeycomb cysts. The characteristic cluster formed are pointed out by arrows. (Figure modified from Raghu et al. 2018)

3.4 Histopathological features

The histopathological hallmarks of IPF are referred to as usual interstitial pneumonia (UIP) pattern. This UIP pattern is characterized by a patchy distributed interstitial fibrosis with subsequent architectural distortion and honeycombing, a cystic airspace filled with mucus and lined with bronchiolar epithelium (Richeldi, Collard and Jones 2017). Fibroblast foci, defined as aggregates of activated (myo-)fibroblasts with adjacent hyperplastic alveolar epithelium, are located at the interface of fibrotic and normal lung parenchyma. They presumably represent areas of active fibrogenesis (Jones et al. 2016, Yanagi et al. 2015). Inflammation, that was historically thought be the cause of IPF, is only mild with lymphocytes and plasma cell infiltrations (Raghu et al. 2011). Notably, mortality was shown to correlate with the number of fibrotic foci in IPF patients, but not with inflammatory activity (King et al. 2001, Harada et al. 2013, Jones et al. 2016, Selman, King and Pardo 2001).

3.5 Pathophysiological features

Historically, IPF was thought to result from chronic inflammation with subsequent fibrosis formation and architectural distortion. However, both the absence of active inflammation in histopathology and the ineffectiveness of anti-inflammatory therapeutics led to re-consideration of the prevailing hypothesis (Selman and Pardo 2002, Selman et al. 2001). In the present paradigm, IPF is believed to result from an exaggerated repair process in response to impaired alveolar epithelium leading to a dysregulated epithelial-mesenchymal-crosstalk, subsequent fibroblast activation and proliferation and excessive extracellular matrix deposition (King et al. 2011, Richeldi et al. 2017). In more detail, alveolar type (AT) II cell impairment is caused by both genetic predisposition, aging processes and repetitive injury due to occupational exposure to toxins (Selman and Pardo 2012, Boucher 2011). As a result, AT II cells, that are crucial for maintenance of lung homeostasis secreting surfactant protein C (SP-C) to reduce surface tension and serve as precursors of AT I cells, 1) become either hyperplastic or elongated large cells, which then 2) synthesize various pro-fibrotic growth factors and cytokines, such as Transforming growth factor- β (TGF- β) and matrix-metalloproteinases (MMPs) and 3) lose their regenerative capacity by becoming increasingly apoptotic or senescent (Selman and Pardo 2002). These aberrantly

activated epithelial cells secreting a plethora of growth factors subsequently cause to the expansion of the (myo-)fibroblasts population by inducing the proliferation of resident fibroblasts (Warshamana, Corti and Brody 2001), attracting circulating fibrocytes (Andersson-Sjoland et al. 2008) and epithelial-to mesenchymal-transition (EMT) (DeMaio et al. 2012). *In-vivo* studies demonstrated EMT to constitute to a small portion of (myo-)fibroblasts in fibrosis, however it remains unclear if these cells substantially contribute to ECM formation in fibrosis (Fernandez and Eickelberg 2012b, Wolters, Collard and Jones 2014, Rock et al. 2011). Thus, the aberrant functioning of epithelial cells results in (myo-)fibroblast activation and proliferation, excessive ECM deposition and subsequent fibroblast foci formation. An aberrant epithelial-mesenchymal crosstalk starts with not only alveolar epithelial cells but (myo-)fibroblasts driving disease progression by inducing epithelial cell apoptosis (Selman and Pardo 2014, Hagimoto et al. 2002, Waghray et al. 2005). These (myo-)fibroblasts undergo phenotypic and functional changes exhibiting an invasive and proliferative phenotype including the resistance to apoptosis (Li et al. 2011, Ramos et al. 2001, Wolters et al. 2014). Moreover, not only (myo-)fibroblasts but the deposited ECM is profoundly altered in IPF (Parker et al. 2014, Zhou et al. 2013). For instance, the ECM stiffening in IPF alters (myo-)fibroblast behavior by inducing fibroblast to myofibroblast transdifferentiation and increasing ECM gene expression. A positive feedback loop is formed with altered ECM regulating miRNA expression in adjacent cells, thus inducing matrix gene expression (Parker et al. 2014).

The recovery of the alveolar epithelial barrier is crucial for maintenance of lung homeostasis; however, repetitive impairment of the alveolar epithelium leads to an aberrant repair response eventually resulting in fibrosis. During the normal wound healing process alveolar epithelial cell migrate towards the denuded area. Upon a provisional matrix, mainly consisting of fibronectin, AT II cells proliferate and transdifferentiate to AT I, thus closing the wounded area (Yanagi et al. 2015). Activated (myo-)fibroblasts simultaneously proliferate and migrate to the site of injury rebuilding the ECM scaffold (Kendall and Feghali-Bostwick 2014). This process is accompanied by close epithelial-mesenchymal-crosstalk with AT II secreting a plethora of chemokines and growth factors and transient reactivation of developmental pathways. In fibrosis impaired epithelial cell integrity due to genetic predisposition and aging processes (e.g. cellular senescence, telomere

attrition) causes the alveolar epithelial cells to respond improperly to repetitive injury upon occupational exposures (Figure 2). An excessive wound healing response is initiated and perpetuates as the disease progresses.

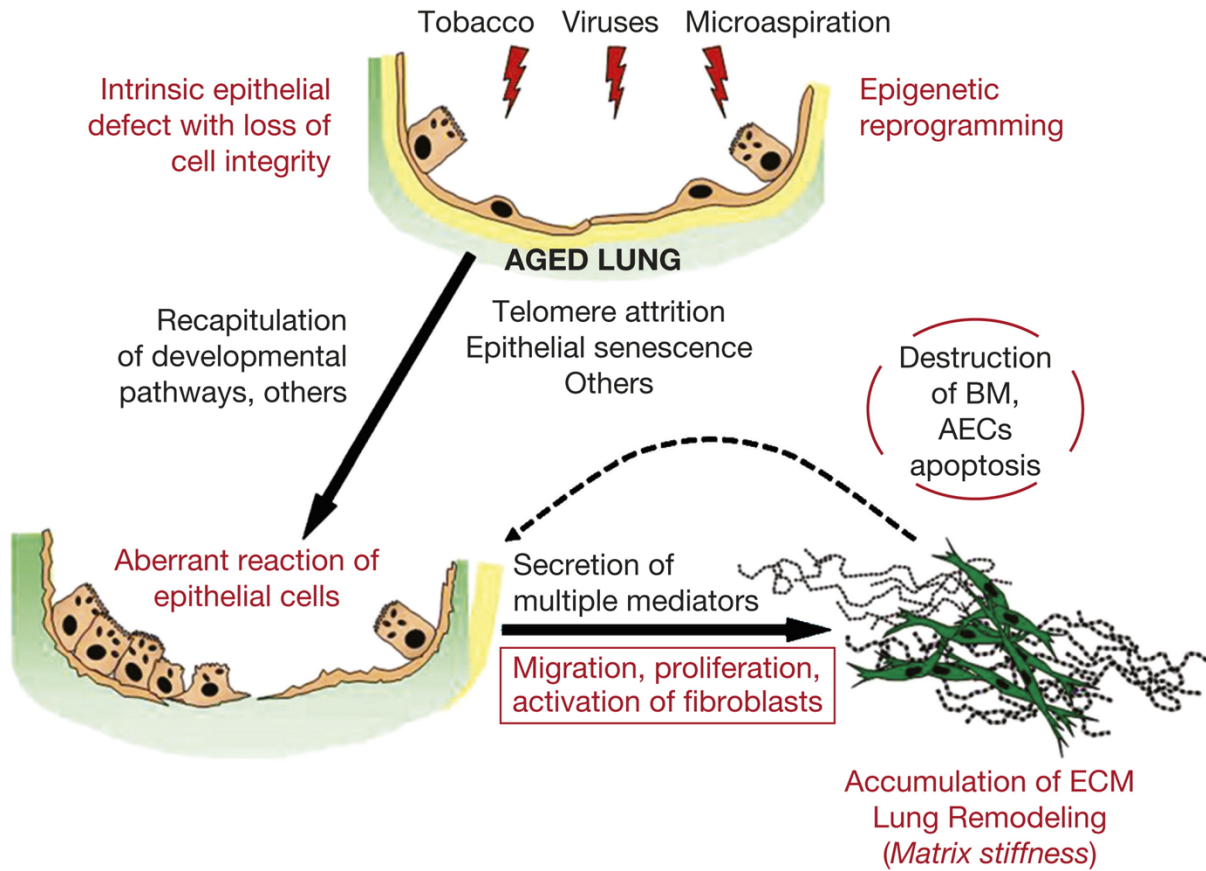


Figure 2: An integral model of genetic and environmental factors contributing to alveolar epithelial cell disintegration in the aged lung. (Figure modified from Selman et al. 2014)

3.5.1 Deregulated pathways

A large number of aberrantly activated signaling pathways, including TGF- β , connective tissue growth factor (CTGF), platelet-derived growth factor (PDGF), tumor necrosis factor α and wingless/in1 (WNT)- signaling, contribute to IPF pathogenesis (Martinez et al. 2017, Selman, Pardo and Kaminski 2008). TGF- β , in particular, is a main driver of fibrosis development and progression exhibiting pleiotropic pro-fibrotic properties (Fernandez and Eickelberg 2012a). TGF- β superfamily is involved in embryonic lung morphogenesis, maintaining organ homeostasis and tissue repair in the adult (Shi and Massague 2003). Although all TGF- β (β 1, β 2, β 3) isoforms are known to be involved in IPF pathogenesis, TGF- β 1 plays a predominant role (Fernandez and Eickelberg 2012a). Activation of latent TGF- β 1 is facilitated via α _v β ₆ integrin which is increasingly expressed on alveolar epithelial cells in IPF (Munger et al. 1999). TGF- β 1 overexpression in alveolar type II (AT II) cells subsequently resulted in AT II hyperplasia along with fibroblast proliferation, myofibroblast formation and enhanced ECM deposition (Xu et al. 2003). Moreover, TGF- β 1 was shown to induce epithelial to mesenchymal transition (EMT) and apoptosis in alveolar epithelial cells in the disease (Siegel and Massague 2003, Xu, Lamouille and Derynck 2009, Ding et al. 2017). Targeting TGF- β signaling substantially reduced the fibrotic burden in experimental fibrosis mouse models; however, these findings have not been successfully translated into the clinics yet. Because TGF- β signaling is important for maintaining physiological functions, its inhibition might be detrimental to organ homeostasis (Varga and Pasche 2008). More recently, a clinical phase II trial showed α _v β ₆ inhibition to substantially reduce active TGF- β signaling with good tolerability in IPF (Mouded et al.). Further results must be awaited.

Developmental pathways, such as WNT, Sonic Hedgehog and Notch signaling, are known to be reactivated in IPF (Martinez et al. 2017, Baarsma and Konigshoff 2017, Selman et al. 2008). Thus, WNT family member expression along with β -catenin nuclear translocation, a sign for activated WNT-signaling, was shown to be increased in lung tissue of IPF patients (Konigshoff et al. 2008). Moreover, WNT-target gene expression, especially WNT1-inducible signaling protein-1 (Wisp1) expression was enhanced in IPF lung tissue suggesting increased functional WNT-signaling in the diseased lung (Konigshoff et al. 2009, Baarsma and Konigshoff 2017). The subsequent inhibition of WISP1 resulted in attenuated Bleomycin induced lung fibrosis proving genes regulated by WNT

signaling to be promising therapeutic targets (Konigshoff et al. 2009). It was shown that AT II to AT I transdifferentiation is regulated by WNT/ β -catenin signaling suggesting that WNT-signaling which might be beneficial in the initial repair response following injury (Flozak et al. 2010). However, with disease progression the persistent activation of WNT-signaling results in aberrant alveolar epithelial cell functioning (Baarsma and Konigshoff 2017). Thus, it was shown that the induction of WNT/ β -catenin signaling in the alveolar epithelium (*in-vitro*) leads to both phenotypic and functional changes, such as EMT and secretion of pro-inflammatory and pro-fibrotic cytokine secretion, respectively (Aumiller et al. 2013, Ulsamer et al. 2012). Similar to WNT-/ β -catenin signaling, both Sonic Hedge Hog (SHH) ligands and receptors (e.g. PTCH1), regulating mesenchymal proliferation and branching morphogenesis during lung development (Kugler et al. 2015), was upregulated in IPF lung tissue but not in healthy controls (Coon et al. 2006, Stewart et al. 2003). Interestingly, inhibition of SHH failed to prevent the development of fibrosis in the Bleomycin mouse model (Moshai et al. 2014) whereas overexpression worsened experimental lung fibrosis (Liu et al. 2013). *In-vitro* studies showed prolonged survival and increased proliferation of fibroblasts after SHH induction suggesting that SHH signaling is crucial for fibrosis perpetuation (Liu et al. 2013, Kugler et al. 2015).

Many developmental pathways that are essential in organ development and silenced later on, are aberrantly reactivated in idiopathic pulmonary fibrosis (Selman et al. 2008). They have been linked to both pathogenesis and progression of the disease and subsequent inhibition led to the attenuation of experimental fibrosis making them to promising targets for future therapies in IPF.

3.5.2 Aging

There is a clear link, both biological and epidemiological, between IPF and aging (Collard 2010b, Thannickal 2013). Aging is indeed accompanied with the loss of cell integrity and function resulting in an increased vulnerability to disease development. However, not only the natural aging process but its acceleration due to repetitive injury and repair plays a critical role in the induction and perpetuation of IPF. Thus, the major hallmarks of aging have been shown to contribute to IPF pathogenesis (Lopez-Otin et al. 2013). Alveolar epithelial impairment in the

disease specifically is linked to age-related changes, such as telomere attrition, increased cellular senescence and mitochondrial dysfunction (Selman and Pardo 2014, Collard 2010b). Recurring damage to the alveolar epithelial barrier with subsequent division of adjacent cells is known to lead to progenitor cell exhaustion and cellular dysfunction making proper wound healing impossible (Chilosi et al. 2013). For instance, abnormally abbreviated telomeres are not only documented in the epithelium of IPF patients (Alder et al. 2008), but the length is associated with a worse survival in IPF patients (Stuart et al. 2014). Moreover, genetic mutations in familial IPF are related to telomere biology highlighting the impact of aging-related changes in the pathogenesis of the disease (Armanios et al. 2007). Similarly, cellular senescence is increased in the alveolar epithelium of IPF patients contributing to disease pathogenesis by secreting a plethora of soluble molecules and thus, affecting the adjacent cellular microenvironment (Minagawa et al. 2011, Disayabutr et al. 2016). This “Senescence-Associated Secretory Phenotype” (SASP) consists of pro-inflammatory cytokines (e.g. IL-6) and metalloproteinases, such as MMP7, known to be upregulated in IPF (Coppé et al. 2010, Takizawa et al. 1997, Rosas et al. 2008). Moreover, depletion of senescence cells restored epithelial cell function in *in-vitro* and *ex-vivo* 3D-Lung Tissue Cultures (3D-LTCs) representing a novel therapeutic option in the treatment of age-related diseases (Lehmann et al. 2017). However, the role of cellular senescence in fibrosis remains controversial exhibiting both anti- and pro-fibrotic effects (Minagawa et al. 2011, Cui et al. 2017).

Furthermore, not only IPF but other chronic lung diseases, such as chronic obstructive pulmonary disease (COPD) exhibit certain hallmarks of aging (e.g. telomere attrition, cellular senescence and mitochondrial dysfunction) raising the question what makes patients specifically prone to IPF. In this context, it has been proposed that genetic predisposition along with distinct gene expression patterns and epigenetic reprogramming could potentially be decisive (Selman and Pardo 2014).

3.5.3 Genetics

Genetic susceptibility is known to substantially contribute to disease development both in familial and sporadic IPF. Known genetic mutations in familial IPF, which can be held accountable

for 20% of overall IPF cases, are related to telomere maintenance (*TERT*, *TERC*, *RTEL*, *PARN*) and surfactant malfunction (*SFTPC*, *SFTPA2*) highlighting the impact of both impaired epithelial cell integrity and aging processes in disease pathogenesis (Richeldi et al. 2017). A genome wide linkage screen revealed a MUC5B promotor polymorphism (rs35705950) to be the most abundant genetic mutation in both sporadic and familial IPF with 38% and 34%, respectively (Spagnolo and Cottin 2017, Yang et al. 2015). MUC5B is expressed in the bronchiolar epithelium maintaining mucociliary clearance as part of immune defense indicating the potential impact of altered distal airways epithelium in disease pathogenesis. Intriguingly, carrier of the MUC5B variant showed improved overall survival suggesting that increased mucin production due the MUC5B polymorphism is linked to improved host defense (Peljto et al. 2013, Yang et al. 2015). As the MUC5B promotor variant is the most common genetic risk factor for the development of IPF in the general population, it was further proposed as biomarker for early fibrosis detection (Yang et al. 2015). However, the MUC5B promotor polymorphism is present in 19 % of the population whereas IPF is found in less than 1% indicating that other genetic mutations and environmental toxins contribute to the development of IPF (Yang et al. 2015). Therefore, other genetic risk factors for sporadic IPF have been identified, including genes associated with DNA repair (*TERT*, *TERC*) and cell-cell-contact (*DSP* and *DPP9*) (Yang et al. 2015). Interestingly, Toll interacting protein (*TOLLIP*) variants, regulating TGF- β signaling as well as Toll-like receptor mediated immune response, were associated with reduced susceptibility for IPF. However, patients who developed IPF despite carrying the TOLLIP polymorphism exhibited increased mortality (Noth et al. 2013).

Genetic factors combined with environmental exposure substantially contribute to IPF development in patients. This can have potential implications both for the understanding of the disease pathogenesis and detection/treatment of IPF (Spagnolo and Cottin 2017): 1) Surfactant protein and telomerase-associated gene mutations in familial IPF are both related to alveolar epithelial cell maintenance, thus emphasizing the importance of impaired of epithelial cell integrity at the onset of the disease, 2) testing for the abundantly expressed MUC5B promotor variant combined with HRCT gives the unique opportunity to detect subclinical IPF stages and thus improving the patients prognosis by early treatment, 3) testing for genetic mutations might

help to predict the course of the disease as the MUC5B promotor mutation is associated with better prognosis whereas patients with the TOLLIP variant have higher mortality and 4) genetic mutations potentially change the response to anti-fibrotic treatment.

3.5.4 Epigenetic reprogramming

Common risk factors for the development of IPF, such as aging, male gender, cigarette smoking and genetic alteration, are also potent inducer of epigenetic reprogramming (Helling and Yang 2015). These epigenetic changes, such as DNA methylation, histone alterations and microRNA deregulation alter the individual's gene expression profile, thus translating environmental influences into genetic regulation (Yang and Schwartz 2015). Yang et al. demonstrated 2 130 gene regions to be differentially methylated in IPF patients compared to control, from which 738 exhibited significant gene expression changes. Approximately 10-15% of the detected differentially methylated genes were associated with IPF pathogenesis, highlighting the impact of DNA methylation on gene regulation in IPF (Yang et al. 2014). Similarly, microRNAs (miRNA), regulating protein translation by targeting mRNA, are differentially expressed in IPF tissue compared to control (Pandit et al. 2010). By interacting with pro-fibrotic signaling pathways, such as TGF- β , these miRNAs exhibit both pro- and anti-fibrotic effects. For instance, miRNA-21 is highly increased in IPF tissue and Bleomycin mouse fibrosis promoting TGF- β signaling by targeting SMAD7. The subsequent miRNA- 21 neutralization resulted in attenuated Bleomycin induced lung fibrosis in mice (Liu et al. 2010). On the contrary, miRNA led-7d was shown to be significantly decreased by TGF- β in IPF (Pandit et al. 2010). Studies investigating structural chromatin changes in IPF showed that, for instance, deficient acetylation of histone with consecutive hypermethylation led to repression of anti-fibrotic genes, such as cyclooxygenase-2, thus contributing to disease progression (Coward et al. 2010). In line with this, histone deacetylases (HDACs) were found to be highly upregulated in IPF tissue (Korfei et al. 2015).

Epigenetic profiling facilitates a better understanding of IPF pathogenesis and further helps to develop innovative therapeutic and diagnostic approaches (Yang et al. 2014). DNA methylation targeting drugs as well as histone deacetylase inhibitors are already utilized in the treatment of

lung cancer and myelodysplastic syndrome highlighting the feasibility of this approach (Yang et al. 2014).

3.6 Pharmacotherapy

IPF patients are treated according to the American Thoracic Society, European Respiratory Society, Japanese Respiratory and Latin American Thoracic Association consensus statement updated in 2015. In the course of recent clinical trials many emerging therapies have been identified as either harmful or ineffective (Richeldi et al. 2017). Therefore, strong recommendations were made against the combination of prednisone, azathioprine and N-acetylcysteine, a recent worldwide standard in the treatment of fibrosis, due to the PANTHER study showing an increased mortality and hospitalization rate (Izumi, Ikura and Hirano 2012). Similar to the immunosuppressive therapy the usage of Ambrisentan, a selective endothelin receptor antagonist, and anticoagulation with warfarin lack any favorable effect more likely accelerating disease progression (Raghu et al. 2013, Noth et al. 2012). N-acetyl-cysteine monotherapy might have beneficial effects in patients with a certain TOLLIP polymorphism (Oldham et al. 2015); however, conditional recommendations were made against its use (Martinez et al. 2017). Thus, Nintedanib and Pirfenidone, remain to be the only approved drugs for the treatment of IPF known to be effective. The underlying mechanisms of action remain poorly understood, though.

3.6.1 Pirfenidone

Pirfenidone (5-methyl-1-phenyl-2-[1H]-pyridon) is a synthetic pyridine derivative that has been approved for treatment of mild-to moderate IPF in 2011 by the European Medicines Agency (EMA) and 2014 by the Food and Drug Administration (FDA) (Richeldi et al. 2017). Originally being developed as an analgesic and anti-pyretic agent in 1974, its anti-fibrotic properties were first described in 1994 in an animal fibrosis model by Margolin et al. (Gan, Herzog and Gomer 2011, George and Wells 2017). The first phase III trial by Taniguchi et al. in 2010 reported a significant reduction in vital capacity decline which is known to correlate with survival (Taniguchi

et al. 2010) whereas following CAPACITY trials showed differential results one supporting the initial findings while the other one being not significant (Noble et al. 2011). Due to the discordance the ASCEND phase III trial was performed showing reduced disease progression and increased progression-free survival in the Pirfenidone group compared to placebo (King et al. 2014, Richeldi et al. 2017). More recently, Pirfenidone was shown to have potential pro-survival effects (Nathan et al. 2017). Reported adverse events were gastrointestinal symptoms such as dyspepsia and vomiting, photosensitivity, skin rash and elevated liver enzymes leading to discontinuation of treatment in one fifth (20%) of the patients (Richeldi et al. 2017).

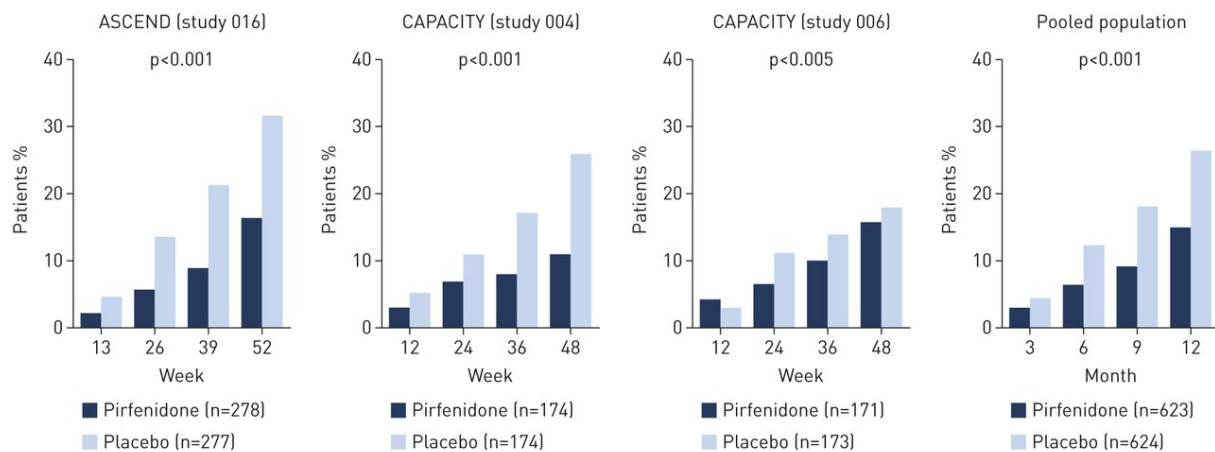


Figure 3: FVC outcomes from all Pirfenidone phase-III trials. A treatment benefit in reduced FCV decline was observed at each timepoint. (Figure modified from Noble et al. 2016)

3.6.1.1 Pharmacokinetics

Pirfenidone is an orally available small molecule. With absorption it is rapidly degraded mainly by cytochrome CYP1A2 into three metabolites, 5-carboxypirfenidone, 5-hydroxypirfenidone and 4-hydroxypirfenidone and subsequently eliminated via urine (Togami, Kanehira and Tada 2015). These metabolites were shown to partially exhibit anti-fibrotic effects. Pirfenidone concentration reaches its maximum at (T_{max}) 0.5 hours and is eliminated within 3 hours (Rubino et al. 2009, Shi et al. 2007, Schaefer et al. 2011). Togami et al. demonstrated the tissue distribution to be relatively low in the lung compared to kidneys and liver. This can potentially be held accountable

for the need of high dosing (2403mg/day) in clinical therapy and subsequent side effects (Togami et al. 2015).

3.6.1.2 Mode of action

Pirfenidone was shown to combine anti-inflammatory, anti-oxidant and anti-fibrotic properties in both animal and *in-vitro* fibrosis models of the lung, liver, kidney and heart (Schaefer et al. 2011, Carter 2011). However, the precise mode of action remains unknown.

Anti-fibrotic action

The anti-fibrotic action of Pirfenidone can be mainly attributed to the downregulation of pro-fibrotic growth factors TGF- β , PDGF-A/-B and bFGF expression, thus inhibiting (myo-)fibroblast activation and proliferation, collagen synthesis and deposition of extracellular matrix (Oku et al. 2008, Iyer, Gurujeyalakshmi and Giri 1999b). *In-vitro* studies demonstrated Pirfenidone to significantly inhibit TGF- β mediated cellular events, including fibroblast to myofibroblast differentiation and proliferation, ECM production and EMT. Pirfenidone was shown to inhibit key regulating factors of the TGF- β signaling pathway, such as phosphorylation of SMAD3, p38 and Akt (Conte et al. 2014). Similar effects were observed in a human retinal pigment epithelial (RPE) cell line with Pirfenidone impeding the accumulation of Smad2/3 in the nucleus (Choi et al. 2012). *In-vivo*, it has been demonstrated that Pirfenidone sufficiently inhibits TGF- β and SMAD mRNA expression levels (Iyer et al. 1999b). These studies suggest that Pirfenidone directly modulate TGF- β signaling by blocking its downstream targets. However, it has been recently proposed that Pirfenidone also regulates TGF- β *via* suppression of GLI transcription factors (Didiasova et al. 2017). Furthermore, Pirfenidone was shown to substantially downregulate PDGF and FGF levels in a Bleomycin hamster model (Gurujeyalakshmi, Hollinger and Giri 1999). Moreover, PDGF-induced hepatic stellate cell proliferation and collagen secretion was reduced by Pirfenidone treatment. However, direct PDGF pathway regulation by Pirfenidone *via* receptor auto-phosphorylation, ERK 1/2 or pp70 activation was not shown (Di Sario et al. 2002).

Major ECM component collagen I, in particular, plays a central role in fibrogenesis (Decaris et al. 2014). Several studies demonstrated that Pirfenidone affects collagen (I) expression, secretion and fibril formation in both human fibroblasts and epithelial cells (Nakayama et al. 2008, Hisatomi et al. 2012, Knuppel et al. 2017, Shin et al. 2015). Collagen specific chaperone Heat shock protein (HSP) 47 was shown to be decreased by Pirfenidone upon TGF- β treatment (Nakayama et al. 2008). Animal studies supported the *in-vitro* findings with Pirfenidone decreasing hydroxyproline secretion (Oku et al. 2008). Moreover, Pirfenidone significantly downregulated MMP 2 and TIMP-1 levels in a liver fibrosis model (Di Sario, 2004).

Anti-inflammatory action

Pirfenidone exerts its anti-inflammatory properties *via* suppressing pro-inflammatory cytokine levels including IL-6, IL-8, IL-12, TNF- α and IL-1 β , increasing anti-inflammatory agents (e.g. IL-10) and reducing inflammatory cell recruitment and proliferation (Oku et al. 2002, Nakazato et al. 2002, Oku et al. 2008). However, the exact mode of action remains elusive. For instance, *in-vivo* studies demonstrated Pirfenidone to inhibit TNF- α production at a translational level while IL-10 expression was enhanced at a transcriptional level (Nakazato et al. 2002). Moreover, Pirfenidone was shown to reduce macrophage (M1, M2) and neutrophil infiltration by inhibiting chemotactic cytokines, such as MCP-1 and CINC (Tsuchiya et al. 2004, Chen et al. 2013). Additionally, Pirfenidone inhibited TCR-induced CD4+ lymphocyte proliferation *in-vitro* and *in-vivo* (Visner et al. 2009). Pro-inflammatory cytokines and chemokines released by both macrophages and lymphocytes were subsequently diminished by Pirfenidone (Visner et al. 2009, Chen et al. 2013).

Anti-oxidant action

Increased oxidative stress has been previously implicated in the IPF pathogenesis. The imbalance towards the enhanced production of reactive oxidant species (ROS) was shown to result in cellular dysfunction and consecutive tissue damage leading to fibrosis formation (Kliment and Oury 2010). Pirfenidone was demonstrated to exert anti-oxidant properties in both *in-vitro* and

in-vivo fibrosis models (Giri et al. 1999, Iyer, Gurujeyalakshmi and Giri 1999a). Pirfenidone both acts as anti-oxidant scavenger neutralizing ROS by complex formation (Mitani et al. 2008, Misra and Rabideau 2000) and induces cellular antioxidant glutathione synthesis (Macias-Barragan et al. 2014). Moreover, it was shown that Pirfenidone regulates Nrf2/Bach1 balance, two key regulators of (anti-)oxidant gene expression, resulting in the increased Nrf2 dependent production of anti-oxidants *in-vitro* and *in-vivo* (Liu et al. 2017).

3.6.2 Nintedanib

Nintedanib (formerly known as BIBF 1120) is a tyrosine kinase receptor inhibitor that was initially designed as an antiangiogenic agent for cancer treatment (Wollin et al. 2015a). Tyrosine kinase receptors, including VEGFR, PDGFR and FGFR have been implicated in IPF pathogenesis being key regulators of fibroblast proliferation, migration and myofibroblast transformation (Wollin et al. 2014). Nintedanib was approved in 2014 by the FDA followed by EMA in 2015 for the treatment of IPF patients based on the findings of TOMORROW phase II trial and INPULSIS-1 and -2, two phase III trials. Both phase II and III trials demonstrated Nintedanib to reduce the annual FVC decline by approximately 50% compared to placebo and the number of acute exacerbations, thus decelerating disease progression in IPF patients (Richeldi et al. 2011, Richeldi et al. 2014). Long-term treatment with Nintedanib showed a reduced all-cause mortality compared to placebo and deceleration of disease progression beyond 52 weeks (Richeldi et al. 2018). The most reported side effect was diarrhea leading to termination of treatment in 5% of the patients (Richeldi et al. 2014).

With IPF and other ILDs sharing clinical and pathophysiological hallmarks, the potential benefit of Nintedanib and Pirfenidone, in the treatment of non-IPF ILD has recently gained attention (Collins and Raghu 2019). *In-vitro* and *in-vivo* preclinical studies demonstrated Nintedanib to exert anti-fibrotic effects in non-IPF ILDs (Wollin et al. 2019a). Moreover, the INBUILD study showed Nintedanib to reduce the annual decline of the FVC rate compared to placebo making the anti-fibrotic agent to be a feasible therapeutic option in non-IPF ILDs (Flaherty et al. 2019)

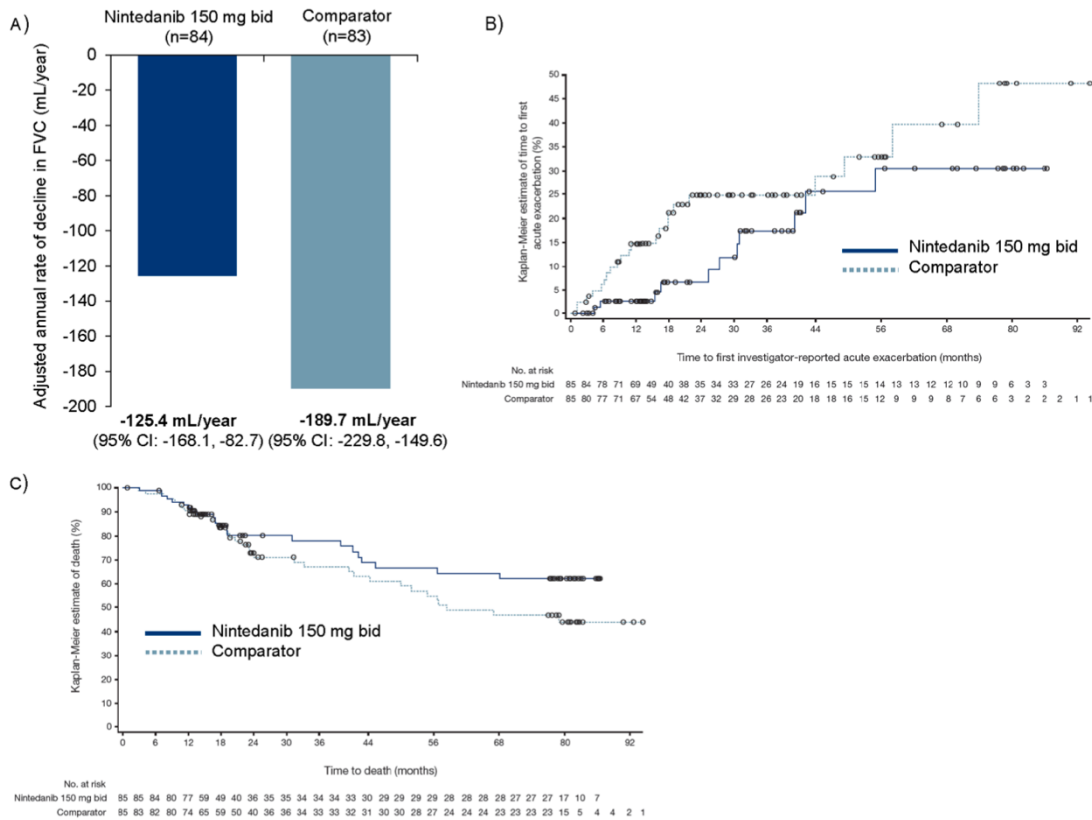


Figure 4: Long-term results of the TOMORROW study. (A) Annual FVC decline (B, C) Kaplan-Meier survival curves for (B) time until first acute exacerbation and (C) time until death. Patients of the TOMORROW study (phase 1 and 2) and its open-label extension were included. The comparator group was treated with placebo in phase 1 and a daily dose of 50mg of Nintedanib in phase 2. They were able to increase to 150mg twice daily of Nintedanib in the open-label extension. The Nintedanib group was treated with 150mg twice daily of Nintedanib. (Figure modified from Richeldi et al. 2018)

3.6.2.1 Pharmacokinetics

After oral administration small-molecule Nintedanib is promptly absorbed reaching its maximum concentration within 2-4 h [0,14 (ng/mL)/mg]. The half-life is 10-15 hours. Due to high first-pass-metabolism, the bioavailability is only around 5%. Nintedanib showed high plasma albumin binding with approximately 98% in humans. Nintedanib is predominantly degraded by hydrolytic ester cleavage into BIBF 1202 with following glucuronidation and elimination *via* bile. A small fraction is demethylated by CYP3A4 into BIBF 1053. However, CYP dependent metabolism and interaction with CYP modulating drugs of Nintedanib is negligible (Roth et al. 2015, Wind et al. 2019).

3.6.2.2 Mode of action

Nintedanib binds competitively to the ATP-binding pocket of following intracellular kinase receptor kinase domains: VEGFR 1–3, PDGFR- α and - β and FGFR 1–3, thereby blocking autophosphorylation and downstream signaling cascade of these receptors (Wind et al. 2019). Additionally, Nintedanib was shown to directly target non-receptor kinases Src, Lyn, Lck, Flt-3 and RET (Roth et al. 2009, Hilberg et al. 2008a). It can be assumed that Nintedanib exerts its anti-fibrotic action via binding to these tyrosine kinase receptors. Hostettler et al. showed PDGF, FGF and VEGF induced fibrotic changes are significantly inhibited by Nintedanib (Hostettler et al. 2014). However, the impact of yet partly known targets on the mode of action still remains to be further elucidated.

Anti-fibrotic action

Targets of Nintedanib therapy, PDGF(R), FGF(R) and VEGF(R), are potent fibroblast mitogens inducing excessive proliferation, migration and myofibroblast transdifferentiation of fibroblasts in the context of disease. Nintedanib was shown to block PDGF, FGF and VEGF induced fibroblast proliferation and motility as well as collagen secretion in IPF and control fibroblasts. Sato et al. also demonstrated Nintedanib to directly interfere with fibrocyte function, mesenchymal progenitor cells, which have been proposed to be major source for fibroblasts in IPF (Sato et al. 2017, Andersson-Sjoland et al. 2008). Moreover, Nintedanib increased matrix metalloproteinase (MMP)-2 levels while reducing its counterpart tissue inhibitor of metalloproteinase (TIMP)-2, contributing to enhanced degradation of ECM (Hostettler et al. 2014, Wollin et al. 2014). It was further shown that Nintedanib directly interferes with TGF- β signaling, thus inhibiting TGF- β dependent fibroblast to myofibroblast transdifferentiation, ECM protein expression and collagen fibril formation (Hostettler et al. 2014, Rangarajan et al. 2016). However, whether this effect is conveyed by Nintedanib binding directly to TGF- β receptor (TGFR β II) and/or nonreceptor SRC kinases remained inconclusive (Rangarajan et al. 2016). Furthermore, Nintedanib was demonstrated to reduce the fibrotic burden following bleomycin induced lung fibrosis in mice

assessed by histologic analysis as well as TGF- β mRNA levels and pro-collagen I (Wollin et al. 2014).

Anti-inflammatory action

Anti-inflammatory activity of Nintedanib was demonstrated in animal models of pulmonary fibrosis by attenuation of inflammatory cell counts and pro-inflammatory cytokines in bronchoalveolar lavage fluids (BALF) (Wollin et al. 2014). It can be assumed that these anti-inflammatory effects are partly conveyed by Nintedanib blocking non-receptor kinase Lck dependent T-cell proliferation and pro-inflammatory chemokine production (Hilberg et al. 2008a, Wollin et al. 2019b). It was further shown that Nintedanib blocks M2 macrophage polarization, a pro-fibrotic phenotype releasing CCL18, thereby promoting fibroblasts depositing collagen (Zhang et al. 2018, Wollin et al. 2019b).

Anti-angiogenic action

The potential impact of dysregulated angiogenesis on IPF pathogenesis remains controversial (Renzoni 2004). However, antiangiogenic agent Nintedanib was shown to restore microvascular architecture by reducing vessel density in mice exposed to Bleomycin (Ackermann et al. 2017). *In vitro*, Nintedanib attenuated proliferation of pericytes, endothelial cells and smooth muscle cells which have been shown to be crucial for lung angiogenesis (Hilberg et al. 2008b, Wollin et al. 2015b). Whether this effect contributes to the anti-fibrotic action of Nintedanib remains inconclusive.

3.7 Aims of the study

It is well accepted that repetitive epithelial injury and the consecutive secretion of pro-fibrotic mediators by aberrant epithelium contribute to the development of IPF. Therefore, targeting the abnormal alveolar epithelium in fibrosis can be of particular interest. To date, the only therapeutic options known to be effective in decelerating disease progression are Nintedanib and Pirfenidone. However, if these drugs potentially affect epithelial functioning remains elusive. Therefore, in this study we aim to investigate this question as follows:

“Do Nintedanib and Pirfenidone affect alveolar epithelial cell behavior and function in a favorable way?”

To do so, we used *ex-vivo* 3D- Lung Tissue Cultures (3D-LTCs) generated from mice and human tissue to resemble the *in-vivo* situation as close as possible. For a more in depth understanding we additionally used murine primary alveolar type II (pmAT II) cell monoculture. Both murine 3D-LTCs and pmAT II cells were either derived from Bleomycin-treated mice or treated with TGF- β as fibrotic stimulus *in-vitro*. We further validated our findings using the human 3D-LTCs subjected to TGF- β or a novel fibrotic cocktail to mimic an “early fibrosis like” stage which was established in our lab.

Additional questions were addressed as follows:

- 1) Are both murine and human 3D-LTCs an adequate tool for testing the anti-fibrotic action of these drugs?
- 2) Which concentrations are effective for *ex-vivo* treatment without compromising cell viability? Do they correspond with concentrations found in patients?
- 3) Thus, can Nintedanib and Pirfenidone sufficiently inhibit mesenchymal gene expression in murine and human 3D-LTCs as previously reported in fibroblast monoculture?

4. MATERIALS AND METHODS

4.1 Materials

4.1.1 Laboratory Equipment

Table 1: Laboratory Equipment

Product	Company
+4° Fridge, Medline	Liebherr; Biberach, Germany
-20° Freezer, Medline	Liebherr; Biberach, Germany
-80° Freezer, U570 Premium	New Brunswick; Hamburg, Germany
Autoclave DX -45	Systemec; Wettenberg, Germany
Autoclave VX -120	Systemec; Wettenberg, Germany
Balance XS4002S	Mettler Toledo, Greifensee, Germany
Centrifuge Mikro 200R	Hettich Zentrifugen; Tuttlingen, Germany
Centrifuge Rotina 420R	Hettich Zentrifugen; Tuttlingen, Germany
Cell incubator BBD6620	Thermo Fisher Scientific; Darmstadt, Germany
Gel imaging system ChemiDoc XRS+	Biorad; Hercules, CA, USA
Herasafe KS180, Cell Culture bench	Pierce, Thermo Fisher Scientific; Schwerte, Germany
Light Cycler LC480 II	Roche Diagnostics; Mannheim, Germany
Mastercycler Nexus	Eppendorf; Hamburg, Germany
Micro-Dismembrator S	Thermo Fisher Scientific; Darmstadt, Germany
Microscope LSM 710 (confocal)	Zeiss; Jena, Germany
Microsprayer Aerosolizer	Penn-Century, Wyndmoor, PA, USA
MilliQ Advantage A10	Merck Millipore; Darmstadt, Germany
Mini Microcentrifuge 230 V	Corning LSE, Kaiserslautern, Germany
Mini-PROTEAN Tetra Cell	Biorad, USA
Multipipette Stream	Eppendorf; Hamburg, Germany
Nano Drop ND-1000	PeqLab; Erlangen, Germany
Sunrise™ (ELISA-Reader)	Tecan; Crailsheim, Germany
Syringe pump "Aladdin" AL-1000	World Precision instruments; Sarasota, FL, USA
Thermomixer Compact	Eppendorf; Hamburg, Germany
Tissue Lyser II	Quiagen; Hilden, Germany

4.1.2 Software

Table 2: Software

Software	Company
Endnote X7.0.2	Thomson Reuters; San Francisco, CA, USA
GraphPad Prism 5.00	GraphPad Software; La Jolla, CA, USA
Image Lab Version 5.0	Biorad; Hercules, CA, USA
IMARIS x 64	Bitplane,, Zurich, Switzerland
LightCycler® 480 SW 1.5	Roche Diagnostics; Mannheim, Germany
Magelan Software	Tecan; Crailsheim, Germany
Zen 2010	Zeiss; Jena, Germany

4.1.3 Chemicals and reagents

Table 3: Chemicals and reagents

Product	Company
Acetone	AppliChem; Darmstadt, Germany
Agarose, low melting point	Sigma-Aldrich; Taufkirchen, Germany
Amphotericin B solution (250µg/ml)	Sigma-Aldrich; Taufkirchen, Germany
Biopsy punch (4mm, 6mm diameter)	pfm medical; Köln, Germany
Bleomycin sulfate	Almirall; Barcelona, Spain
Bovine serum albumin (BSA)	Sigma-Aldrich; Taufkirchen, Germany
Cell Proliferation Reagent WST-1	Roche Diagnostics; Mannheim, Germany
Complete® Mini without EDTA	Roche Diagnostics; Mannheim, Germany
DAPI	Sigma-Aldrich; Taufkirchen, Germany
Desoxyribonucleotides mix (dNTPs)	Thermo Fisher Scientific; Heidelberg, Germany
Dimethyl sulfoxide (DMSO)	Carl Roth; Karlsruhe, Germany
Dithiothreitol (DTT)	AppliChem; Darmstadt, Germany
D-MEM/F12	Gibco, Life Technologies; Carlsbad, CA, USA
DNase/RNase-free water	Gibco, Life Technologies; Carlsbad, CA, USA
Ethanol (p.a.)	AppliChem; Darmstadt, Germany
Fetal bovine serum (FBS)	PAA/GE Healthcare; Fairfield, CT, USA
Fluorescence mounting medium	Dako; Hamburg, Germany

Glucose	AppliChem; Darmstadt, Germany
HEPES	Life Technologies; Carlsbad, CA, USA
Ketamine	Bela-pharm; Vechta, Germany
Lysophosphatidic acid (LPA)	Cayman Chemical; Ann Arbor, MI, USA
Methanol	AppliChem; Darmstadt, Germany
MuLV Reverse Transcriptase 5,000 U	Applied Biosystems, Invitrogen, Life Technologies; Carlsbad, USA
Nintedanib	Selleck; Houston, TX, USA
Non-fat dried milk powder	AppliChem; Darmstadt, Germany
Plated derived growth factor- AB (PDGF-AB)	Gibco, Life Technologies; Carlsbad, CA, USA
Penicillin-Streptomycin	Gibco, Life Technologies; Carlsbad, CA, USA
Phosphate buffered saline	Gibco, Life Technologies; Carlsbad, CA, USA
PhosSTOP Phosphatase Inhibitor	Roche Diagnostics; Mannheim, Germany
Pirfenidone	Selleck; Houston, TX, USA
Proteinase K	Pierce, Thermo Fisher Scientific; Schwerte, Germany
Protein marker V	Peqlab; Erlangen, Germany
Random hexamers	Applied Biosystems, Life Technologies; Carlsbad, CA, USA
Rekombinant TGF- β 1 protein	R&D Systems; Minneapolis, USA
Restore Plus Western Blot Stripping Buffer	Pierce, Thermo Fisher Scientific; Schwerte, Germany
RNase inhibitor 20 U/ μ l	Applied Biosystems, Invitrogen, Life Technologies; Carlsbad, USA
Rotiphorese Gel 30 (37,5:1) 500 ml	Carl Roth; Karlsruhe, Germany
Sodium dodecyl sulphate (SDS) pellets	Carl Roth; Karlsruhe, Germany
Sodium chloride	AppliChem; Darmstadt, Germany
SuperSignal West Dura Extended Duration Substrate	Pierce, Thermo Fisher Scientific; Schwerte, Germany
SuperSignal West Femto Substrate	Pierce, Thermo Fisher Scientific; Schwerte, Germany
SybrSafe (10,000x in DMSO)	Invitrogen Life Technologies; Carlsbad, CA, USA
TEMED	AppliChem; Darmstadt, Germany
Tumor necrosis factor- α	R&D Systems; Minneapolis, USA
T-PER Tissue Protein Extraction Reagent	Pierce, Thermo Fisher Scientific; Schwerte, Germany
Tris base, buffer grade	AppliChem; Darmstadt, Germany
Triton X-100	AppliChem; Darmstadt, Germany
Tween 20	AppliChem; Darmstadt, Germany
UltraPure DNase/RNase-Free Distilled Water	Invitrogen Life Technologies; Carlsbad, CA, USA

WST-1
Xylazinhydrochloride

Roche Diagnostics; Mannheim, Germany
cp-pharma; Burgdorf, Germany

4.1.4 Consumables

Table 4: Consumables

Product	Company
Cell culture flask	Thermo Fisher Scientific; Darmstadt, Germany
Cell culture well (6-well, 12-well, 96-well)	TPP; Trasadingen, Switzerland
Cryotubes	Thermo Fisher Scientific; Darmstadt, Germany
Falcon tubes (15ml, 50ml)	BD Bioscience, Heidelberg, Germany
Filter tips	Biozym Scientific; Hessisch Oldendorf, Germany
Grinding steel balls	Neolab; Heidelberg, Germany
Multipipette tips	Eppendorf; Hamburg, Germany
Nitrocellulose membrane	Sigma-Aldrich; Taufkirchen, Germany
Nylon Meshes (pore size 100µm, 20µm, 10µm)	Sefar; Heiden, Germany
Scalpel	B.Braun; Melsungen, Germany
Syringes	B.Braun; Melsungen, Germany
Parafilm Sealing Film	Bemis Packaging; Neenah, WI, USA
PCR plates and sealing foil	Kisker Biotech; Steinfurt, Germany
PVDF membranes	Sigma-Aldrich; Taufkirchen, Germany
Reaction tubes	Greiner Bio-One; Frickenhausen, Germany
Whatman Blotting Papers	GE Healthcare; München, Germany

4.1.5 Buffers, solutions and media

Table 5: Buffers, solutions and media

Buffer/solutions	Compounds	Concentration
Cultivation medium for 3D-LTCs - DMEM-F12	Penicillin/Streptomycin	1%
	Amphotericin B	2.5 µg/ml
	Fetal bovine serum	0.1%
Cultivation medium for pmAT II cells- DMEM-F12	Penicillin/Streptomycin	1%
	Fetal bovine serum	10%
	HEPES	1 M
	1-Glutamine	2 mM
	Glucose	3.6 mg/ml
Laemmli loading buffer (4x)	Bromophenol blue	traces
	DTT	400 mM
	Glycerol	40%
	Tris/HCL, pH 6,8	2 mM
	SDS	8%
PBS 10x, pH 7.6	NaCl	1.37 M
	KCl	27 mM
	Na ₂ HPO ₄	100 mM
	KH ₂ PO ₄	20 mM
RIPA buffer	NaCl	150 mM
	Tris/HCL	10 mM
	SDS	0,1%
	Triton X-100	1%
	Sodiumdeoxycholate	1%
	EDTA	5 mM
Running Buffer	Tris	25 mM
	Glycine	1.92 M
	SDS	1%
TBS 10x, pH 7.6	Tris	10 mM
	NaCl	150 mM
TBS-T	TBS	1:10
	Tween	0,1%
Transfer Buffer	Tris	25 mM
	Glycine	200 mM

4.1.6 Kits

Table 6: Kits

Product	Company
BCA Protein Assay Kit	Pierce, Thermo Fisher Scientific; Schwerte, Germany
IL-6 ELISA	R&D, Minneapolis, Minnesota, USA
Peqlab Total RNA Kit	Peqlab, Erlangen, Germany
PerfectPure RNA Fibrous Tissue Kit	5Prime; Hilden, Germany
RNeasy Mini Kit	Qiagen; Hilden, Germany
SFTPC ELISA	Cusabio; Wuhan, China
WISP1 ELISA	R&D, Minneapolis, Minnesota, USA

4.1.7 Antibodies

Table 7: Primary Antibodies for immunofluorescence

antibody	origin	company, catalog number	dilution
alpha-SMA	mouse	Sigma-Aldrich; Taufkirchen, Germany; A5228	1:500
Collagen 1	rabbit	Rockland; Gilbertsville, PA, USA; 600-401-103	1:100
E-Cadherin	mouse	BD Biosciences; Heidelberg; Germany; 610181	1:200
Fibronectin	rabbit	Santa Cruz Biotechnology, TX, USA; sc-9068	1:100
Podoplanin	goat	R&D; Minneapolis, MN, USA; AF3244	1:100
SFTPC, pro-	rabbit	Millipore; Billerica, MA, USA; AB3786	1:500
Tenc	mouse	Abcam; Cambridge, UK; ab58954-100	1:100

Table 8: Primary Antibodies for Western Blot

antibody	origin	company, catalog number	dilution
β -actin	mouse	Sigma-Aldrich; Taufkirchen, Germany; A3854	1:50,000
Collagen 1	rabbit	Rockland; Gilbertsville, PA, USA; 600-401-103	1:1000
E-Cadherin	mouse	BD Biosciences; Heidelberg; Germany; 610181	1:1000

antibody	origin	company, catalog number	dilution
SFTPC, pro-	rabbit	Abcam; Cambridge, UK; ab40879	1:1000

Table 9: Secondary Antibodies for immunofluorescence

antibody	origin	company, catalog number	dilution
Goat-IgG (H+L), Alexa Fluor 488 conjugated	donkey	Invitrogen Life Technologies; Carlsbad, CA, USA; A-11055	1:1,000
Mouse-IgG (H+L), Alexa Fluor 555 conjugated	rabbit	Invitrogen Life Technologies; Carlsbad, CA, USA; A-21424	1:1,000
Rabbit-IgG (H-L), Alexa Fluor 555 conjugated	goat	Invitrogen Life Technologies; Carlsbad, CA, USA; A-21429	1:1,000

Table 10: Secondary Antibody for Western Blot, HRP linked

antibody	origin	company, catalog number	dilution
Mouse IgG	sheep	GE Healthcare; Freiburg, Germany	1:4,000
Rabbit IgG	donkey	GE Healthcare; Freiburg, Germany	1:10,000

Table 11: Antibodies used for FACS analysis (primary and secondary)

antibody	origin	company, catalog number	dilution
SFTPC, pro-	rabbit	Millipore, ab3786	1:2000
Rabbit-IgG (H-L), Alexa Fluor 488 conjugated	goat	Invitrogen Life Technologies; Carlsbad, CA, USA; A-21429	1:50

4.1.8 Primers

Table 12: Murine quantitative PCR primers

Gene	Sequence 5' - 3'	
<i>Acta2</i>	fw GCTGGTGATGATGCTCCCA	rv GCCCATTCCAACCATTACTCC
<i>Col1a1</i>	fw CCAAGAAGACATCCCTGAAGTCA	rv TGCACGTCATCGCACACA
<i>Fn1</i>	fw GGTGTAGCACAACCTCCAATTACG	rv GGAATTTCCGCTCGAGTCT
<i>Hopx</i>	fw TCTCCATCCTTAGTCAGACGC	rv TCTCCATCCTTAGTCAGACGC
<i>HPRT</i>	fw CCTAAGATGAGCGCAAGTTGAA	rv CCACAGGACTAGAACACCTGCTAA
<i>Nkx2.1</i>	fw AGGACACCATGCGGAACAG	rv CCATGCCGCTCATATTCATGC
<i>Sftpc</i>	fw AGCAAAGAGGTCCTGATGGA	rv GAGCAGAGCCCCTACAATCA
<i>T1α</i>	fw ACAG GTGCTACTGGAGGGCTT	rv TCCTCTAAGGGAGGCTTCGTC

Table 13: Human quantitative PCR Primers

Gene	Sequence 5' - 3'	
<i>FN1</i>	fw CCGACCAGAAGTTTGGGTTCT	rv CAATGCGGTACATGACCCCT
<i>COL1A1</i>	fw CAAGAGGAAGGCCAAGTCGAG	rv TTGTCGCAGACGCAGATCC
<i>CDH1</i>	fw ATACACTCTTCTCTCACGCTGTGT	rv CATTCTGATCGTTACCGTGATC
<i>NKX2.1</i>	fw AGCACACGACTCCGTTCTC	rv GCCCACTTTCTGTAGCTTTCC
<i>SFTPC</i>	fw GCCCAGTGACCTGAAACGC	rv GCCCAGTGACCTGAAACGC
<i>ZO1</i>	fw TCTGAGCCTGTAAGAGAGGAC	rv GCTTCTGCTTTCTGTTGAGAGG

4.2 Methods

4.2.1 Human tissue

Macroscopically tumor-free lung tissue obtained from patients undergoing lung cancer resection surgeries was used for the generation of 3D-LTCs. The absence of IPF/ILD was verified by pathology and CT. Human tissue samples subsequently subjected to the fibrotic cocktail were attained from two patients (one male 62 years, one female, 80 years) with squamous cell carcinoma and one patient being diagnosed with a carcinoid lung tumor (male, 48 years). The smoking history of these patients was not known. Human 3D-LTCs were generated and cultured as previously described (Uhl et al. 2015). Human tissue samples were provided by the Asklepios Biobank of Lung Diseases and the CPC BioArchive CPC-M at the University Hospital Grosshadern of the Ludwig Maximilian University (LMU). All experiments using human tissue were approved by the local ethic committee of the LMU (project number: 333-10,455-12). Written informed consent by all participants of this study was obtained.

4.2.2 Animal experiments

Six to eight-month-old female pathogen-free C57BL/6 mice obtained from Charles River were used throughout all studies. All experiments were conducted according to the ethics committee of the Helmholtz Zentrum Munich (Germany) guidelines and approved by the regional council of Upper Bavaria (Germany). The mice had free access to water and food and were housed in facilities with constant temperature, humidity and 12h light cycles. To induce experimental lung fibrosis, Bleomycin was applied intratracheally as a single dose (2U/kg/body weight) using the Micro-Sprayer Aerosolizer. Control mice received PBS only. At day 14 post-installation, the mice were sacrificed and the lungs were obtained for 3D-LTCs and pmAT II generation.

4.2.3 Primary murine alveolar type II cell isolation and culture

Primary murine alveolar type II cells (pmAT II) were isolated from mice as previously described (Mutze et al. 2015, Demaio et al. 2009). In brief, after flushing the pulmonary circulation system with sterile PBS, the lung was inflated with dispase followed by low gelling agarose. The lungs were subsequently incubated for 45 minutes at room temperature. After digestion the tissue was minced and filtered through 100 μ m, 20 μ m and 10 μ m nylon meshes. After centrifugation the pellets were re-suspended and fibroblast negative selection was done by adherence using cell culture dishes. Lymphocytes, macrophages and endothelial cells were removed from the cell suspension with CD45 and CD31 conjugated magnetic beads, respectively. Cell purity was checked routinely by cell morphology and immunofluorescence analysis. After plating the pmAT II were cultured in DMEM-F12 complemented with 10% FCS, 2mM 1-glutamine, 1% penicillin/streptomycin, 3,6 mg/ml glucose and 10M HEPES for 24h to promote attachment. Before stimulation, cells were synchronized by culturing them for 12h hours in 0.1% FCS starvation medium with identical composition as medium for cell attachment. Fibrotic pmAT II cell were then treated with Nintedanib (0,1 μ M) or Pirfenidone (100 μ M) and respective DMSO control. pmAT II derived from wild-type mice were pre-treated with Nintedanib ((0,1 μ M, 1 μ M) or Pirfenidone (100 μ M, 500 μ M) and respective DMSO control for 1 hour and subsequently treated with transforming growth factor- β (TGF- β , 2 ng/ml) for 48h.

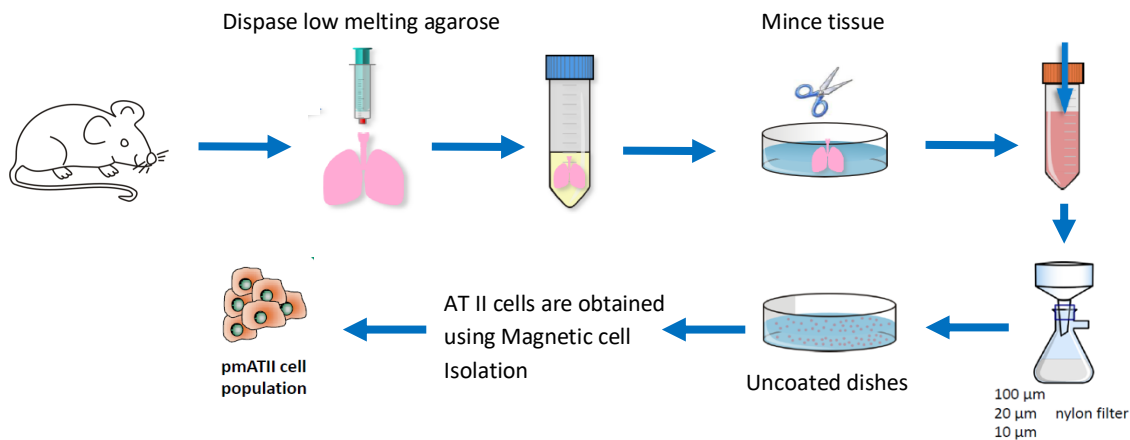


Figure 5: Primary murine alveolar epithelial type II cell isolation. The pmATII cells were obtained either from wild-type or Bleomycin/PBS-treated mice. Mice lungs were filled with agarose, minced and filtered through meshes. The pmATII cells were separated from other cell types using Magnetic Cell Isolation.

4.2.4 Murine *ex-vivo* 3D-Lung tissue culture

Murine 3D-LTCs were generated as described afore (Uhl et al. 2015). Briefly, the anaesthetized mice were intubated using an endotracheal tube and the chest cavity was opened after dissecting the diaphragm. After flushing the pulmonary circulation system through the heart with sterile PBS, the lungs were inflated via an endotracheal tube with warm low gelling agarose dissolved in cultivation medium (2% by weight in DMEM-F12) using a syringe pump. After harvesting the lung, the lobes were separated and cut into 300 μ m thick slices using the vibratome at a speed of 10-12 μ m/s, an amplitude of 1mm and frequency of 100Hz. The 3D-LTCs were cultured in DMEM-F12 supplemented with 0.1% FCS and antibiotics (1% penicillin/streptomycin and amphotericin B). 3D-LTCS obtained from healthy mice were pre-treated with Pirfenidone (100 μ M, 500 μ M, 2.5mM) or Nintedanib (0.1 μ M, 1 μ M, 10 μ M) and the respective DMSO control. After one hour TGF- β (2ng/ml) was added. 3D-LTCs obtained from PBS- or Bleomycin-treated mice at day 14 post-installation were stimulated either with Pirfenidone (100 μ M, 500 μ M, 2.5mM) or Nintedanib (0.1 μ M, 1 μ M, 10 μ M) and respective DMSO control. The murine 3D-LTCs were kept in culture for 48h. For harvest two to three 3D-LTCs were pooled, frozen in liquid nitrogen and subsequently stored at -80°C.

4.2.5 Human *ex-vivo* 3D-Lung tissue cultures

Human 3D-LTCs were obtained as previously described (Uhl et al. 2015). The freshly excised human tissue was filled with warm low gelling agarose (3% by weight (dissolved in DMEM-F12 supplemented with antibiotics and amphotericin B) *via* a prominent bronchus using a cannula and subsequently cooled for 30 min to allow agarose gelling. Small pieces were then cut into 500 μ m thick slices to a speed of 6-10 μ m/s, amplitude of 1.2mm and frequency of 100Hz. The human 3D-LTCs were cultured in DMEM-F12 complemented with 0.1% FCS and antibiotics (1% penicillin/streptomycin and amphotericin B). 3D-LTCs were pre-treated with Nintedanib (1 μ M) or Pirfenidone (500 μ M) for 1 hour. After adding TGF- β (5ng/ml) the 3D-LTCs were kept in culture for 48h. For harvest, two 3D-LTCs were collected and frozen in liquid nitrogen. The samples were subsequently stored at -80°C.

4.2.6 Fibrotic cocktail

Human 3D-LTCS/ 4-mm punches were generated as described afore (Uhl et al. 2015, Alsafadi et al. 2017) and subjected to a fibrotic cocktail (FC) comprising recombinant TGF- β (5 ng/ml), platelet-derived growth factor-AB (PDGF-AB, 5 μ M), tumor necrosis factor (TNF- α , 10ng/ml) and lysophosphatidic acid (LPA, 5 μ M) or control cocktail (CC) (Alsafadi et al. 2017). After 48h the FC was replenished and the 3D-LTCs subjected to Nintedanib (1 μ M) or Pirfenidone (500 μ M). 3D-LTCs/punches were subsequently harvested after 72h for downstream analysis.

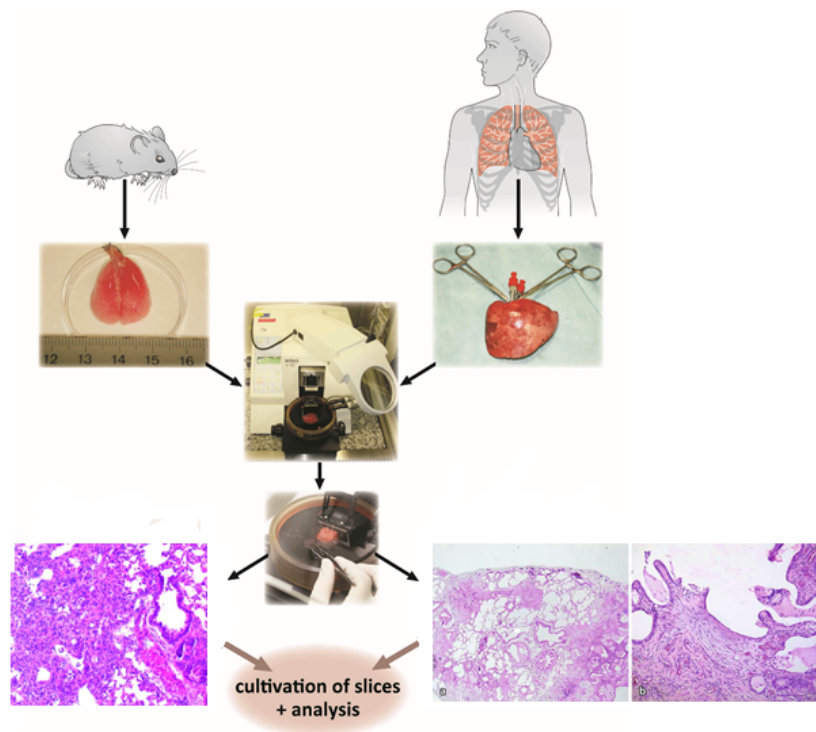


Figure 6: Generation of ex-vivo 3D-lung tissue cultures. The lungs were explanted from wild-type or Bleomycin/PBS-treated mice and filled with agarose. The lung lobes were then cut into slices (300 μ M) with the vibratome. Human material was filled with agarose and cut into 500 μ M thick slices. The 3D-LTCs were cultivated up to 48h. (Image modified from Uhl et al.2015)

4.2.7 RNA isolation

For RNA isolation two to three 3D-LTCs were collected, subsequently frozen in liquid nitrogen and pulverized using a tissue lyser (2x 30 s at 3,000 rpm). Murine 3D-LTCs were digested using RNA lysis buffer containing TCEP for 1h and subsequently incubated with Proteinase K for 10min at 55 $^{\circ}$ C. Total RNA was extracted from murine 3D-LTCS using the PeqLap Total RNA kit with minor

alterations to the manufacturer’s protocol (Uhl et al. 2015). RNeasy Fibrous tissue kit was utilized for RNA isolation from human 3D-LTCs. After being pulverized the human 3D-LTCs were incubated with RTT buffer containing DTT for 1h and subsequently incubated with Proteinase K for 15min at room temperature. Peqlab DNA removing columns were applied prior to the RNA binding step. After isolation the RNA concentration and quality were determined using the NanoDrop spectrophotometer.

4.2.8 cDNA Synthesis

1µg RNA in 20µl RNase/DNase free water was denatured for 10 minutes at 70°C. The reverse transcription was performed by adding 20µl of the reagent mixture as listed below. After the transcription was performed the samples were diluted 1:5 (less if the RNA concentration was low).

Table 14: Mastermix for cDNA Synthesis

Reagent	Stock concentration	Final concentration in 40µl	Volume
10x Buffer II	100mM	20mM	4µl
MgCl ₂	25mM	10mM	8µl
dNTPs	10mM	1mM	2µl
Random Hexamers	50µM	5µM	2µl
RNase-Inhibitor	5 U/µl	0.5 U/µl	1µl
Reverse Transcriptase	50 U/µl	5 U/µl	2µl
H ₂ O			1µl
Final Volume			20µl

4.2.9 Quantitative PCR

Quantitative PCR was conducted using SYBR Green and the LC480 Light Cycler. Gene expression analysis of each sample was run in duplicates using 2.5µl of cDNA and 7.5µl master mix per well. The master mix compounds and reaction conditions are listed below. Hypoxanthine-guaninephosphoriboyltransferase (HPRT) for mouse and human was utilized as a reference gene in all experiments. Relative gene expression was expressed as ΔCt value ($\Delta Ct = [Ct \text{ Hprt}] - [Ct \text{ gene}]$)

of interest]). Relative changes upon treatment are displayed as fold change $\Delta\Delta Ct$ value ($\Delta\Delta Ct = \Delta Ct^{\text{treated}} - \Delta Ct^{\text{control}}$). The primers used are listed above.

Table 15: qPCR Mastermix

Reagent	Stock concentration	Final concentration	Volume
Light Cycler 480 SYBR Green Master Mix	2x	1x	5 μ l
Primer mix	10 μ M each	0.5 μ M	0.5 μ l
H ₂ O			2 μ l
cDNA	5ng/ μ l	12.5ng/ μ l	2.5 μ l
total			10 μ l

Table 16: LC480 Light cycler reaction program

Steps	Repetitions	Temperature	Time
Initial Denaturation	1x	95°C	5 min
Denaturation		95°C	5 sec
Annealing	45x	59°C	5 sec
Elongation		72°C	10 sec
		95°C	5 sec
Melting Curve	1x	60°C	1 min
		60°C-95°C	
Cooling	1x	4°C	on hold

4.2.10 Immunofluorescence

For immunofluorescence analysis 3D-LTCs or 4mm punches were fixed with acetone/methanol for 20 min. The 3D-LTCs were subsequently blocked for nonspecific binding with 5% bovine serum albumin (BSA) diluted in PBS for 1h at room temperature, followed by incubation with the respective primary antibody in PBS comprising 0.1% BSA over night at 4°C. After washing indirect immunofluorescence staining was performed by adding the fluorescently labeled secondary antibody for 1h. To visualize cell nuclei DAPI staining was used. The 3D-LTCs were fixated with 4% formalin for 20 min. After washing the fixated 3D-LTCs were stored at 4°C in PBS containing 0.1% BSA. Imaging through the 300 μ m thick z-axis of the 3D-LTCs was performed using the LSM710 confocal microscope. 3D reconstruction was done with IMARIS x 64.

4.2.11 Immunoblotting

PmAT II cells or pulverized 3D-LTCs were lysed using Tissue Protein Extraction Reagent (T-PER) lysis buffer supplemented with protease and phosphatase inhibitors. The extracted protein was clarified from cell detritus by centrifugation (10 000g at 4°C). Protein concentration was measured by bicinchoninic acid (BCA) protein assay according to the manufacturer's protocol. After denaturation at 95°C for 5min 15 µg of total protein was loaded with 4x Laemmli loading buffer on SDS-polyacrylamide gels, separated by gel electrophoresis and transferred onto polyvinylidene difluoride (PVDF) membranes. The SDS polyacrylamid gel concentration (6%-10%) was adjusted according to the size of the protein to be detected. The membranes were subsequently blocked in 5% nonfat dry milk and incubated with the respective primary antibody at 4°C overnight and for 1 h at room temperature. After washing, the membrane was incubated with the appropriate HRP-linked secondary antibody for 1 hour at room temperature. The protein was visualized using enhanced chemiluminescence and ChemiDoc™ XRS+ system for detection.

4.2.12 Enzyme-linked immunosorbent assay (ELISA)

Supernatants were obtained from pmAT II cells, murine and human 3D-LTCs. Secreted protein concentrations (SP-C, WISP1, IL-6) were assessed by enzyme-linked immunosorbent assay (ELISA) according to the manufacturer's protocol, respectively.

4.2.13 WST-1 based cell toxicity assay

4-mm punches from murine 3D-LTCS were generated and treated as indicated. After 48h each punch was subsequently incubated in 200µl cultivation medium containing 15 µL·mL⁻¹ WST-1 for 2h. The WST-1 reagent is cleaved into a formazan dye by viable cells. After incubation, the punches were removed and the formazan dye formation was quantified using a plate reader at 450nm. For each treatment a minimum of three punches were measured. The samples were all normalized to control containing cultivation medium only.

4.2.14 Fluorescence-activated cell sorting (FACS)

proSPC expression of pmAT II cells was evaluated by flow cytometry. Following cultivation pmAT II were fixed and permeabilized using IntraPrep™ Permeabilization Reagent and subsequently stained with pro-SPC antibody for 15 min at room temperature. After washing, the cell suspension was incubated with secondary antibody Alexa Fluor 488 goat anti-rabbit IgG. After another washing step, the cells were re-suspended in FACS Buffer. The amount of proSPC⁺/EpCAM⁺ cells was analyzed using FACS LSRII cell analyzer (BD Bioscience, USA).

4.2.15 Statistical analysis

All results are presented as mean ± SEM and were analyzed with GraphPad Prism 5 or 8. Statistical significance was determined either by paired Student's t-test or one-sample t-test compared to the theoretical value of 0/1. Differences were regarded to be significant when $P < 0.05$.

5. RESULTS

5.1 Murine *ex-vivo* 3D-Lung Tissue Cultures (3D-LTCs)

5.1.1 Characterization of murine *ex-vivo* 3D-LTCs as fibrosis model

We initially characterized the murine 3D-LTCs as *ex-vivo* fibrosis model by investigating pro-fibrotic gene and protein expression over the culture period of 48h. For this approach we used both 3D-LTCs generated from wild-type mice which were subsequently treated with Transforming Growth Factor- β (TGF- β) *ex-vivo* and fibrotic 3D-LTCs from Bleomycin treated mice.

We first sought to evaluate if TGF- β as single pro-fibrotic stimulus induces sufficient fibrotic changes in 3D-LTCs after 48h. Indeed, fibrotic marker, *Fibronectin 1 (Fn1)* and *Collagen 1 (Col1a1)*, gene expression was significantly upregulated with increased collagen deposition verified by immunofluorescence staining (Figure 8B-C). Similarly, pro-inflammatory marker Interleukin-6 (IL-6) and Wnt-inducible signaling protein 1 (Wisp1) secretion was sufficiently induced by TGF- β *ex-vivo* (Figure 8D).

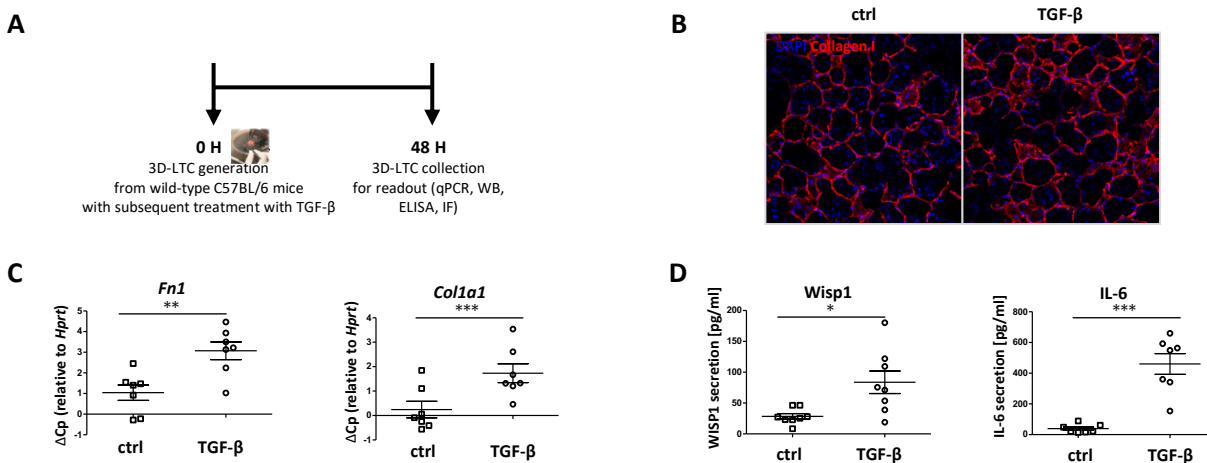


Figure 7: Induction of fibrotic marker expression in *ex-vivo* murine 3D-LTCs upon TGF- β treatment. (A) Treatment scheme of 3D-LTCs with TGF- β or respective control and subsequent downstream analysis. After generation *ex-vivo* murine 3D-LTC were treated with TGF- β and cultivated for 48h. **(B)** Representative immunofluorescence images of 3D-LTCs subjected to TGF- β and respective control stained for Collagen I. **(C)** Fibrotic marker *Fn1* and *Col1a1* gene expression was investigated by qPCR (n=7), paired Student's t-test. **(D)** Wisp1 and IL-6 secretion was determined by ELISA (n = 7), paired Student's t-test. *p < 0.05, **p < 0.01, ***p < 0.001

As a single fibrotic stimulus naturally cannot recapitulate the *in-situ* development of fibrosis we proceeded using fibrotic murine 3D-LTCs. For induction of fibrosis *in-vivo* mice were intratracheally subjected to Bleomycin and sacrificed at day 14 post-installation as the fibrosis is known to be established (Jenkins et al. 2017). Morphological analysis showed maintained fibrotic lung structure of the newly generated 3D-LTCs with increased collagen and myofibroblast marker α -SMA staining (Figure 9B). Simultaneously, E-cadherin (E-Cad), a marker for epithelial cell integrity, was decreased (Figure 9B). We further confirmed that 3D-LTCs maintain their fibrotic phenotype over the culture time with fibrotic marker gene expression, *Fn1* and *Col1a1*, being significantly upregulated compared to PBS control after 48h of culture (Figure 9C). Similarly, collagen secretion, being assessed by Western Blotting, was significantly increased after 48h (Figure 9D). We further observed increased IL-6 and Wisp1 secretion as a sign of ongoing inflammation and activation of pro-fibrotic pathways after 48h of culture (Figure 9E-F). Therefore, major hallmarks of fibrosis such as increased ECM deposition, sustained inflammation and impaired epithelial cell integrity were retained in fibrotic 3D-LTCs proving it to be feasible for assessment of the anti-fibrotic action of Nintedanib and Pirfenidone.

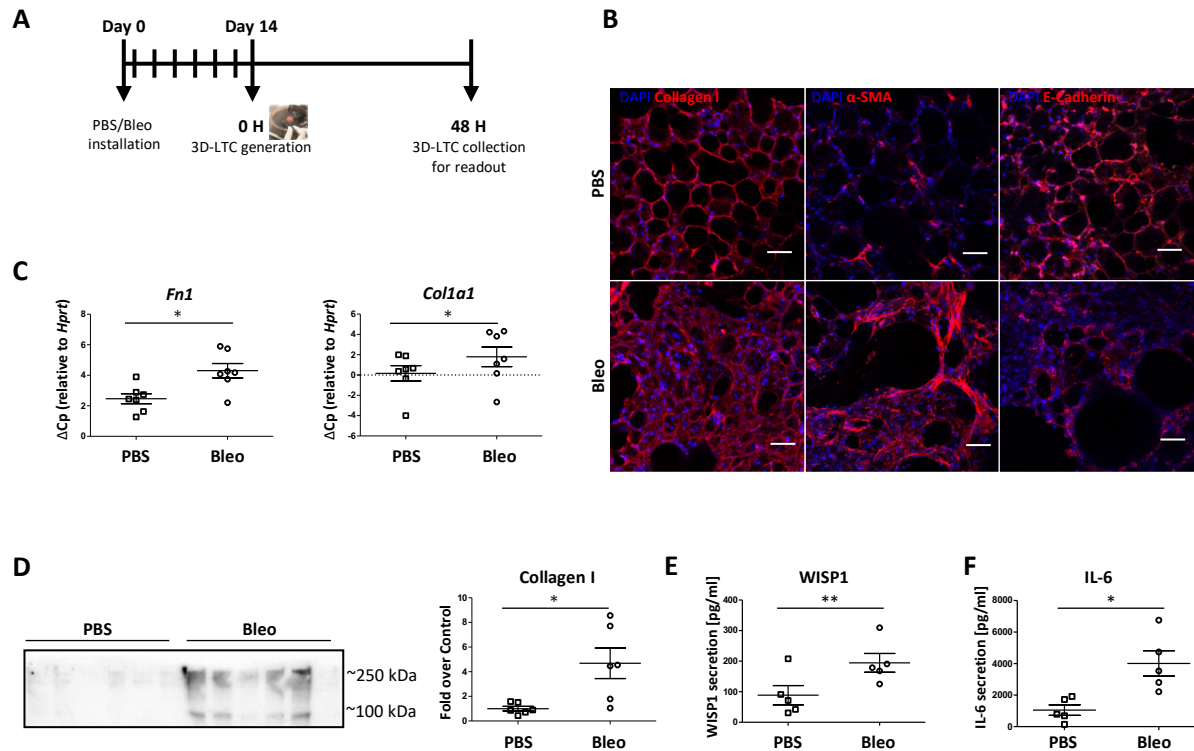


Figure 8: Maintenance of pro-fibrotic phenotype of murine 3D-LTCs during cultivation. (A) Scheme of fibrotic 3D-LTCs generation from Bleomycin treated mice. **(B)** Representative immunofluorescence images of fibrotic 3D-LTCs and PBS control stained for Collagen I, α -SMA and E-Cadherin. **(C)** Fibrotic marker *Fn1* and *Col1a1* gene expression in fibrotic 3D-LTCs and PBS control was investigated by qPCR (n=7), paired Student's t-test. **(D)** Collagen I secretion of fibrotic 3D-LTCs and PBS control was assessed by Western blot (n=6), paired Student's t-test. **(D, E)** WISP1 and IL-6 secretion of fibrotic 3D-LTCs and PBS was measured by ELISA (n= 5), paired Student's t-test. *p < 0.05, **p < 0.01

5.1.2 Nintedanib and Pirfenidone dose-dependently inhibit fibrotic marker expression in murine *ex-vivo* 3D-LTCs

Next, we sought to evaluate whether Nintedanib and Pirfenidone inhibit the pro-fibrotic phenotype in both murine 3D-LTCs subjected to TGF- β 1 *ex-vivo* and fibrotic 3D-LTCs from Bleomycin treated mice. For this purpose, we assessed fibrotic and inflammatory marker gene and protein expression upon drug treatment. Prior to drug treatment we performed WST-1 assay and found the cell proliferation to be reduced upon higher drug concentrations (Nintedanib: 10 μ M; Pirfenidone: 2.5.mM) which led to decision to hereafter precede with the lower, more physiological concentrations for both drugs and that have been used in *in-vitro* studies before (Nintedanib: 0.1 μ M, 1 μ M; Pirfenidone 100 μ M, 500 μ M) (Knuppel et al. 2017) (Figure S1).

Thus, we found TGF- β 1 induced fibrotic marker, *Fn1* and *Col1a1*, gene and protein expression decreased upon Nintedanib and Pirfenidone treatment in a dose dependent manner (Figure 10A-B). Similarly, inflammatory marker IL-6 secretion was inhibited by both Nintedanib and Pirfenidone. Noteworthy, Pirfenidone significantly diminished IL-6 secretion at 100 μ M but not at 500 μ M (Figure 10C).

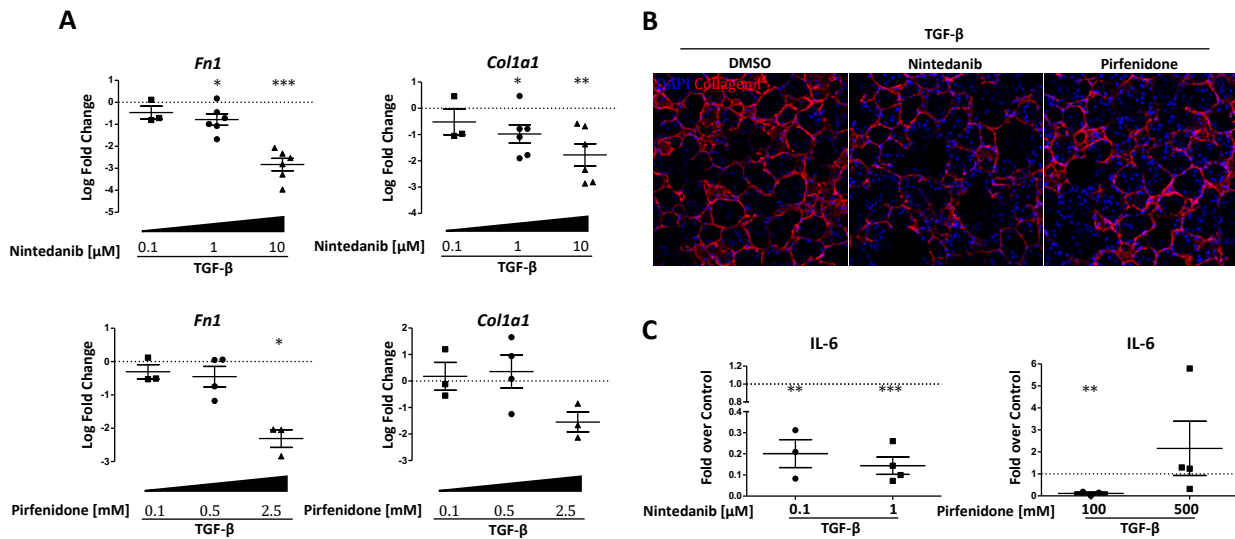


Figure 9: Effect of Nintedanib and Pirfenidone on fibrotic marker expression in TGF- β treated 3D-LTCs. (A) Murine 3D-LTCs were pretreated with Nintedanib and Pirfenidone for 1h. After adding TGF- β the 3D-LTCs were cultured for 48h. Fibrotic marker *Fn1* and *Col1a1* gene expression was investigated by qPCR (n=3-6), one-sample t-test compared to the theoretical value of 0. **(B)** Representative immunofluorescence images of TGF- β treated 3D-LTCs and Nintedanib or Pirfenidone and stained for Collagen I. **(C)** IL-6 secretion was measured by ELISA (n = 5), one-sample t-tests compared to the theoretical value of 1. *p < 0.05, **p < 0.01, ***p < 0.001

We further assessed the effectiveness of Nintedanib and Pirfenidone treatment in already established fibrosis using fibrotic 3D-LTCs derived from Bleomycin treated mice. Consistently, we observed a dose-dependent downregulation of fibrotic marker gene expression by both Nintedanib and Pirfenidone (Figure 11A). We observed a trend of Nintedanib but not for Pirfenidone reducing collagen secretion in fibrotic 3D-LTCs (Figure 11B).

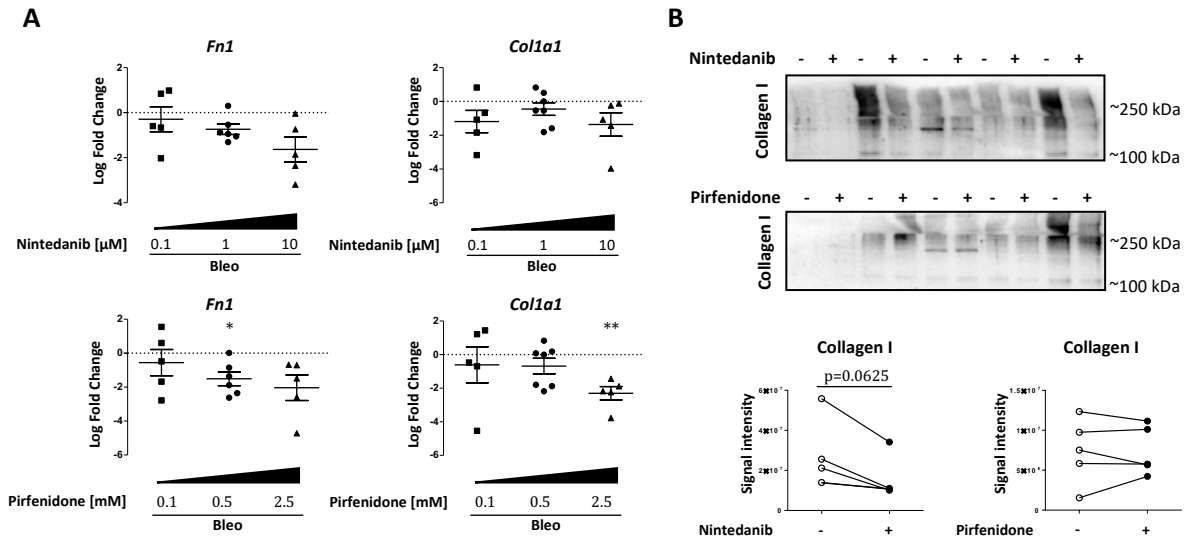


Figure 10: Effect of Nintedanib and Pirfenidone on fibrotic marker expression in fibrotic 3D-LTCs. (A) Fibrotic murine 3D-LTCs were subjected to Nintedanib or Pirfenidone and cultured for 48h. Fibrotic marker *Fn1* and *Col1a1* gene expression was investigated by qPCR (n=5-6), one-sample t-test compared to the theoretical value of 0. **(B)** Collagen I secretion of fibrotic 3D-LTCs subjected to Nintedanib (1 μM) or Pirfenidone (500 μM) was assessed by Western blot (n=4), paired Student's t-test. *p < 0.05, **p < 0.01, ***p < 0.001

5.1.3 Double treatment with Nintedanib and Pirfenidone shows an additive effect in downregulating fibrotic marker expression in fibrotic murine *ex-vivo* 3D-LTCs

Pirfenidone and Nintedanib presumably exert their anti-fibrotic action via different targets indicating that co-treatment might have a synergistic effect, thus improving the overall outcome in IPF patients (Vancheri et al. 2018). For proof of concept, we co-treated fibrotic murine 3D-LTCs with Nintedanib (0.1 μM) and Pirfenidone (100 μM) for 48h. Notably, the double treatment showed an additive effect significantly downregulating *Fn1* gene expression compared to Nintedanib (0.1 μM) and Pirfenidone (100 μM) alone, analyzed by qPCR. A similar trend was observed for *Col1a1* (Figure 12).

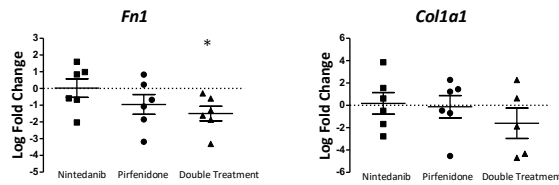


Figure 11: Double treatment with Nintedanib and Pirfenidone in fibrotic 3D-LTCs. Fibrotic murine 3D-LTCs were subjected to Nintedanib (0.1 μ M), Pirfenidone (100 μ M) or double treatment (Nintedanib (0.1 μ M) + Pirfenidone (100 μ M)) for 48h. Fibrotic marker *Fn1* and *Col1a1* gene expression was assessed by qPCR (n=5-6), one-sample t-tests compared to the theoretical value of 0. *p < 0.05

Altogether, the data presented here confirms the findings of previous *in-vivo* investigations of the anti-fibrotic action of Nintedanib and Pirfenidone and proves *ex-vivo* 3D-LTCs to be a suitable tool for preclinical drug testing.

5.1.4 Nintedanib and Pirfenidone differentially affect epithelial cell function in murine *ex-vivo* 3D-LTCs

Impaired epithelium is known to play a crucial role in the pathogenesis of IPF. However, while most studies on the anti-fibrotic action of Nintedanib and Pirfenidone have been performed on fibroblasts, little is known about these drugs affecting epithelial cell function. Therefore, we next evaluated the distinct effect of Nintedanib and Pirfenidone on alveolar epithelial type II cells in TGF- β treated 3D-LTCs. TGF- β 1 is known to induce epithelial cell apoptosis and EMT in fibrosis (Schuster and Kriegelstein 2002, Xu, Lamouille and Derynck 2009). We first analyzed AT II cell marker pro-SPC protein expression by Western Blotting and found it to be decreased upon TGF- β treatment (Figure 13). Notably, we observed a trend of Nintedanib (1 μ M) and Pirfenidone (500 μ M) increasing pro-SPC protein expression in murine 3D-LTCs upon TGF- β 1 treatment (Figure 13).

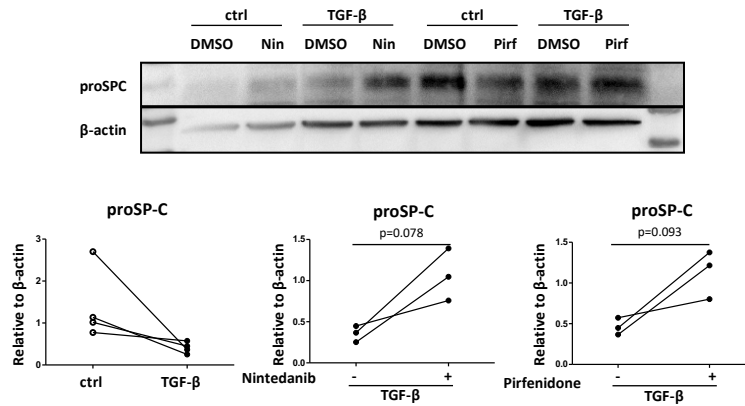


Figure 12: Effect of Nintedanib and Pirfenidone on proSP-C protein expression in TGF-β treated 3D-LTCs. Murine 3D-LTCs were pretreated with Nintedanib (1μM) and Pirfenidone (500μM) for 1h, subsequently subjected to TGF-β and cultured for 48h. Western blot analysis of pro-SPC expression (n=5), paired Student's t-test.

Along with this, Wisp1, a pro-fibrotic mediator mainly secreted by altered epithelium in fibrosis, was significantly inhibited by both Nintedanib and Pirfenidone in 3D-LTCs upon TGF-β1 treatment, as analyzed by ELISA. Nintedanib showed sufficient downregulation at 0.1 μM with no additive effect at 1μM potentially indicating target saturation. Again, Pirfenidone significantly decreased Wisp1 secretion at 100μM, but not at 500μM (Figure 14).

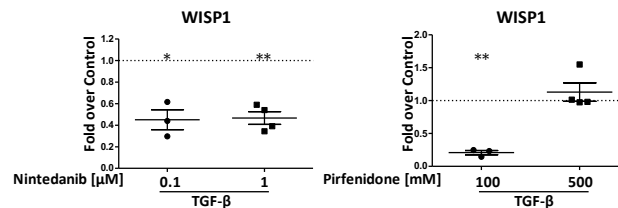


Figure 13: Effect of Nintedanib and Pirfenidone on epithelial cell function in TGF-β1 treated 3D-LTCs. (A, B) Murine 3D-LTCs were pretreated with Nintedanib and Pirfenidone for 1h, subsequently subjected to TGF-β and cultured for 48h. WISP1 secretion was determined by ELISA (n=3-4), one-sample t-test compared to the theoretical value of 1. *p < 0.05, **p < 0.01

We further confirmed our findings using fibrotic murine 3D-LTCs. Consistently, we observed Nintedanib significantly increasing AT II cell marker pro-SPC protein expression and secretion. Notably, Pirfenidone failed to sufficiently induce epithelial cell marker expression in fibrotic 3D-LTCs (Figure 15-16A).

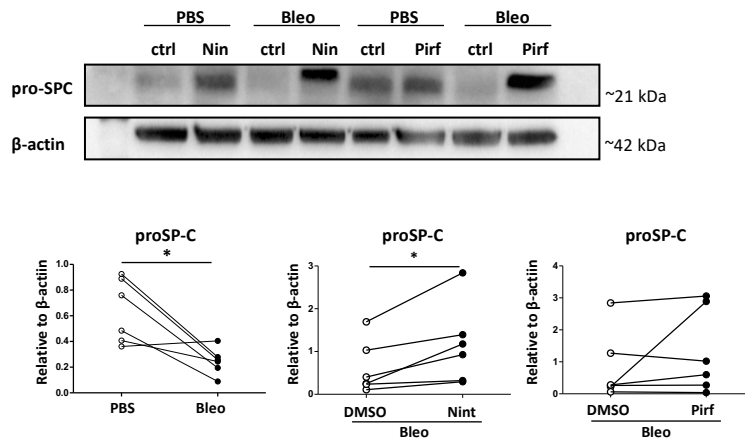


Figure 14: Effect of Nintedanib and Pirfenidone on proSP-C protein expression in fibrotic 3D-LTCs. Fibrotic murine 3D-LTCs were treated with Nintedanib (1 μ M) and Pirfenidone (500 μ M) for 48h. Western blot analysis of pro-SPC expression (n=6), paired Student's t-test. *p < 0.05

Similarly, pro-fibrotic mediator Wisp1 was decreased upon Nintedanib but not Pirfenidone treatment (Figure 16B).

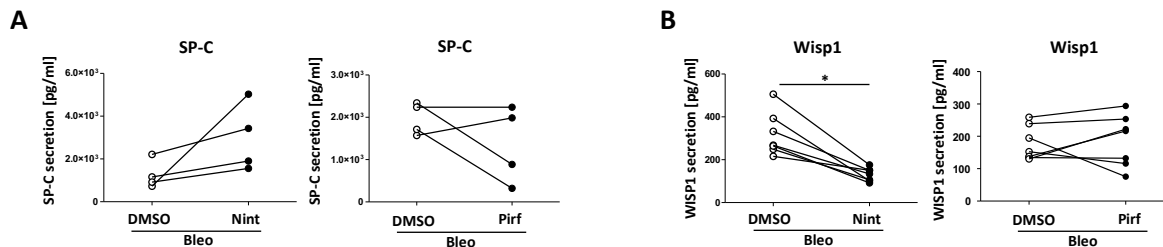


Figure 15: Effect of Nintedanib and Pirfenidone on epithelial cell function in fibrotic 3D-LTCs. Fibrotic murine 3D-LTCs were treated with Nintedanib (1 μ M) and Pirfenidone (500 μ M) for 48h. **(A)** SP-C secretion and **(B)** WISP1 secretion was assessed by ELISA (n=4-6), paired Student's t-test. *p < 0.05

5.2 Primary murine alveolar type II (pmAT II) cell monoculture

5.2.1 Nintedanib and Pirfenidone inhibit fibrotic marker expression in pmAT II cells

Based on our findings in 3D-LTCs we further sought to delineate the effects of Nintedanib and Pirfenidone on epithelial cell function using primary murine alveolar type (pmAT) II cell monoculture. For this approach we utilized both pmAT II cells derived from wild-type mice and subsequently subjected to TGF- β 1 *in-vitro* and fibrotic pmAT II cells from Bleomycin treated mice. The model of cultivating pmAT II cells *in-vitro* itself has been widely used to recapitulate repair processes upon injury with pmAT II cells differentiating to AT I cells during cultivation time (Mutze et al. 2015, Demaio et al. 2009). Alveolar epithelial cells are known to exhibit a pro-fibrotic phenotype upon TGF- β 1 with losing epithelial and subsequently acquiring mesenchymal cell properties (Ding et al. 2017). Thus, we first confirmed fibrotic marker, *Fn1* and *Col1a1*, gene expression levels to be upregulated upon TGF- β 1 stimulation in pmAT II cells after 48h (Figure 17).

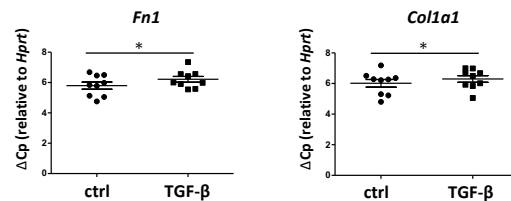


Figure 16: Induction of fibrotic marker expression in pmAT II upon TGF- β treatment. PmAT II were treated with TGF- β for 48h. Fibrotic marker *Fn1* and *Col1a1* gene expression in control and TGF- β treated pmAT II cells (n=9), paired Student's t-test. *p < 0.05

Both Nintedanib (0,1 μ M, 1 μ M) and Pirfenidone (100 μ M, 500 μ M) subsequently decreased TGF- β 1 induced fibrotic marker gene expression (Figure 18A). On protein level Nintedanib, but not Pirfenidone sufficiently reduced collagen I expression (Figure 18B).

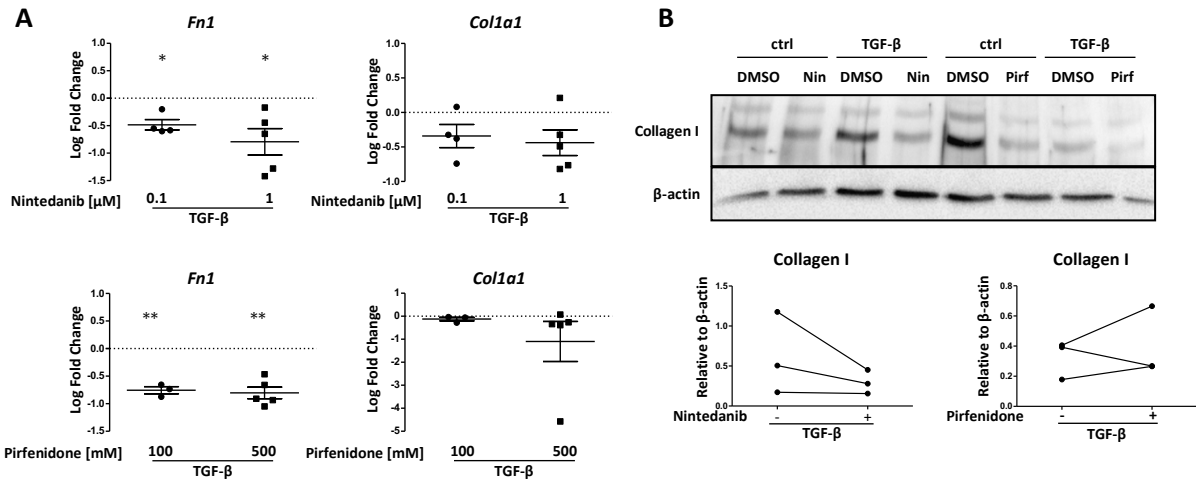


Figure 17: Effect of Nintedanib and Pirfenidone on fibrotic marker expression in TGF- β treated pmAT II cells. (A, B) PmAT II cell were pretreated with Nintedanib (A: 0.1 μ M, 1 μ M; B: 1 μ M) or Pirfenidone (A: 100 μ M, 500 μ M; B: 500 μ M) for 1h, subsequently subjected to TGF- β and cultured for 48h. (A) Fibrotic marker *Fn1* and *Col1a1* gene expression was investigated by qPCR (n=3-5), one-sample t-test compared to the theoretical value of 0. (B) Western blot analysis of collagen I expression (n=3), paired Student's t-test. *p < 0.05, **p < 0.01

Apart from the anti-fibrotic action of Nintedanib and Pirfenidone both drugs significantly decreased pro-inflammatory marker IL-6 secretion in pmAT II cells upon TGF- β treatment. Using two different concentrations for Nintedanib (0.1 μ M, 1 μ M) and Pirfenidone (100 μ M, 500 μ M), we observed a dose dependent effect for Nintedanib. Notably, both Pirfenidone concentrations were similarly efficient attenuating the inflammatory response upon TGF- β treatment (Figure 19).

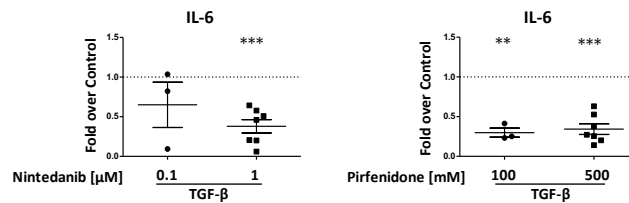


Figure 18: Effect of Nintedanib and Pirfenidone on inflammatory marker IL-6 secretion in TGF- β treated pmAT II cells. PmAT II cell were pretreated with Nintedanib (0.1 μ M, 1 μ M) or Pirfenidone (100 μ M, 500 μ M) for 1h, subsequently subjected to TGF- β and cultured for 48h. IL-6 secretion was determined by ELISA (n=3-7), one-sample t-test compared to the theoretical value of 1. **p < 0.01, ***p < 0.001

We further evaluated our findings using fibrotic pmAT II cells derived from Bleomycin treated mice. We first confirmed pmAT II cells to retain their pro-fibrotic phenotype with increased fibrotic marker, *Fn1* and *Col1a1*, gene expression in culture after 48h (Figure 20).

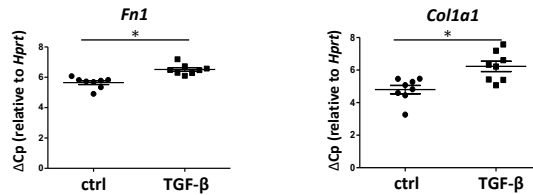


Figure 19: pmAT II derived from Bleomycin treated mice retain their pro-fibrotic phenotype in culture. Fibrotic marker *Fn1* and *Col1a1* gene expression in control and fibrotic pmAT II cells (n=9), paired Student's t-test. **p < 0.01, ***p < 0.001

Nintedanib (1 μ M) and Pirfenidone (500 μ M) subsequently diminished the pro-fibrotic phenotype of pmAT II cells decreasing fibrotic marker *Fn1* and *Col1a1* (Figure 21).

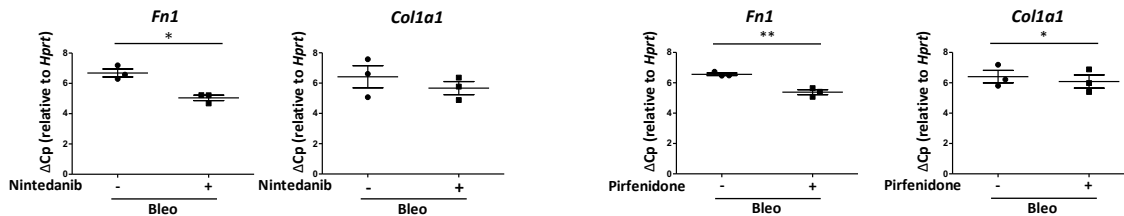


Figure 20: Effect of Nintedanib and Pirfenidone on fibrotic marker expression in fibrotic pmAT II cells. Fibrotic pmAT II cells were treated with Nintedanib (1 μ M) or Pirfenidone (500 μ M) for 48h. Fibrotic marker *Fn1* and *Col1a1* gene expression was assessed by qPCR (n=9), paired Student's t-test. *p < 0.05, **p < 0.01

5.2.2 Nintedanib and Pirfenidone differentially affect epithelial cell marker expression in pmAT II cells

We previously confirmed alveolar epithelial cell function to be affected upon Nintedanib and Pirfenidone treatment in *ex-vivo* 3D-LTCs. To further elucidate, if these drugs directly affect epithelial cell function or this effect is mediated by other cell types, we treated pmAT II cells either with Nintedanib or Pirfenidone upon a fibrotic stimulus and tested for alveolar type II and I cell marker gene expression, *Sftpc* (Surfactant protein C), *Nkx2.1* (NK2 homeobox 1) and *T1 α* (Podoplanin), *Hopx* (Homeodomain only protein X), respectively. We first confirmed *Sftpc* to be

significantly downregulated by TGF- β in pmAT II cells. Notably, AT I cell marker *T1 α* remained unchanged upon TGF- β treatment (Figure 21).

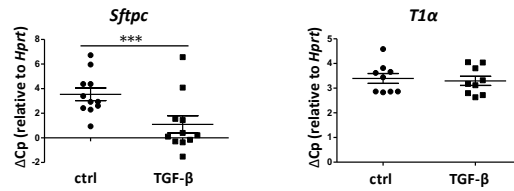


Figure 21: TGF- β treatment affecting epithelial cell marker expression in pmAT II cell monoculture. PmAT II were treated with TGF- β for 48h. Epithelial cell marker *Sftpc* and *T1 α* gene expression was investigated by qPCR (n=9), paired Student's t-test. ***p < 0.001

Nintedanib subsequently increased both AT II cell marker *Sftpc* and AT I cell marker *T1 α* gene expression along with regulatory genes *Nkx2.1* and *Hopx*. Pirfenidone showed a trend for upregulating AT II cell marker *Sftpc* and *Nkx2.1* expression. However, only AT I cell marker *T1 α* gene expression was significantly induced upon Pirfenidone treatment (Figure 22).

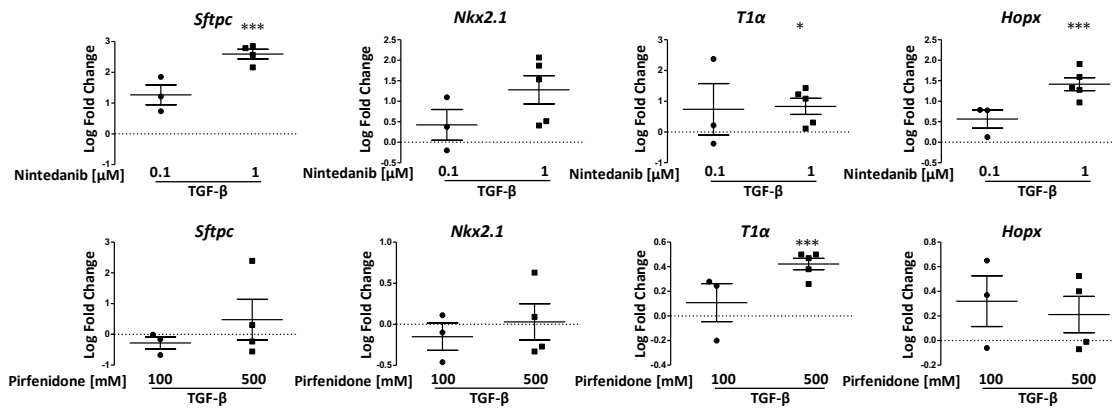


Figure 22: Effect of Nintedanib and Pirfenidone on epithelial cell marker gene expression in TGF- β treated pmAT II cells. PmAT II cell were pretreated with Nintedanib (1 μ M) or Pirfenidone 500 μ M for 1h, subsequently subjected to TGF- β and cultured for 48h. Epithelial cell marker *Sftpc*, *Nkx2.1*, *T1 α* and *Hopx* gene expression was investigated by qPCR (n=3-6), one-sample t-test compared to the theoretical value of 0. *p < 0.05, ***p < 0.001

We next performed fluorescence-activated cell sorting (FACS) analysis for SPC positivity of pmAT II cells subjected to Nintedanib treatment. Noteworthy, overall SPC-positive cells were strongly decreased after four days of cultivation. This is most likely due to profound phenotypic changes as AT II cells both transdifferentiate to AT I cells and acquire a mesenchymal phenotype during

culture subsequently losing AT II cell properties. Nevertheless, we observed a trend of Nintedanib increasing the number of SPC-positive cells compared to control (Figure 23).

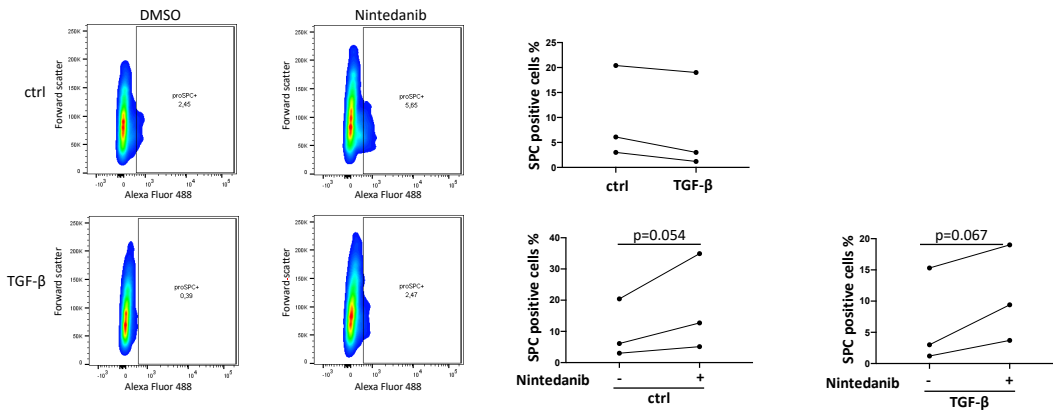


Figure 23: Effect of Nintedanib and Pirfenidone on epithelial cell marker protein expression in TGF- β treated pmAT II cells. PmAT II cells were pretreated with Nintedanib (1 μ M) or Pirfenidone 500 μ M for 1h, subjected to TGF- β and cultured for 48h. PmAT II cells were analyzed for SPC positivity using fluorescence-activated cell sorting (FACS) (n=3), paired Student's t-test.

We further determined the impact of Nintedanib and Pirfenidone on pro-fibrotic mediator Wisp1 mainly secreted by altered epithelium using ELISA and found it to be decreased upon drug treatment (Figure 24).

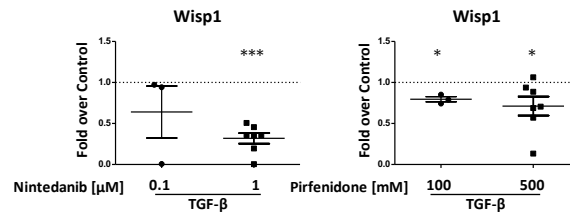


Figure 24: Effect of Nintedanib and Pirfenidone on Wisp1 secretion in TGF- β treated pmAT II cells. PmAT II cells were pretreated with Nintedanib (0,1 μ M, 1 μ M) or Pirfenidone (100 μ M, 500 μ M) for 1h, subjected to TGF- β and cultured for 48h. Wisp1 secretion was investigated by ELISA (n=3-7), one-sample t-tests compared to the theoretical value of 1. *p < 0.05, ***p < 0.001

Further evaluating our findings in pre-injured pmAT II cells we used fibrotic pmAT II cells derived from Bleomycin treated mice. We first verified that the epithelial injury was retained after 48h of culture with decreased *Sftpc* gene expression compared to PBS control. Notably, *T1 α* expression was increased indicating an attempted repair by AT II cells transdifferentiating to AT I cells (Figure 25).

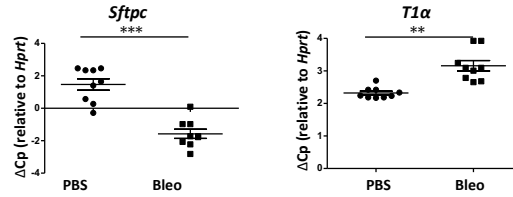


Figure 25: Epithelial cell injury is retained in fibrotic primary murine (pm) AT II cells during culture. Fibrotic pmAT II were cultured for 48h. Epithelial cell marker *Sftpc* and *T1α* gene expression in fibrotic pmAT II cells and PBS control was investigated by qPCR (n=8), paired Student's t-test. **p < 0.01, ***p < 0.001

Similar to our previous findings, Nintedanib significantly increased AT II cell marker *Sftpc* and *Hopx* with a comparable trend for *Nkx2.1* and *T1α*. Pirfenidone solely affected AT I cell marker *T1α* and *Hopx* gene expression (Figure 26). Overall, Nintedanib, but not Pirfenidone restored AT II cell function within the diseased cells.

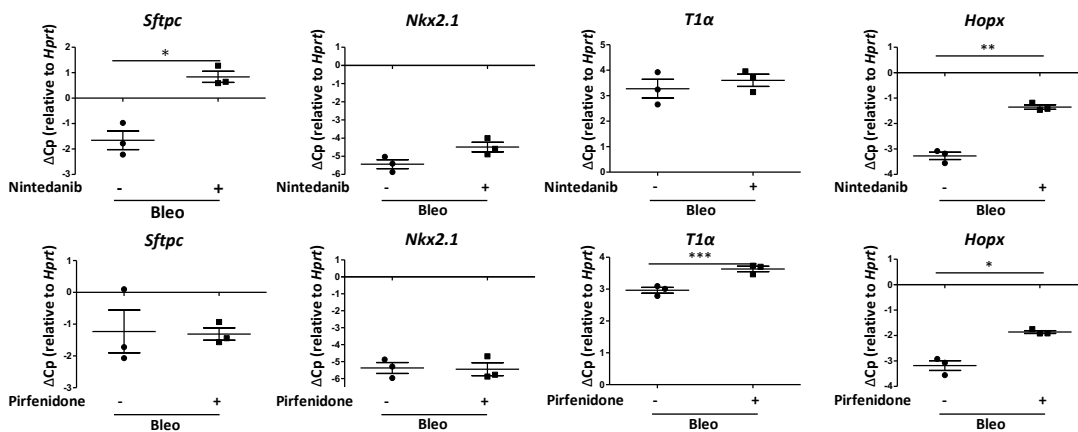


Figure 26: Effect of Nintedanib and Pirfenidone on epithelial cell marker expression in fibrotic pmAT II cells. Fibrotic pmAT II cells were treated with Nintedanib (1μM) or Pirfenidone (500μM) and cultured for 48h. Epithelial cell marker *Sftpc*, *Nkx2.1*, *T1α* and *Hopx* gene expression was investigated by qPCR (n=3), paired Student's t-test. *p < 0.05, **p < 0.01, ***p < 0.001

5.3 Human *ex-vivo* 3D-LTCs

5.3.1 Nintedanib and Pirfenidone don't significantly inhibit fibrotic marker expression in human *ex-vivo* 3D-LTCs

While most studies on the anti-fibrotic action of both Nintedanib and Pirfenidone have been conducted on either isolated cells or in animals, little is known about their actual activity within the intact human system. In this context, human 3D-LTCs represent a valuable tool to mimic the *in-situ* situation as close as possible. Here we used human 3D-LTCs derived from lung cancer resection either treated with TGF- β alone or a fibrotic cocktail consisting of TGF- β , TNF- α , LPA and PDGF α/β .

We first confirmed both *FN1* and *COL1A1* gene and protein expression to be sufficiently upregulated upon TGF- β treatment in the human 3D-LTCs. Interestingly, the increase of fibrotic marker gene expression highly differed between the patient samples suggesting different baseline levels of TGF- β expression (Figure 27).

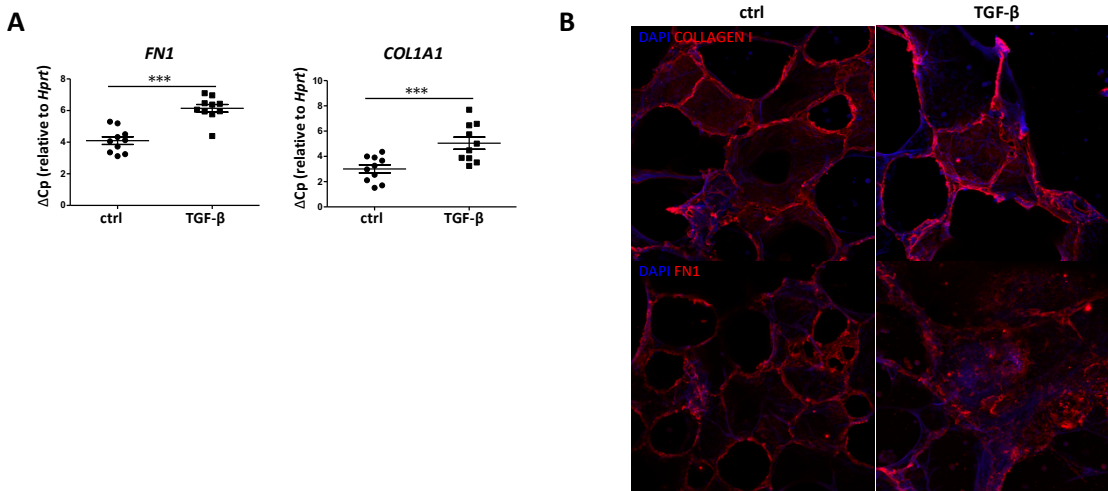


Figure 27: Induction of fibrotic marker expression in *ex-vivo* human 3D-LTCs upon TGF- β treatment. Human 3D-LTCs were subjected to TGF- β for 48h. **(A)** Fibrotic marker *FN1* and *COL1A1* gene expression in human 3D-LTCs treated with TGF- β and respective control was investigated by qPCR (N=9), paired Student's t-test. **(B)** Representative immunofluorescence images of human 3D-LTCs treated with TGF- β and respective control stained with Fibronectin. *** $p < 0.001$

However, neither Nintedanib nor Pirfenidone were able to significantly inhibit the pro-fibrotic marker gene expression following TGF- β treatment. Nintedanib solely showed a trend towards fibrotic gene, *FN1* and *COL1A1*, downregulation (Figure 28).

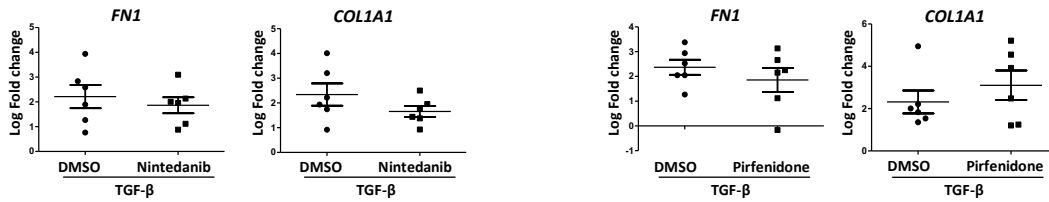


Figure 28: Ex-vivo effect of Nintedanib and Pirfenidone on fibrotic gene expression in TGF- β treated human 3D-LTCs. Human 3D-LTCs were pretreated with Nintedanib (1 μ M) or Pirfenidone (500 μ M) for 1 h, subsequently subjected to TGF- β and cultured for 48h. Fibrotic marker *FN1* and *COL1A1* gene expression was investigated by qPCR (N=5), paired Student's t-test.

In respect of the limited availability of IPF tissue we next used a fibrotic cocktail that has previously been established in our lab mimicking “early fibrotic like” changes in human 3D-LTCs. After the induction of an “early fibrosis like” phenotype within the first 48h of culture we subsequently treated the 3D-LTCs with either Nintedanib (1 μ M) or Pirfenidone (500 μ M) for 72h before harvesting. The detailed treatment scheme is depicted in Figure 29.

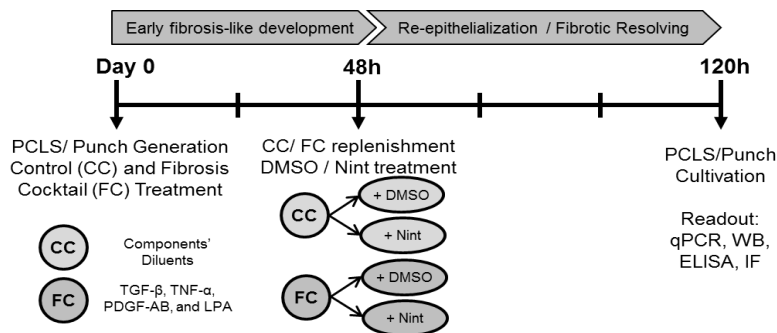


Figure 29: Treatment scheme with fibrotic cocktail (FC) or control cocktail (CC) and Nintedanib (1 μ M) or Pirfenidone (500 μ M) and subsequent downstream analysis. Human 3D-LTCs were subjected to FC or CC. After 48h FC or CC was renewed and Nintedanib or Pirfenidone were added. Human 3D-LTCs were harvested after 120h and downstream analysis was performed.

We first confirmed the early fibrosis like changes after 120 hours of cultivation by fibrotic marker *FN1* and *COL1A1* gene expression analysis and immunofluorescence staining visualizing fibronectin accumulation in the 3D-LTCs. Indeed, we observed a significant increase of *FN1* gene and protein expression upon FC cocktail exposure (Figure 30).

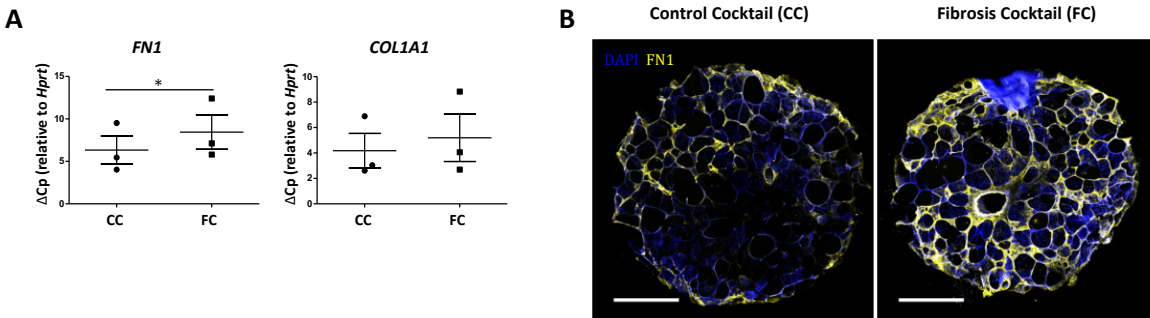


Figure 30: Fibrotic cocktail induces fibrotic marker gene and protein expression in human 3D-LTCs *ex-vivo*. (A) Fibrotic marker *FN1* and *COL1A1* gene expression was investigated by qPCR (N=3), paired Student's t-test. (B) Representative immunofluorescence images of punches subjected to FC and respective control and stained for Fibronectin. Scale bar represents 1mm. *p < 0.05

Subsequent treatment with Nintedanib and Pirfenidone did not significantly decrease *FN1* and *COL1A1* gene expression in FC- treated human 3D-LTCs. However, a trend of Nintedanib and Pirfenidone inhibiting baseline fibrotic marker transcript levels was observed (Figure 31).

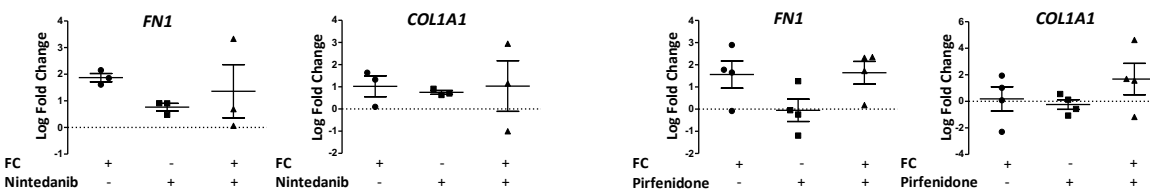


Figure 31: *Ex-vivo* effect of Nintedanib and Pirfenidone on fibrotic cocktail induced “early fibrosis like changes” in human 3D-LTCs. Fibrotic marker *FN1* and *COL1A1* gene expression was investigated by qPCR (N=4), one-sample t-test compared to the theoretical value of 0.

5.3.2 Nintedanib and Pirfenidone differentially influence epithelial cell function in human *ex-vivo* 3D-LTCs upon TGF- β treatment

We next sought to investigate the differential effects of Nintedanib and Pirfenidone on epithelial cell functioning in human 3D-LTCs. We first analyzed transcript levels of epithelial cell marker upon TGF- β treatment in human 3D-LTCs. Notably, TGF- β alone was not able to sufficiently induce epithelial cell injury in human 3D-LTCs (Figure 32).

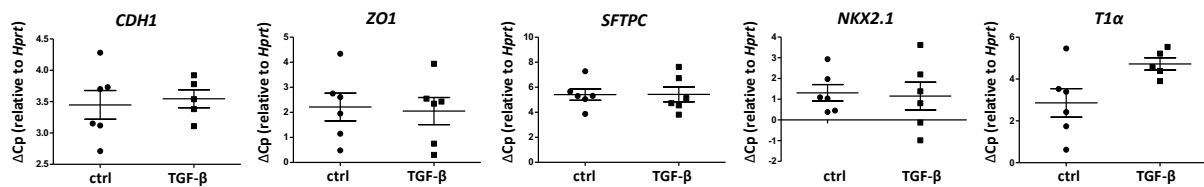


Figure 32: Effect of TGF- β on epithelial cell marker expression in human 3D-LTCs. Human 3D-LTCs were subjected to TGF- β for 48h. Epithelial cell marker *CDH1*, *ZO1*, *SFTPC*, *NKX2.1* and *T1a* gene expression was investigated by qPCR (N=6), paired Student's t-test.

Nintedanib subsequently increased epithelial cell integrity marker *CDH1* and *ZO1* expression upon TGF- β treatment. A similar trend was observed for *SFTPC* and *NKX2.1* gene expression. On protein level pro-SPC secretion was induced by Nintedanib. On the contrary, Pirfenidone neither influence epithelial cell marker gene expression nor pro-SPC secretion in human 3D-LTCs (Figure 32A-B).

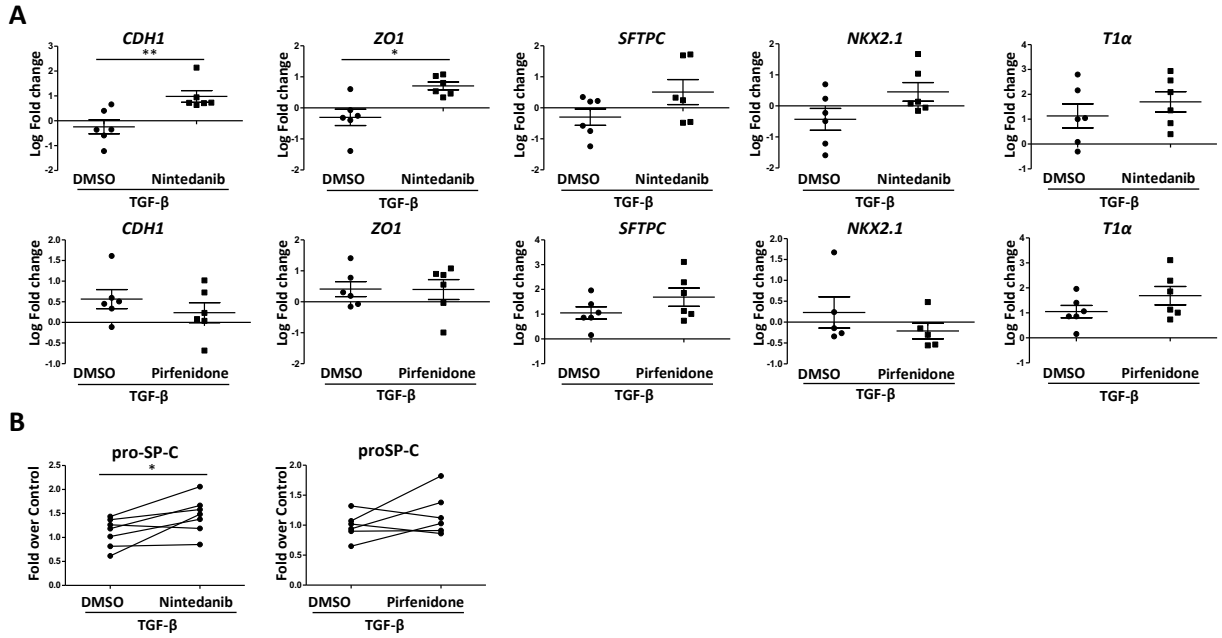


Figure 33: Ex-vivo effect of Nintedanib and Pirfenidone on epithelial cell function in TGF- β treated human 3D-LTCs. Human 3D-LTCs were pretreated with Nintedanib (1 μ M) or Pirfenidone (500 μ M) for 1 h, subsequently subjected to TGF- β and cultured for 48h. **(A)** Epithelial cell marker *CDH1*, *ZO1*, *SFTPC*, *NKX2.1* and *T1 α* gene expression was investigated by qPCR (N=5). **(B)** ProSP-C secretion was determined by ELISA (N=6), paired Student's t-test *p < 0.05, **p < 0.01

5.3.3 Nintedanib and Pirfenidone affecting epithelial cell function in human *ex-vivo* 3D-LTCs subjected to the Fibrotic Cocktail

Because TGF- β solely was insufficient to derange epithelial cell integrity in human 3D-LTCs we next utilized human 3D-LTCs treated with the fibrotic cocktail (FC). Alsafadi et al. previously demonstrated epithelial cell injury to be induced upon the fibrotic cocktail after 120 h of culture (Alsafadi et al. 2017). Similarly, we showed epithelial cell marker gene expression to be reduced upon FC and subsequently observed a trend for both Nintedanib and Pirfenidone to restore epithelial cell marker on transcript level (Figure 27).

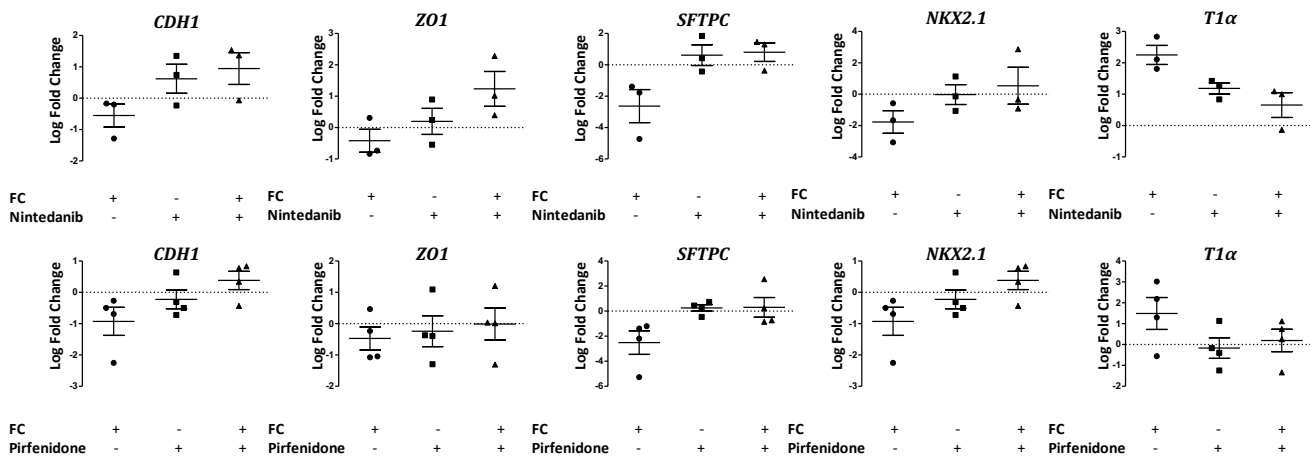


Figure 34: *Ex-vivo* effect of Nintedanib and Pirfenidone on epithelial cell marker gene expression in fibrotic cocktail (FC) treated human 3D-LTCs. Epithelial cell marker *CDH1*, *ZO1*, *SFTPC*, *NKX2.1* and *T1α* gene expression was investigated by qPCR (N=4), one-sample t-test compared to theoretical value of 0.

We further checked for corresponding epithelial cell marker protein expression and found both SPC-secretion in the supernatant and expression as evaluated by immunofluorescence staining increased in human 3D-LTCs upon Nintedanib treatment. Similarly, general alveolar epithelial marker E-Cadherin protein expression was induced (Figure 34).

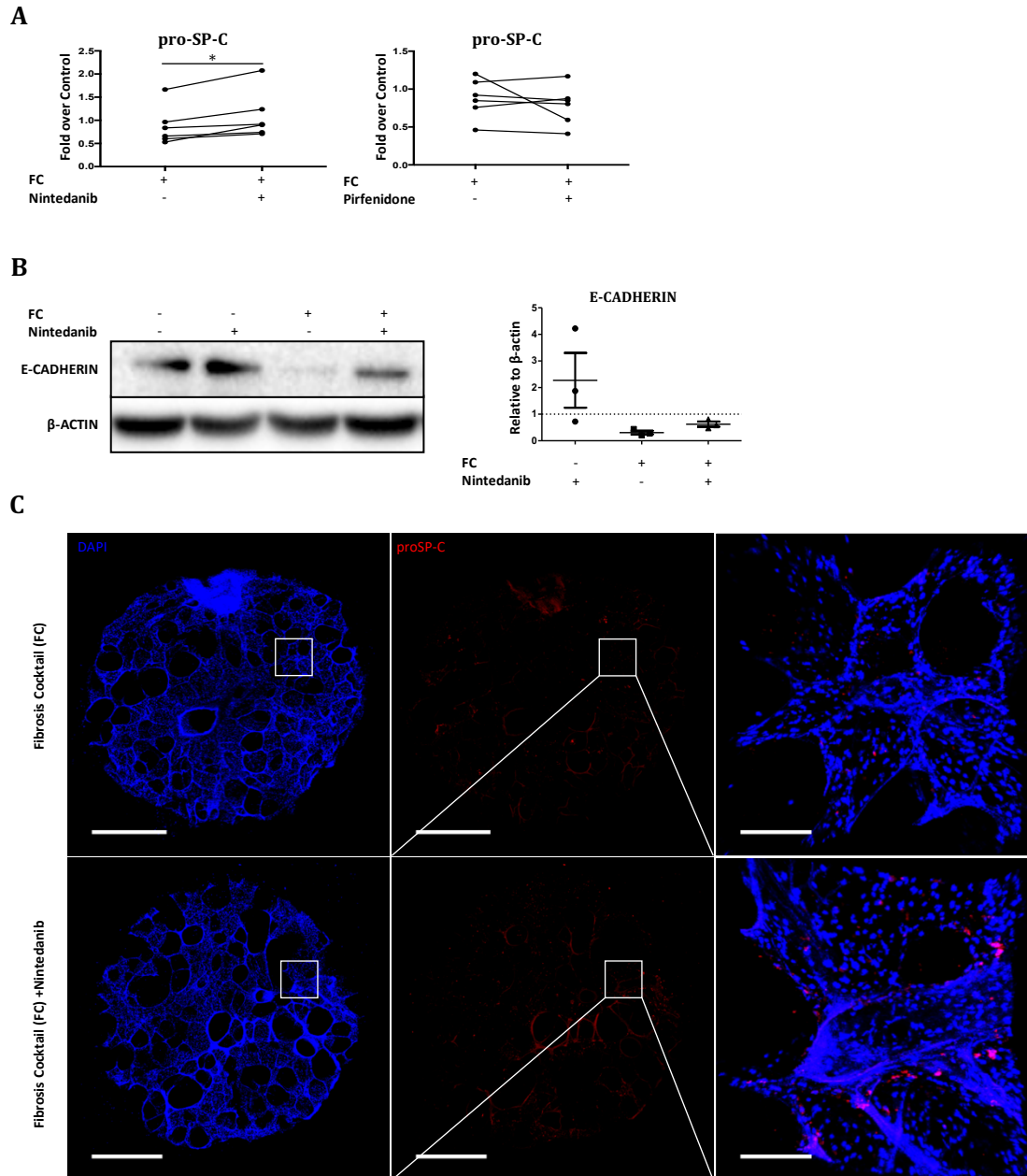


Figure 35: Ex-vivo effect of Nintedanib on epithelial cell marker protein expression in fibrotic cocktail (FC) treated human 3D-LTCs. (A) Pro-SPC secretion was determined by ELISA. (N=6), paired Student's t-test. **(B)** E-CADHERIN protein expression was investigated by Western blot (N=3), one-sample t-test compared to theoretical value of 1. **(C)** Representative immunofluorescence images of pro-SPC of human 3D-LTCs treated with FC and Nintedanib and respective control. Scale bar represents 140 μ m. * $p < 0.05$

6. DISCUSSION

IPF is a fatal interstitial lung disease characterized by unremitting extracellular matrix accumulation which results in the irreversible destruction of the lung architecture and impaired gas exchange in patients. The pathogenesis of IPF is incompletely understood. However, over the past decades the concept of an “epithelial-driven disorder” emerged, in which repetitive epithelial cell injury and genetic predisposition lead to the formation of a dysfunctional epithelial cell phenotype, which then initiates fibroblast activation and ECM accumulation (Selman and Pardo 2020). Nintedanib and Pirfenidone, two recently approved drugs and a major breakthrough in the treatment of IPF, decelerate but not stop disease progression. Therefore, novel therapeutic options for the treatment of IPF are needed. In this process, a better understanding of Nintedanib and Pirfenidone affecting epithelial cell function and how this possibly contribute to the general anti-fibrotic action of these drugs is key and might ultimately reveal new targets for alternative therapeutic approaches. Therefore, the here presented data is of special interest as most mechanistic studies solely focused on how Nintedanib and Pirfenidone potentially affect fibroblast (Wollin et al. 2015, Hostettler et al. 2014, Knuppel et al. 2017), but not epithelial cell function.

In the present study we report that Nintedanib and Pirfenidone differentially affect alveolar epithelial cell function, with Nintedanib significantly inducing alveolar type II cell marker and interfering with the aberrant epithelial-mesenchymal-crosstalk (by reducing WISP1 secretion) in both 3D-LTCs and pmAT II cell monoculture. We demonstrated that Nintedanib and Pirfenidone exert their anti-fibrotic action in murine 3D-LTCs by inhibiting fibrotic and inflammatory marker expression and thus, proving the murine 3D-LTCs to be a valuable tool for testing the mechanism of action of anti-fibrotic drugs. We further demonstrated that Nintedanib affecting epithelial cell function had a more conserved effect than downregulating pro-fibrotic gene expression in human 3D-LTCs.

6.1 The applicability of *ex-vivo* 3D-LTCs for pre-clinical drug testing

At the onset of our study, we aimed to evaluate the *ex-vivo* 3D-LTCs as suitable model for preclinical drug testing in the context of fibrosis. *Ex-vivo* 3D-LTCs show distinct advantages compared to the traditional 2D culture. Cells undergoing cell isolation and being plated on supra-physiological stiff surfaces naturally behave differently than in the *in-vivo* situation which complicates the translation of mechanistic findings *in-vitro* into efficient therapies for patients (Bailey et al. 2018, Uhl et al. 2015). Thus, 90% of all novel compounds fail in clinical trials, most of them in phase II highlighting the need for more accurate preclinical models (Perry and Lawrence 2017). In contrast to *in-vitro* monoculture 3D-LTCs resemble the *in-vivo* situation more closely retaining the cellular and structural complexity including cell-to-cell and cell-to-matrix interactions. Cell viability and function such as ciliary beating was shown to be maintained up to 7 days in culture (Uhl et al. 2015). Additionally, the use of murine 3D-LTCs in particular reduces the overall animal numbers needed for experimentation. However, the complexity of the *in-vivo* situation can still not be fully emulated by *ex-vivo* 3D-LTCs lacking air-liquid-interfaces within the alveoli, the recruitment of immune and progenitor cells via the bloodstream and the cyclic stretch deflection while breathing mechanically stimulating the cells (Uhl 2015, Lehmann et al. 2018, Zscheppang et al. 2018). Additionally, the cutting process along with potential hypoxia in the middle of the slices, are possible stressors altering cellular behavior (Neuhaus et al. 2017). Considering these limitations, animal models for testing compounds within a living organism are still pivotal (Jenkins et al. 2017). Nevertheless, as animal models cannot fully resemble human disease especially the usage of human 3D-LTCs is a unique possibility to perform preclinical drug validation within an intact human microenvironment. However, a major challenge of human tissue remains the inter-individual variability of the samples together with the complexity of the model itself making a proper data interpretation more complicated. Additionally, most human tissue is obtained from lung cancer surgeries and thus, any finding can be potentially altered due to the underlying disease (Zscheppang et al. 2018). Therefore, the acquired data needs to be evaluated in respect of the systems limitations and confirmed by complementary approaches in order to improve result precision and accurately anticipate drug responsiveness in patients (Zscheppang et al. 2018).

Previous studies demonstrated the applicability of human and murine 3D-LTCs for preclinical drug testing investigating the effect of caffeine in murine fibrotic 3D-LTCs and PI3 kinase/mTOR inhibitor in human IPF 3D-LTCs (Tatler et al. 2016, Mercer et al. 2016). Especially, fibrotic 3D-LTCs derived from Bleomycin treated mice represent a suitable tool for *ex-vivo* drug testing in already established fibrosis. Tatler et al. showed that 3D-LTCs obtained from Bleomycin treated mice retain their fibrotic properties over the culture time of 5 days (Tatler et al. 2016). Similar to these findings, we observed both mesenchymal and inflammatory marker to be increased after 48h of culture in fibrotic 3D-LTCs. Within 7 days of culture, we found extracellular matrix compounds, *Fn1* and *Col1a1*, even more elevated indicating that fibroblasts remain viable and continue to deposit extracellular matrix proteins in culture. On the contrary alveolar type II cell marker *Sftpc* was decreased suggesting the epithelial injury upon bleomycin treatment was retained during culture. Along with this, *Wisp1*, a WNT-target gene and pro-fibrotic mediator mainly secreted by altered epithelium (Konigshoff et al. 2009), was upregulated, thus proving epithelial functioning with recapitulation of developmental pathways to be still impaired in culture. Overall, it can be assumed, that pre-injured 3D-LTCs not only continue to exhibit pro-fibrotic hallmarks during culture, but the culture itself induces pro-fibrotic changes. In fact, prolonged culture of precision cut liver slices was proposed as a model of early fibrosis with increased ECM deposition (Westra et al. 2014). However, these pro-fibrotic changes also limit cell functionality and viability of 3D-LTCs in culture and therefore restrict overall culture duration (Uhl et al. 2015, Umachandran, Howarth and Ioannides 2004). Interestingly, Bailey et al. demonstrated murine 3D-LTCs to remain viable for at least 21 days after being encapsulated in hydrogel and replenished with cell-adhesive components, thus supporting the longevity of epithelial cells while inhibiting fibroblast overgrowth in culture (Bailey et al. 2020). Indeed, it supports the notion that the alveolar epithelium is crucial to sustain tissue homeostasis *in-situ* and *ex-vivo*.

For a more mechanistic approach we additionally sought to investigate the distinct anti-fibrotic action of Nintedanib and Pirfenidone on TGF- β as a single pro-fibrotic stimulus in *ex-vivo* 3D-LTCs. For this purpose, we first evaluated the impact of TGF- β 1 on murine and human *ex-vivo* 3D-LTCs. TGF- β 1 is known to be a main driver of fibrosis development secreted by alveolar epithelial cells and fibroblasts (Fernandez and Eickelberg 2012a). We found mesenchymal marker to be

significantly increased upon TGF- β 1 in both human and murine 3D-LTCs. Similarly, alveolar type II cell marker SP-C was decreased with TGF- β inducing epithelial cell apoptosis and epithelial-mesenchymal-transition (EMT) (Ding et al. 2017) in 3D-LTCs *ex-vivo*. Notably, we observed a high expression variability of pro-fibrotic genes, such as *FN1* and *COL1A1*, on baseline and after TGF- β 1 induction between each patient sample. It again highlights the great inter-individual differences that need to be taken into account.

TGF- β as a single fibrotic stimulus cannot induce profound structural changes in *ex-vivo* 3D-LTCs as highlighted by immunofluorescence staining. Therefore, also in respect of the limited availability of IPF tissue we further used a model for “early fibrosis like changes” in human *ex-vivo* 3D-LTCs that was previously established in our lab. Alsafadi et al. showed pro-fibrotic and inflammatory mediators to be upregulated along with enhanced ECM deposition and alveolar epithelial cell injury upon a fibrotic cocktail (FC) treatment comprising TGF- β , TNF- α , LPA and PDGF α/β (Alsafadi et al. 2017). However, myofibroblast marker α -SMA was not sufficiently increased indicating that fibroblast to myofibroblast transdifferentiation, a major hallmark of IPF pathogenesis, was not induced by fibrotic cocktail treatment *ex-vivo*. The authors proposed the lack of profound ECM remodeling with increased matrix stiffening in the non-ILD tissue to be the reason for the insufficient myofibroblast differentiation. Indeed, TGF- β induced (myo-) fibroblast activation was shown to be highly dependable on matrix stiffness (Marinković, Liu and Tschumperlin 2013). Interestingly, we similarly observed in fibrotic murine 3D-LTCs α -SMA protein expression to be still retained when the difference on gene expression level was already diminished. This might be indicative for an insufficient fibroblast to myofibroblast transdifferentiation in *ex-vivo* 3D-LTCs independent of matrix stiffness. However, further investigations are needed to support this notion.

Taken together both murine and human fibrotic 3D-LTCs recapitulate certain characteristics of fibrosis such as the upregulation of pro-inflammatory and pro-fibrotic cytokines, prolonged alveolar epithelial cell injury along with impaired epithelial-mesenchymal crosstalk and increased extracellular matrix deposition in culture. However, the two systems mimic an acute state of the disease. Bleomycin induced lung fibrosis in mice, in particular, was shown to be partially

reversible within weeks (Moeller et al. 2008). In fact, developing IPF as a patient is a process of decades with innumerable co-activated pathways and interactions leading to the irreversible destruction of the lung architecture. Therefore, both models naturally fail to fully recapitulate the complexity of disease pathogenesis in patients. Nevertheless, taken these limitations into account, both murine and human fibrotic 3D-LTCs can be valuable complementary approach in pre-clinical drug testing.

6.2 Investigating the effect of Nintedanib and Pirfenidone on pro-fibrotic marker expression in murine and human *ex-vivo* 3D-LTCs

6.2.1 Nintedanib and Pirfenidone inhibit fibrotic marker expression in murine *ex-vivo* 3D-LTCs

In-vitro monoculture was previously used to single out the distinct impact of Nintedanib and Pirfenidone on diseased lung fibroblasts as main contributor of excessive ECM deposition (Conte et al. 2014, Knuppel et al. 2017, Lehtonen et al. 2016, Nakayama et al. 2008, Wollin et al. 2015). However, a recent study showed only little concordance when comparing gene expression profiles of lung fibroblasts derived from Pirfenidone treated individuals with IPF fibroblasts treated with Pirfenidone *in-vitro* (Kwapiszewska et al. 2018). This fact highlights the complexity of the anti-fibrotic action of both Nintedanib and Pirfenidone *in-situ* and the need of more accurate models to resemble the *in-vivo* setting. In this context, 3D-LTCs retaining much of the cellular and structural complexity of the lung tissue can be of special interest. Here we report that Nintedanib and Pirfenidone reduce pro-fibrotic marker gene expression both upon TGF- β 1 treatment and in fibrotic murine 3D-LTCs in a dose dependent manner. Additionally, both drugs inhibited inflammatory marker IL-6 secretion and functional collagen secretion in murine 3D-LTCs. Notably, we observed Nintedanib in therapeutically relevant concentrations (0.1 μ M, 1 μ M) to be more effective in decreasing pro-fibrotic marker gene expression and secretion compared to Pirfenidone. In fact, Pirfenidone exerted significant anti-fibrotic effects at 2.5mM. This effect is presumably related to cell toxicity of the DMSO solvent or Pirfenidone itself with decreasing cell proliferation. Moreover, Pirfenidone concentration of 2.5mM is much higher than the plasma concentration of Pirfenidone achieved in IPF patients after therapeutic dosing (Wollin 2015).

Similar observations have been made by Knüppel et al. with Nintedanib being more effective in downregulating pro-fibrotic marker expression in IPF fibroblasts (Knüppel et al. 2017). Interestingly, despite of these *in-vitro* findings both Nintedanib and Pirfenidone show a similar efficacy in the real-life treatment of IPF patients although much higher therapeutic dosing is required for Pirfenidone (Bargagli et al. 2018, Cottin 2017). This discrepancy of clinical effectiveness and experimental results might be due to methodic limitations of both *in-vitro* and *ex-vivo* cell culture and/or the selection of readouts and time points of analysis. For instance, Pirfenidone is partly degraded into its metabolites *in-situ* which were also shown to exhibit an anti-fibrotic activity (Togami et al. 2013). Moreover, Pirfenidone treatment in IPF patients was demonstrated to induce profound alterations in inflammatory processes (Kwapiszewska et al. 2018). However, the potential impact of Pirfenidone metabolites and on circulating immune cells that are known to contribute to fibrogenesis (Fernandez et al. 2016) cannot be fully recapitulated using fibroblast monoculture or *ex-vivo* 3D-LTCs. This underlines again the intricate anti-fibrotic action of Nintedanib and Pirfenidone *in-situ* and might explain the differences of the actual clinical effectiveness of both drugs and our results.

6.2.2 Double treatment with Nintedanib and Pirfenidone show a synergistic effect in downregulating pro-fibrotic marker expression in murine *ex-vivo* 3D-LTCs

Despite Nintedanib and Pirfenidone decelerating disease progression, IPF continues to progress. Therefore, novel therapeutic options are needed. Pirfenidone and Nintedanib differentiate in their molecular structure and mode of action suggesting that concomitant treatment might show additive effects. Recent trials already showed side-effects of co-treatment being tolerable in IPF patients (Ogura et al. 2015). Vancheri et al. observed the co- treatment to be superior compared to Nintedanib alone regarding the reduced decline of FVC after 12 weeks observation (Vancheri et al. 2018a). However, further clinical trials must be awaited. As proof of concept, we co-treated fibrotic murine 3D-LTCs with both low concentration of Nintedanib and Pirfenidone and found an additive effect in decreasing mesenchymal gene expression *ex-vivo*. With our findings recapitulating the *in-situ* findings we further confirmed the feasibility of 3D-LTCs for *ex-vivo* drug testing.

6.2.3 The anti-fibrotic action of Nintedanib and Pirfenidone in human *ex-vivo* 3D-LTCs

Human 3D-LTCs represent a unique possibility for *ex-vivo* preclinical drug testing within an intact human microenvironment. Thus, investigating the anti-fibrotic impact of Nintedanib and Pirfenidone in human 3D-LTCs, in particular, can be of special interest. For this approach we used human 3D-LTCs from lung cancer resections either treated with TGF- β alone or a fibrotic cocktail in the presence of Nintedanib or Pirfenidone. Interestingly, both Nintedanib and Pirfenidone did not sufficiently downregulate pro-fibrotic marker expression in human 3D-LTCs upon a fibrotic stimulus (TGF- β and FC). This might be due the heterogeneity of the utilized human material, for instance due to genetic polymorphism and the potential impact of the underlying disease. In this regard, further evaluation with more replicates and a detailed characterization of the clinical cohort is needed.

Our results might also reflect the great heterogeneity within the IPF patient collective regarding course of disease and drug efficacy that need to be addressed in both daily clinical practice and basic science (Ley, Collard and King 2011, Selman et al. 2007). Therefore, the identification of distinct subgroups cannot only help to predict drug responsiveness but allow a more personalized therapy (Magnini et al. 2017). In this context, *ex-vivo* preclinical models can possibly help to distinguish between the different disease endotypes according to their molecular characteristics and may predict *in-situ* drug efficacy. For instance, 3D pulmospheres generated from IPF lung tissue biopsies have already been utilized as a multicellular model to evaluate the anti-fibrotic drug responsiveness in patients *ex-vivo*. In fact, Surolia et al. were able to show that the generated 3D pulmospheres treated with either Nintedanib or Pirfenidone *ex-vivo* reflected how well a patient responded to anti-fibrotic therapy *in-situ* (Surolia et al. 2017). However, the multi-step process necessary to form 3D pulmospheres with the ECM being digested can induce profound cellular alterations. In this regard, 3D-LTCs punches directly generated from lung biopsies can be a possible alternative approach to predict drug efficacy *ex-vivo*. However, a detailed characterization of the system will be necessary to identify suitable marker for treatment response.

6.3 Differential effects of Nintedanib and Pirfenidone on epithelial cell phenotype and function in pmAT II cell culture and *ex-vivo* 3D-LTCs

IPF disease is driven by impaired epithelium secreting a plethora of pro-fibrotic cytokines which initiates fibroblast activation and extracellular matrix accumulation and a vicious cycle of impaired epithelial-mesenchymal crosstalk starts thereof. Hence, targeting the abnormal alveolar epithelium in fibrosis can be a considerable therapeutic option (Königshoff and Bonniaud 2014). However, the question in which way the epithelium should be targeted can be raised as both proliferation of hyperplastic alveolar epithelium and apoptosis/cellular senescence have been demonstrated to contribute to fibrosis (Uhal 2003, Königshoff and Bonniaud 2014, Lehmann et al. 2017). Subsequent inhibition of alveolar epithelial cell proliferation via a deoxycytidine kinase (DCK) inhibitor as well as depletion of senescent alveolar epithelial cells showed favorable effects in the treatment of experimental fibrosis (Weng et al. 2014, Lehmann et al. 2017). In this context it can be of particular interest, if Nintedanib and Pirfenidone, the two approved drugs in the treatment of IPF, affect alveolar epithelial cell function in a favorable way. Furthermore, the delineation of the exact mode of action can possibly help to identify novel therapeutic targets. Yet, up to date little is known about Nintedanib and Pirfenidone affecting not only fibroblast but also epithelial cell function. Kamio et al. reported Surfactant protein D (SP-D) expression in human alveolar epithelial cells to be induced upon Nintedanib treatment via the c-Jun N-terminal kinase-activator protein-1 pathway (Kamio et al. 2015). SP-D has been previously linked to mortality predictions in IPF patients and was, therefore, used as biomarker for increased lung injury in the disease (Barlo et al. 2009). However, these findings can be a matter of debate as they used supraphysiological concentrations of Nintedanib (3-5 μ M) while Nintedanib plasma levels are around 70nM when treating patients with the standard dose (150mg twice a day). Therefore any observations using these high concentrations might be without clinical relevance (Wollin 2015). In the case of Pirfenidone it can be similarly reasoned with any concentration above 100 μ M being not relevant in the clinical setting. Here we argue as we use concentrations slightly exceeding the plasma concentrations of patients that these might still recapitulate the concentration found in the lung with the compound accumulating in the

tissue. Moreover, the drug availability in 3D-LTCs might differ from the pharmacokinetics within as living organism due to altered cell metabolism and drug distribution. Nevertheless, it cannot be excluded that using concentrations exceeding the *in-situ* plasma levels in patients and the direct exposure of cells results in further off target effects.

6.3.1 Nintedanib and Pirfenidone inhibit TGF- β induced EMT in alveolar epithelial cells

EMT plays a crucial role in early life during lung development and later in the pathogenesis of cancer metastasis and chronic lung diseases (Jolly et al. 2018). However, EMT as potential myofibroblast source in IPF pathogenesis remains controversial (Fernandez and Eickelberg 2012b, Wolters, Collard and Jones 2014, Rock et al. 2011). Recent fate mapping studies in mice showed alveolar epithelial cells to express mesenchymal marker upon TGF- β or Bleomycin treatment (Kim et al. 2006, Tanjore et al. 2009). Willis et al. similarly demonstrated cellular subpopulations expressing both mesenchymal and epithelial cell markers in IPF tissue (Willis et al. 2005). However, the detection of this hybrid cell phenotype doesn't necessarily implicate a complete epithelial cell into myofibroblast transdifferentiation (Jolly et al. 2018). Nevertheless, these cells can promote fibrogenesis by secreting multiple pro-fibrotic factors without directly contributing to the myofibroblast population (Lovisa, Zeisberg and Kalluri 2016, Hill et al. 2019). Initially, EMT is part of a physiological repair process occurring in response to injury. After injury, adjacent epithelial cells and subsequently progenitor cells spread and migrate to reestablish the disrupted epithelial layer upon the secretion of a plethora of growth factors and cytokines (Crosby and Waters 2010). In this process these cells partially undergo phenotypic changes including EMT. It is characterized by the loss of E-cadherin mediated cell-cell contact and apical-basal polarity and the simultaneous gain of mesenchymal markers leading to the formation of a reversible hybrid epithelial-mesenchymal cell phenotype (Jolly et al. 2015). EMT can be triggered by multiple growth factors/cytokines including TGF- β and Wnt-signaling and cellular stress responses, such as ER stress and unfolded protein response (UPR) (Jolly et al. 2018, Yu et al. 2008). However, the perpetuation of EMT-initiating signals causes an aberrant repair process resulting in ECM accumulation, ultimately leading to organ fibrosis (Salton, Volpe and Confalonieri 2019). Recent studies reported that both Nintedanib and Pirfenidone suppress TGF-

β induced epithelial to mesenchymal transition (EMT) in cancer cell lines with Nintedanib upregulating E-cadherin expression (Fujiwara et al. 2017, Huang et al. 2015, Kurimoto et al. 2017). Along with this, we show the inhibition of fibrotic marker, *Fn1* and *Col1a1*, by Nintedanib and Pirfenidone in pmAT II cells after TGF- β treatment. However, *E-cadherin* was not reconstituted on gene expression level (data not shown). Interestingly, we observed *E-cadherin* and *Zo1* expression to be increased upon Nintedanib treatment in human 3D-LTCs. It highlights again the differences of results dependent on the selected read-out and demonstrates the potential impact of retained microenvironment and/or particular human epithelial cell properties that might play a role in restoring epithelial cell integrity.

6.3.2 Nintedanib and Pirfenidone differentially affect alveolar epithelial cell phenotype

It is well accepted that alveolar type II (AT II) cells serve as progenitor cells during lung homeostasis and injury reconstituting the intact barrier by differentiating to ATI cells (Selman and Pardo 2006). In fibrosis the renewal capacity of AT II cells is impaired. Recent studies demonstrated that disturbed regeneration of the epithelium led to severe fibrosis and increased mortality in the bleomycin mouse model (Liang et al. 2016, Richeldi, Collard and Jones 2017). Moreover, the targeted damage of AT II cells subsequently leading to apoptosis resulted in the devolvement of fibrosis in mice highlighting the importance of epithelial cells retaining lung homeostasis (Sisson et al. 2010). However, not only alveolar epithelial cell apoptosis, but induction of p53-dependent cellular senescence in AT II cells was demonstrated to lead to lung fibrosis (Yao et al. 2019). Therefore both epithelial cell apoptosis and cellular senescence upon injury and subsequent hyperplasia contribute to disease perpetuation making it to promising therapeutic targets (Königshoff and Bonniaud 2014). In this context a more in depth understanding of how Nintedanib and Pirfenidone might affect epithelial cells, may lead to novel therapeutic approaches directly targeting alveolar epithelial cells in IPF. Here we show that AT II cell marker Surfactant protein C expression was both downregulated in pmAT II cells and 3D-LTCs upon injury. This can be either due to increased apoptosis of AT II cells or decreased Surfactant protein C expression as AT II cells loose epithelial cell properties undergoing EMT. Interestingly,

AT I cell marker *T1α* expression was upregulated in fibrotic pmAT II possibly indicating an attempted repair mechanism by AT II cells differentiating into AT I cells. Nintedanib, but not Pirfenidone treatment subsequently restored proSP-C protein expression and secretion in murine and human 3D-LTCs. Observing similar effects in pmAT II monoculture it can be argued that the upregulation of pmAT II cell marker is conveyed by a direct impact of Nintedanib on epithelial cells and not as a result of cell-cell interactions. For more mechanistic insights we checked for *Nkx2.1*, a transcription factor pivotal for AT II differentiation and lung morphogenesis (Liebler et al. 2016), and found it to be upregulated by Nintedanib suggesting that pro-SPC expression is partly mediated via *Nkx2.1*. Interestingly, both AT I marker *T1α* and *Hopx* are upregulated upon Nintedanib and Pirfenidone indicating induced increased AT I cell formation. This might be indicative for Nintedanib inducing physiological repair mechanisms in the lung with AT II differentiating to AT I cells. In fact, *Hopx*, which is proposed to be marker for the regenerative capacity of epithelial cells (Ota et al. 2018), is downregulated in fibrotic pmAT II cells after 5 days in culture with epithelial cells losing their ability for renewal and subsequently increased upon Nintedanib and Pirfenidone suggesting that the treatment might be beneficial for restoring the regenerative potential in epithelial cells. However, neither Nintedanib nor Pirfenidone were capable of upregulating *Hopx* in the human 3D-LTCs upon the fibrotic cocktail. Further insights using human alveolar epithelial type II cells could be of benefit in this regard.

We report here that Nintedanib significantly induced the AT II cell marker *Sftpc* (SFTPC) expression in both pmAT II monoculture and murine and human 3D-LTCs whereas Pirfenidone had no such effect. However, whether the AT II cell marker induction represents an increase in the total number of functional viable epithelial cells or the already existing epithelial cells express more Surfactant Protein C needs to be further evaluated.

6.3.3 Nintedanib and Pirfenidone interfere with an aberrant epithelial-mesenchymal-crosstalk by decreasing *Wisp1* secretion

Due to the repetitive injury in fibrosis the epithelial phenotype and function is altered leading to apoptosis and hyperplasia with increased proliferate capacity, recapitulation of developmental

and pro-fibrotic pathways (Richeldi et al. 2017, Königshoff et al. 2009). It is well accepted that canonical WNT/ β -catenin signaling is increased in a variety of cell types in IPF (Baarsma and Königshoff 2017). Königshoff et al. demonstrated the canonical ligand Wnt1 to be largely enriched in both hyperplastic AT II cells and bronchial epithelium with β -catenin and Gsk-3 β being localized to the nucleus (Königshoff et al. 2008). Moreover, targeting Wisp1, a potent inducer of epithelial cell proliferation and EMT *in-vitro*, with neutralizing antibodies led to the attenuation of Bleomycin induced lung fibrosis *in-vivo* proving genes regulated by WNT signaling to be promising therapeutic targets (Königshoff et al. 2009). In order to investigate if Nintedanib and Pirfenidone affect WNT target expression, we analyzed Wisp1 secretion in murine 3D-LTCs and found it to be downregulated leading to the assumption that both drugs partly interfere with the impaired epithelial-mesenchymal-crosstalk in fibrosis *via* Wisp1. As Wisp1 is predominately expressed by AT II cells, we continued by treating pmAT II cells with Nintedanib and Pirfenidone upon TGF- β stimulation. Notably, we observed Wisp1 being induced by TGF- β in pmAT II cells which has been previously described in primary human fibroblasts (Berschneider et al. 2014, Klee et al. 2016). We found Wisp1 secretion to be downregulated by Nintedanib and Pirfenidone in pmAT II cells suggesting that the effect is directly mediated *via* AT II cells. However, whether Pirfenidone and Nintedanib downregulate Wisp1 secretion via inhibiting TGF- β signaling or by directly targeting WNT-signaling remains unclear. Further investigations are needed to unravel the exact mode of action.

6.4 Conclusions

Firstly, we demonstrated that murine 3D-LTCs represent a valuable approach for pre-clinical drug testing *ex-vivo*, thus limiting the number of animals being used for experimentation. We further validated the applicability of the Fibrotic Cocktail inducing “early fibrosis like” changes in human 3D-LTCs for testing the anti-fibrotic action of compounds, using Nintedanib and Pirfenidone as an example. The acquired data can possibly be held as reference standard for testing future compounds using *ex-vivo* 3D-LTCs. However, we also pointed out the systems limitations with highlighting the need of combining multiple approaches for pre-clinical drug testing. Given the

complexity of the system of human 3D-LTCs, the deployment of high throughput analysis in order to identify suitable marker for the treatment response will be crucial.

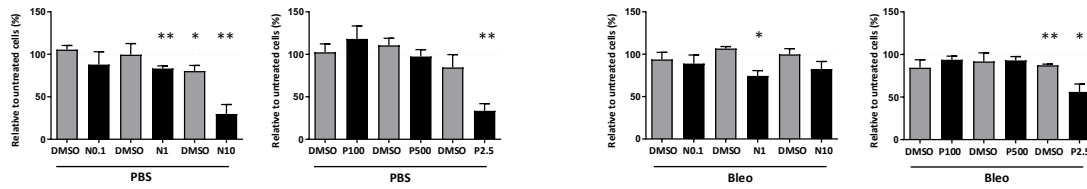
Secondly, we provide evidence of Nintedanib and Pirfenidone affecting alveolar epithelial cell, thus contributing to a better overall understanding of the anti-fibrotic action of both drugs. We present evidence of Nintedanib and Pirfenidone differentially affecting alveolar epithelial cell function both in pmAT II cell culture and *ex-vivo* 3D-LTCs. We demonstrated Nintedanib to stabilize phenotypic marker for alveolar type I and II cells and show evidence of Nintedanib restoring the regenerative potential of the alveolar epithelium. Furthermore, both Pirfenidone and Nintedanib were shown to prevent TGF- β induced EMT in alveolar type II cells. However, to what extent Nintedanib and Pirfenidone restore epithelial cell function and if this adds to the anti-fibrotic action of these drugs *in-situ* needs to be further delineated.

6.5 Future perspective

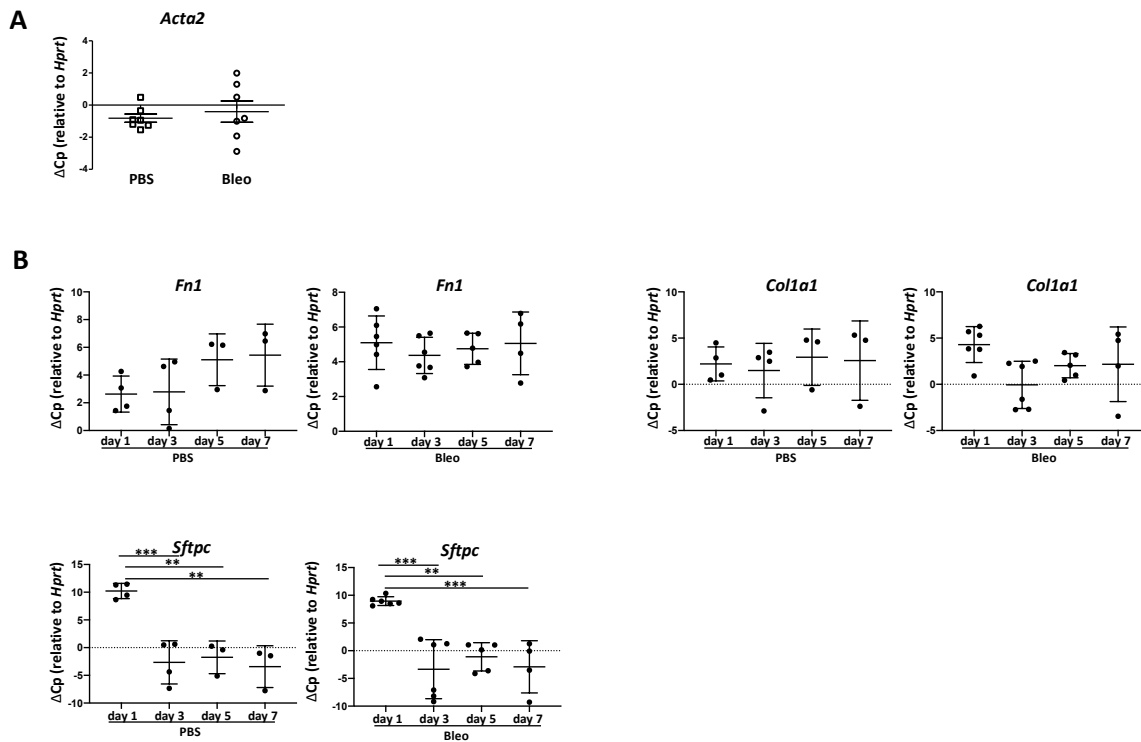
Nintedanib and Pirfenidone are the only approved drugs in the treatment of IPF patients known to decelerate disease progression and reduce mortality (Richeldi et al. 2017). Their clinical success can be mainly attributed to their pleiotropic anti-fibrotic effects on multiple cell types in the disease. However, IPF continues to progress upon Nintedanib or Pirfenidone treatment and novel treatment approaches are needed. In this regard, combined therapy with Nintedanib and Pirfenidone was shown to have additive effects. (Vancheri et al. 2018b). Further clinical trials must be awaited. As recent more selective therapeutic strategies failed to show sufficient anti-fibrotic effects *in-situ* (Daniels et al. 2004, Aono et al. 2005, Daniels et al. 2010), compounds affecting multiple cell types and interfering with various pathways might be the key to clinical success. Moreover, considering the heterogeneity within the IPF disease “personalized combination therapy” as a novel approach using highly diverse anti-fibrotic agents, such as Nintedanib and Pirfenidone, with targeted therapies according to patient’s individual background can be advantageous in order to maximize the clinical success (Hambly and Kolb 2016, Martinez et al. 2017). In this regard, specifically targeting the alveolar epithelial cell dysfunction can be of

particular interest for patients with genetic variants of *SFTPC* and *SFTPA* associated with surfactant malfunction.

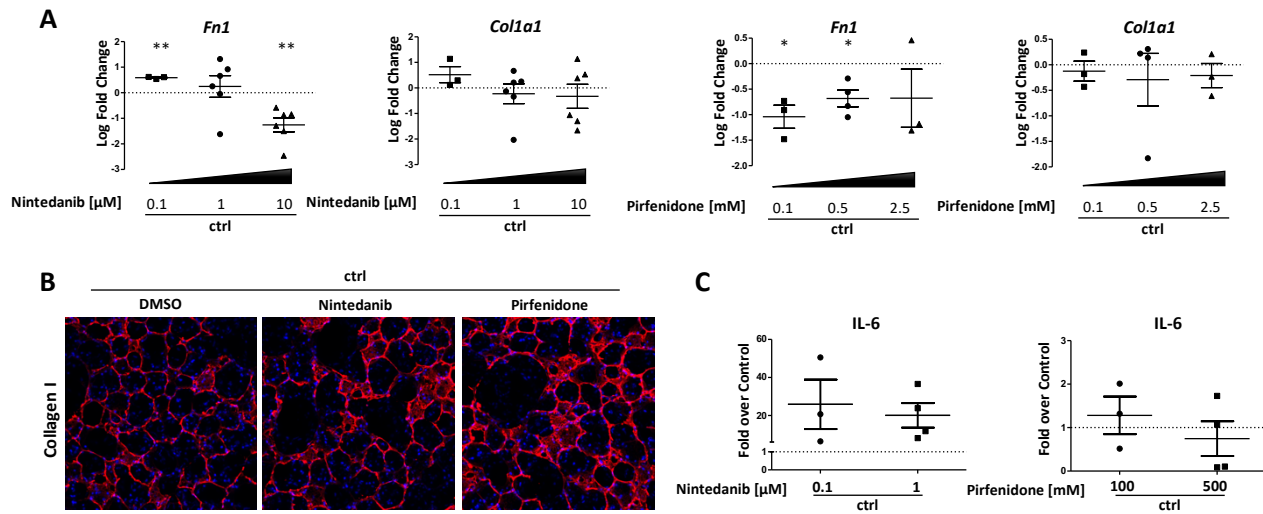
7. SUPPLEMENT



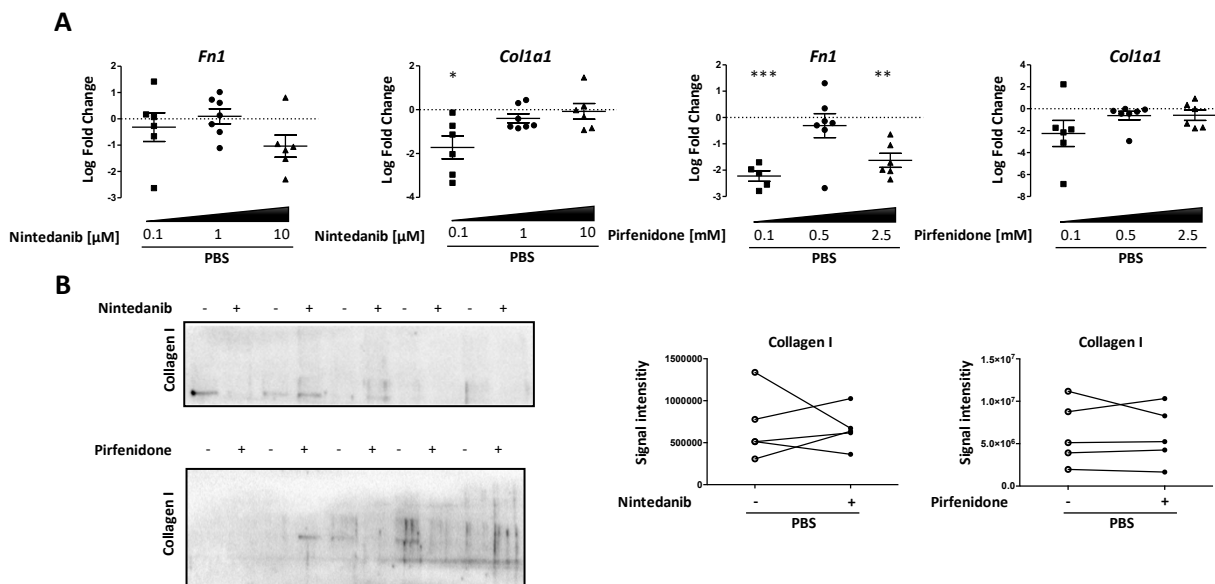
Supplemental Figure 1: Dose dependent effect of Nintedanib and Pirfenidone on murine 3D-LTC metabolic activity. Control and fibrotic 3D-LTCs were subjected to Nintedanib (0.1 μ M, 1 μ M, 10 μ M) and Pirfenidone (100 μ M, 500 μ M, 2.5mM) and cultured for 48h. Metabolic activity was assessed by WST-1 assay, one-sample t-tests compared to the theoretical value of 100. * $p < 0.05$, ** $p < 0.01$, *** $p < 0.001$



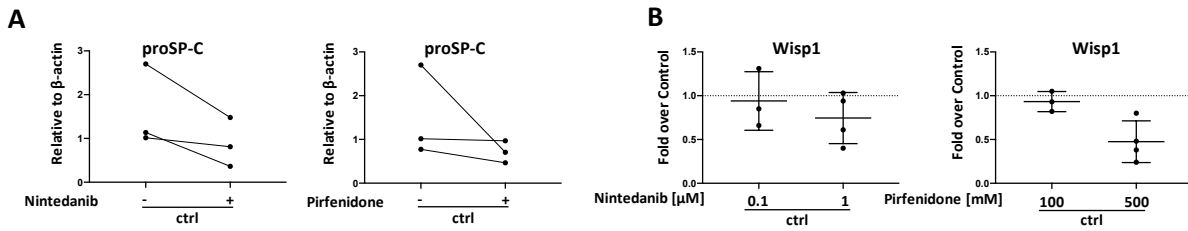
Supplemental Figure 2: Maintenance of control and fibrotic 3D-LTCs in culture. Control and fibrotic 3D-LTCs were generated as previously described. **(A)** 3D-LTCs were cultured for 48h. Fibrotic marker *Acta2* gene expression in fibrotic 3D-LTCs compared to PBS control was investigated by qPCR (n=7), paired Student's t-test. **(B)** 3D-LTCs were cultured up to seven days. Fibrotic marker *Fn1* and *Col1a1* and alveolar type II cell marker *Sftpc* gene expression in fibrotic 3D-LTCs compared to PBS control was investigated by qPCR (n=7), one-way ANOVA followed by Bonferroni's post test. ** $p < 0.01$, *** $p < 0.001$



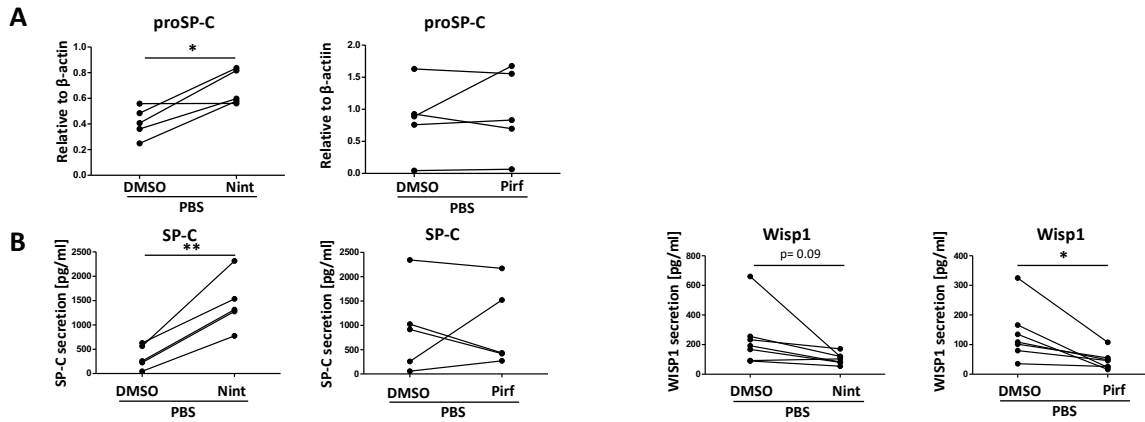
Supplemental Figure 3: Nintedanib and Pirfenidone affecting fibrotic gene and protein expression in control 3D-LTCs. (A) Murine 3D-LTCs were subjected to Nintedanib or Pirfenidone and cultured for 48h. Fibrotic marker *Fn1* and *Col1a1* gene expression was investigated by qPCR (n=3-6), one-sample t-test compared to the theoretical value of 0. **(B)** Representative immunofluorescence images of Collagen I. **(C)** IL-6 secretion was measured by ELISA (n=3-4), one-sample t-test compared to the theoretical value of 0. *p < 0.05, **p < 0.01



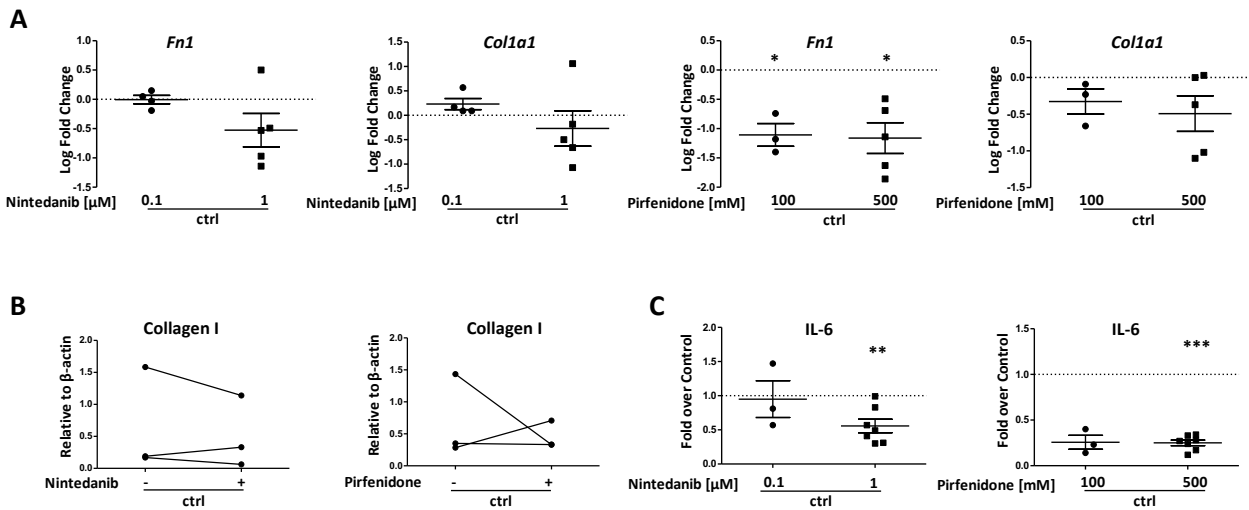
Supplemental Figure 4: Effect of Nintedanib and Pirfenidone on fibrotic marker expression in PBS treated 3D-LTCs. (A) Murine 3D-LTCs were treated with Nintedanib and Pirfenidone for 48h. Fibrotic marker *Fn1* and *Col1a1* gene expression was investigated by qPCR (n=3-6), one-sample t-tests compared to the theoretical value of 0. **(B)** Collagen I secretion was investigated by Western blot (n=4), paired Student's t-test. *p < 0.05, **p < 0.01, ***p < 0.001



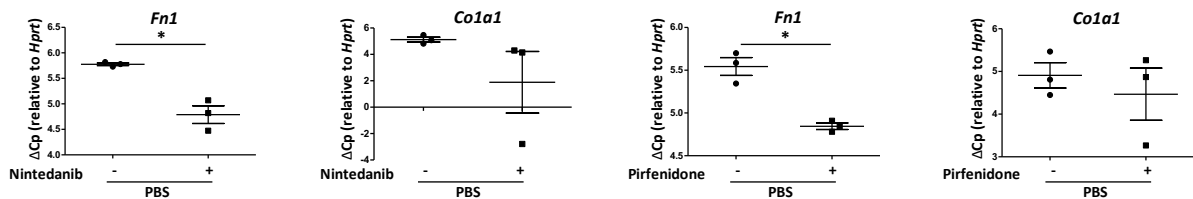
Supplemental Figure 5: Effect of Nintedanib and Pirfenidone on epithelial cell function in control 3D-LTCs. (A, B) Murine 3D-LTCs were subjected to Nintedanib (**A**: 1 μ M; **B**: 0.1 μ M, 1 μ M) and Pirfenidone (**A**: 500 μ M; **B**: 100 μ M, 500 μ M) and cultured for 48h. **(A)** Western blot analysis of pro-SPC expression (n=3), paired Student's t-test. **(B)** Wisp1 secretion was determined by ELISA (n=3), one-sample t-tests compared to the theoretical value of 1.



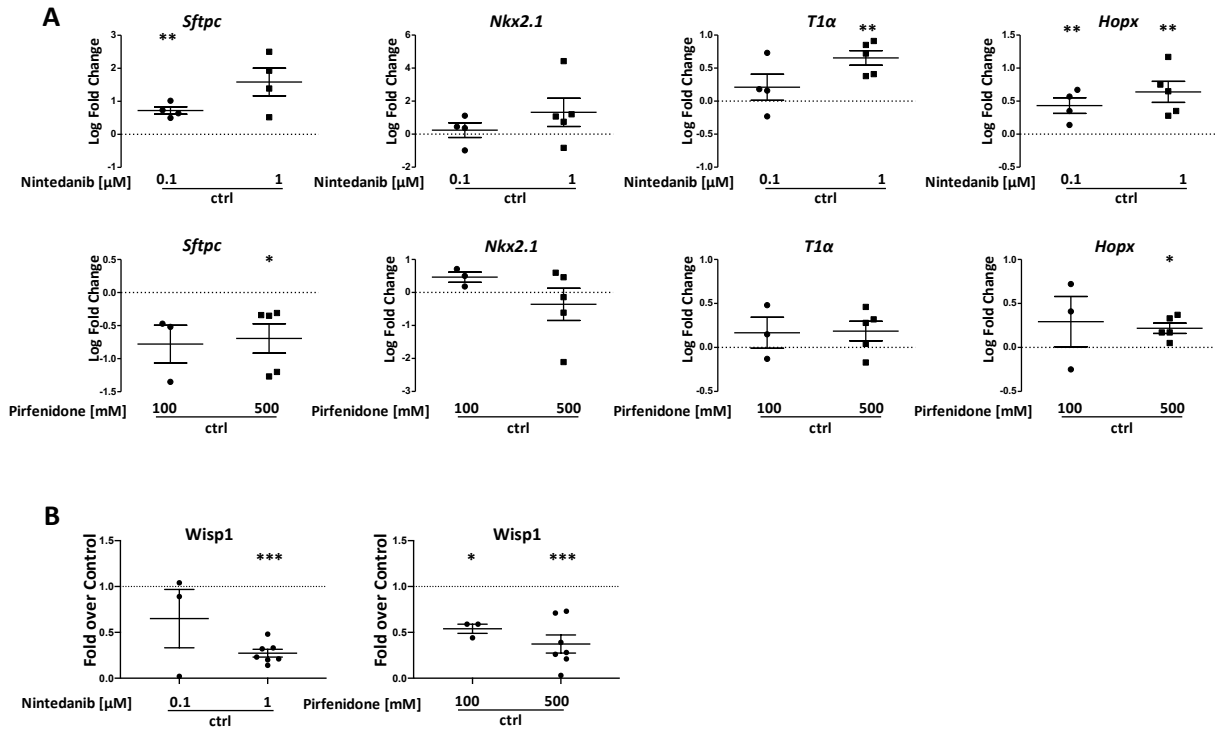
Supplemental Figure 6: Effect of Nintedanib and Pirfenidone on epithelial cell function in PBS treated 3D-LTCs. (A, B, C) Fibrotic murine 3D-LTCs were subjected to Nintedanib (1 μ M) and Pirfenidone (500 μ M) for 48h. **(A)** Western blot analysis of pro-SPC expression (n=4-5), paired Student's t-test. **(B)** SP-C and WISP1 secretion was determined by ELISA, paired Student's t-test. *p < 0.05, **p < 0.01



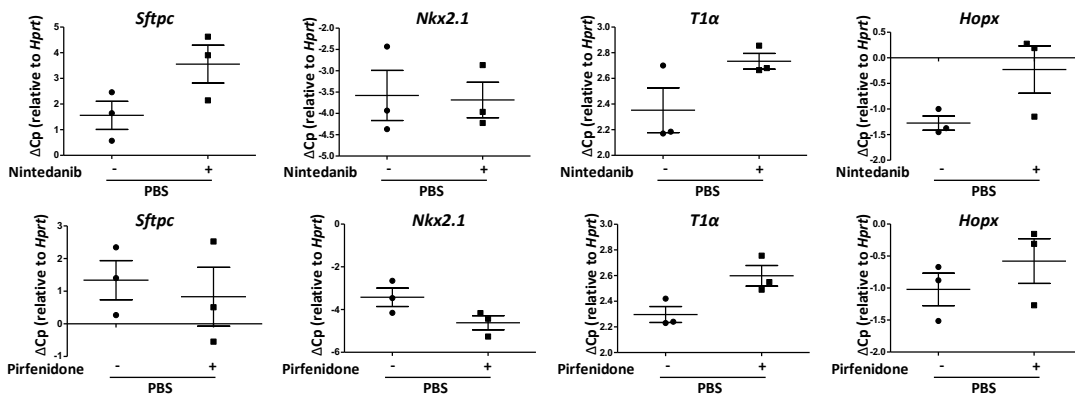
Supplemental Figure 7: Effect of Nintedanib and Pirfenidone on control pmAT II cells. (A, B) PmAT II cell were cultured with Nintedanib (A: 0.1μM, 1μM; B: 1μM) or Pirfenidone (A: 100μM, 500μM; B: 500μM) for 48h. (A) Fibrotic marker *Fn1* and *Col1a1* gene expression was investigated by qPCR (n=3-5), one-sample t-tests compared to the theoretical value of 0. (B) Western blot analysis of collagen I expression (n=3), paired Student's t-test. (C) IL-6 secretion was determined by ELISA (n=3-7), one-sample t-tests compared to the theoretical value of 1. *p < 0.05, **p < 0.01, ***p < 0.001



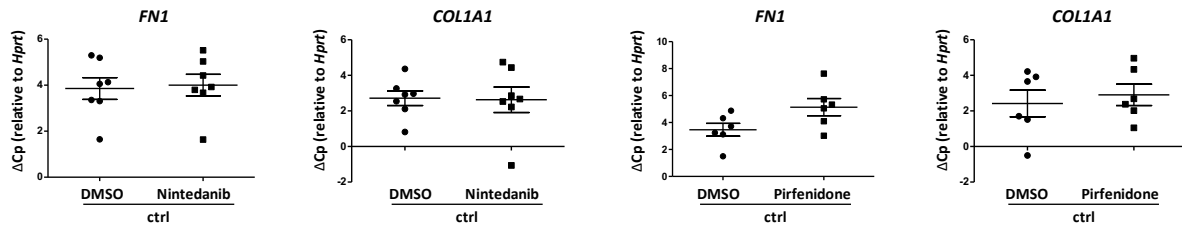
Supplemental Figure 8: Effect of Nintedanib and Pirfenidone on pmAT II cells derived from PBS treated mice. Fibrotic marker *Fn1* and *Col1a1* gene expression in control pmAT II cells treated with Nintedanib (1μM) or Pirfenidone (500μM) for 48h was investigated by qPCR (n=3), paired Student's t-test. *p < 0.05



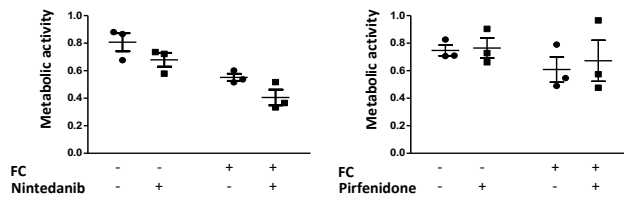
Supplemental Figure 9: Nintedanib and Pirfenidone affecting epithelial cell function in control pmAT II cells. PmAT II cells were cultured with Nintedanib or Pirfenidone for 48h. **(A)** Epithelial cell marker *Sftpc*, *Nkx2.1*, *T1α* and *Hopx* gene expression was investigated by qPCR (n=3-6), one-sample t-tests compared to the theoretical value of 0. **(B)** *Wisp1* secretion was determined by ELISA, one-sample t-tests compared to the theoretical value of 1. *p < 0.05, **p < 0.01, ***p < 0.001



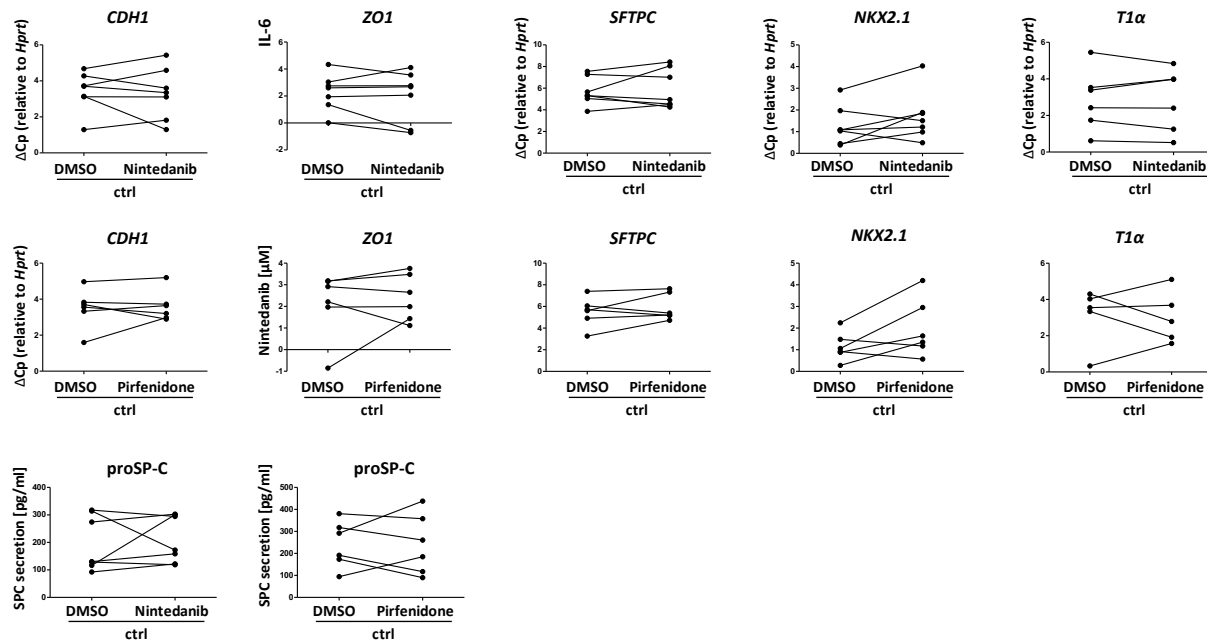
Supplemental Figure 10: Effect of Nintedanib and Pirfenidone on pmAT II cells derived from PBS treated mice. PmAT II cells were cultured with Nintedanib (1 μM) or Pirfenidone (500 μM) for 48h. **(A)** Epithelial cell marker *Sftpc*, *Nkx2.1*, *T1α* and *Hopx* gene expression was investigated by qPCR (n=3), paired Student's t-test.



Supplemental Figure 11: Ex-vivo effect of Nintedanib and Pirfenidone on fibrotic gene expression in control human 3D-LTCs. Human 3D-LTCs were cultured with Nintedanib (1 μ M) or Pirfenidone (500 μ M) for 48h. Fibrotic marker *Fn1* and *Col1a1* gene expression was investigated by qPCR (N=6), paired Student's t-test.



Supplemental Figure 12: Metabolic activity of human 3D-LTCs cultured with CC/FC and Pirfenidone and Nintedanib. Punches were treated with CC/FC and Pirfenidone (5 μ M) and Nintedanib (1 μ M) for 120h. Metabolic activity was assessed by WST-1 assay (N =3), two-way ANOVA followed by Sidak's multiple comparisons test.



Supplemental Figure 13. Ex-vivo effect of Nintedanib and Pirfenidone on epithelial cell function in control human 3D-LTCs. (A, B) Human 3D-LTCs were cultured with Nintedanib (1 μ M) or Pirfenidone (500 μ M) for 48h. (A) Epithelial cell marker *CDH1*, *ZO1*, *SFTPC*, *NKX2.1* and *T1 α* gene expression was investigated by qPCR (N=5-6), paired Student's t-test (B) Pro-SP-C secretion was measured by ELISA (N=6), paired Student's t-test.

8. REFERENCES

Some aspects of this thesis have been published in the following research article:

Lehmann M*, Buhl L*, Alsafadi H, Klee S, Hermann S, Mutze K, Ota C, Lindner M, Behr J, Hilgendorff, Wagner DE and Königshoff M (*contributed equally) “*Differential effects of Nintedanib and Pirfenidone on lung alveolar epithelial cell function in ex vivo murine and human lung tissue cultures of pulmonary fibrosis*”; Respiratory Research, Sept. 2018

This work is licensed under the Creative Commons Attribution 4.0 International License. To view a copy of this license, visit <http://creativecommons.org/licenses/by/4.0/> or send a letter to Creative Commons, PO Box 1866, Mountain View, CA 94042, USA.

8.1. Bibliography

- (2002) American Thoracic Society/European Respiratory Society International Multidisciplinary Consensus Classification of the Idiopathic Interstitial Pneumonias. This joint statement of the American Thoracic Society (ATS), and the European Respiratory Society (ERS) was adopted by the ATS board of directors, June 2001 and by the ERS Executive Committee, June 2001. *Am J Respir Crit Care Med*, 165, 277-304.
- Ackermann, M., Y. O. Kim, W. L. Wagner, D. Schuppan, C. D. Valenzuela, S. J. Mentzer, S. Kreuz, D. Stiller, L. Wollin & M. A. Konerding (2017) Effects of nintedanib on the microvascular architecture in a lung fibrosis model. *Angiogenesis*, 20, 359-372.
- Alsafadi, H. N., C. A. Staab-Weijnitz, M. Lehmann, M. Lindner, B. Peschel, M. Königshoff & D. E. Wagner (2017) An ex vivo model to induce early fibrosis-like changes in human precision-cut lung slices. *Am J Physiol Lung Cell Mol Physiol*, 312, L896-L902.
- Andersson-Sjoland, A., C. G. de Alba, K. Nihlberg, C. Becerril, R. Ramirez, A. Pardo, G. Westergren-Thorsson & M. Selman (2008) Fibrocytes are a potential source of lung fibroblasts in idiopathic pulmonary fibrosis. *Int J Biochem Cell Biol*, 40, 2129-40.
- Aono, Y., Y. Nishioka, M. Inayama, M. Ugai, J. Kishi, H. Uehara, K. Izumi & S. Sone (2005) Imatinib as a novel antifibrotic agent in bleomycin-induced pulmonary fibrosis in mice. *Am J Respir Crit Care Med*, 171, 1279-85.
- Armanios, M. Y., J. J. Chen, J. D. Cogan, J. K. Alder, R. G. Ingersoll, C. Markin, W. E. Lawson, M. Xie, I. Vulto, J. A. Phillips, 3rd, P. M. Lansdorf, C. W. Greider & J. E. Loyd (2007) Telomerase mutations in families with idiopathic pulmonary fibrosis. *N Engl J Med*, 356, 1317-26.
- Aumiller, V., N. Balsara, J. Wilhelm, A. Gunther & M. Königshoff (2013) WNT/beta-catenin signaling induces IL-1beta expression by alveolar epithelial cells in pulmonary fibrosis. *Am J Respir Cell Mol Biol*, 49, 96-104.
- Baarsma, H. A. & M. Königshoff (2017) 'WNT-er is coming': WNT signalling in chronic lung diseases. *Thorax*, 72, 746-759.
- BBailey, K. E., T. J. D'Ovidio, N. Manning, M. Königshoff & C. M. Magin (2018) Hybrid Three-Dimensional Lung Tissue Cultures to Improve Ex Vivo Models of Chronic Obstructive Pulmonary Disease. *Ann Am Thorac Soc*, 15, S288.

- Bailey, K. E., C. Pino, M. L. Lennon, A. Lyons, J. G. Jacot, S. R. Lammers, M. Konigshoff & C. M. Magin (2020) Embedding of Precision-Cut Lung Slices in Engineered Hydrogel Biomaterials Supports Extended Ex Vivo Culture. *Am J Respir Cell Mol Biol*, 62, 14-22.
- Bargagli, E., C. Piccioli, E. Rosi, E. Torricelli, L. Turi, E. Piccioli, M. Pistolesi, K. Ferrari & L. Voltolini (2018) Pirfenidone and Nintedanib in idiopathic pulmonary fibrosis: Real-life experience in an Italian referral centre. *Pulmonology*.
- Barlo, N. P., C. H. van Moorsel, H. J. Ruven, P. Zanen, J. M. van den Bosch & J. C. Grutters (2009) Surfactant protein-D predicts survival in patients with idiopathic pulmonary fibrosis. *Sarcoidosis Vasc Diffuse Lung Dis*, 26, 155-61.
- Berschneider, B., D. C. Ellwanger, H. A. Baarsma, C. Thiel, C. Shimbori, E. S. White, M. Kolb, P. Neth & M. Konigshoff (2014) miR-92a regulates TGF-beta1-induced WISP1 expression in pulmonary fibrosis. *Int J Biochem Cell Biol*, 53, 432-41.
- Boucher, R. C. (2011) Idiopathic Pulmonary Fibrosis — A Sticky Business. 364, 1560-1561.
- Carter, N. J. (2011) Pirfenidone: in idiopathic pulmonary fibrosis. *Drugs*, 71, 1721-32.
- Chen, J. F., H. F. Ni, M. M. Pan, H. Liu, M. Xu, M. H. Zhang & B. C. Liu (2013) Pirfenidone inhibits macrophage infiltration in 5/6 nephrectomized rats. *Am J Physiol Renal Physiol*, 304, F676-85.
- Chilosi, M., A. Carloni, A. Rossi & V. Poletti (2013) Premature lung aging and cellular senescence in the pathogenesis of idiopathic pulmonary fibrosis and COPD/emphysema. *Transl Res*, 162, 156-73.
- Choi, K., K. Lee, S. W. Ryu, M. Im, K. H. Kook & C. Choi (2012) Pirfenidone inhibits transforming growth factor-beta1-induced fibrogenesis by blocking nuclear translocation of Smads in human retinal pigment epithelial cell line ARPE-19. *Mol Vis*, 18, 1010-20.
- Collard, H. R. (2010a) The Age of Idiopathic Pulmonary Fibrosis. 181, 771-772.
- (2010b) The Age of Idiopathic Pulmonary Fibrosis. *American Journal of Respiratory and Critical Care Medicine*, 181, 771-772.
- Collins, B. F. & G. Raghu (2019) Antifibrotic therapy for fibrotic lung disease beyond idiopathic pulmonary fibrosis. *European Respiratory Review*, 28, 190022.
- Conte, E., E. Gili, E. Fagone, M. Fruciano, M. Iemmolo & C. Vancheri (2014) Effect of pirfenidone on proliferation, TGF-beta-induced myofibroblast differentiation and fibrogenic activity of primary human lung fibroblasts. *Eur J Pharm Sci*, 58, 13-9.
- Coon, D. R., D. J. Roberts, M. Loscertales & R. Kradin (2006) Differential epithelial expression of SHH and FOXF1 in usual and nonspecific interstitial pneumonia. *Exp Mol Pathol*, 80, 119-23.
- Coppé, J.-P., P.-Y. Desprez, A. Krtolica & J. Campisi (2010) The Senescence-Associated Secretory Phenotype: The Dark Side of Tumor Suppression. 5, 99-118.
- Cottin, V. (2017) The safety and tolerability of nintedanib in the treatment of idiopathic pulmonary fibrosis. *Expert Opin Drug Saf*, 16, 857-865.
- Coward, W. R., K. Watts, C. A. Feghali-Bostwick, G. Jenkins & L. Pang (2010) Repression of IP-10 by interactions between histone deacetylation and hypermethylation in idiopathic pulmonary fibrosis. *Mol Cell Biol*, 30, 2874-86.
- Crosby, L. M. & C. M. Waters (2010) Epithelial repair mechanisms in the lung. *Am J Physiol Lung Cell Mol Physiol*, 298, L715-31.
- Cui, H., J. Ge, N. Xie, S. Banerjee, Y. Zhou, V. B. Antony, V. J. Thannickal & G. Liu (2017) miR-34a Inhibits Lung Fibrosis by Inducing Lung Fibroblast Senescence. *Am J Respir Cell Mol Biol*, 56, 168-178.
- Daniels, C. E., J. A. Lasky, A. H. Limper, K. Mieras, E. Gabor & D. R. Schroeder (2010) Imatinib Treatment for Idiopathic Pulmonary Fibrosis. 181, 604-610.
- Daniels, C. E., M. C. Wilkes, M. Edens, T. J. Kottom, S. J. Murphy, A. H. Limper & E. B. Leof (2004) Imatinib mesylate inhibits the profibrogenic activity of TGF-beta and prevents bleomycin-mediated lung fibrosis. *J Clin Invest*, 114, 1308-16.

- Decaris, M. L., M. Gatmaitan, S. FlorCruz, F. Luo, K. Li, W. E. Holmes, M. K. Hellerstein, S. M. Turner & C. L. Emson (2014) Proteomic analysis of altered extracellular matrix turnover in bleomycin-induced pulmonary fibrosis. *Mol Cell Proteomics*, 13, 1741-52.
- DeMaio, L., S. T. Buckley, M. S. Krishnaveni, P. Flodby, M. Dubourd, A. Banfalvi, Y. Xing, C. Ehrhardt, P. Minoo, B. Zhou, E. D. Crandall & Z. Borok (2012) Ligand-independent transforming growth factor-beta type I receptor signalling mediates type I collagen-induced epithelial-mesenchymal transition. *J Pathol*, 226, 633-44.
- Demaio, L., W. Tseng, Z. Balverde, J. R. Alvarez, K. J. Kim, D. G. Kelley, R. M. Senior, E. D. Crandall & Z. Borok (2009) Characterization of mouse alveolar epithelial cell monolayers. *Am J Physiol Lung Cell Mol Physiol*, 296, L1051-8.
- Di Sario, A., E. Bendia, G. Svegliati Baroni, F. Ridolfi, A. Casini, E. Ceni, S. Saccomanno, M. Marziani, L. Trozzi, P. Sterpetti, S. Taffetani & A. Benedetti (2002) Effect of pirfenidone on rat hepatic stellate cell proliferation and collagen production. *J Hepatol*, 37, 584-91.
- Didiasova, M., R. Singh, J. Wilhelm, G. Kwapiszewska, L. Wujak, D. Zakrzewicz, L. Schaefer, P. Markart, W. Seeger, M. Lauth & M. Wygrecka (2017) Pirfenidone exerts antifibrotic effects through inhibition of GLI transcription factors. *Faseb j*, 31, 1916-1928.
- Ding, Q., I. Subramanian, T. R. Luckhardt, P. Che, M. Waghray, X. K. Zhao, N. Bone, A. R. Kurundkar, L. Hecker, M. Hu, Y. Zhou, J. C. Horowitz, R. Vittal & V. J. Thannickal (2017) Focal adhesion kinase signaling determines the fate of lung epithelial cells in response to TGF-beta. *Am J Physiol Lung Cell Mol Physiol*, 312, L926-935.
- Disayabutr, S., E. K. Kim, S. I. Cha, G. Green, R. P. Naikawadi, K. D. Jones, J. A. Golden, A. Schroeder, M. A. Matthay, J. Kukreja, D. J. Erle, H. R. Collard & P. J. Wolters (2016) miR-34 miRNAs Regulate Cellular Senescence in Type II Alveolar Epithelial Cells of Patients with Idiopathic Pulmonary Fibrosis. *PLoS One*, 11, e0158367.
- Fernandez, I. E. & O. Eickelberg (2012a) The impact of TGF-beta on lung fibrosis: from targeting to biomarkers. *Proc Am Thorac Soc*, 9, 111-6.
- (2012b) New cellular and molecular mechanisms of lung injury and fibrosis in idiopathic pulmonary fibrosis. *Lancet*, 380, 680-8.
- Fernandez, I. E., F. R. Greiffo, M. Frankenberger, J. Bandres, K. Heinzemann, C. Neurohr, R. Hatz, D. Hartl, J. Behr & O. Eickelberg (2016) Peripheral blood myeloid-derived suppressor cells reflect disease status in idiopathic pulmonary fibrosis. ERJ-01826-2015.
- Flaherty, K. R., A. U. Wells, V. Cottin, A. Devaraj, S. L. F. Walsh, Y. Inoue, L. Richeldi, M. Kolb, K. Tetzlaff, S. Stowasser, C. Coeck, E. Clerisme-Beaty, B. Rosenstock, M. Quaresma, T. Haeufel, R.-G. Goeldner, R. Schlenker-Herceg & K. K. Brown (2019) Nintedanib in Progressive Fibrosing Interstitial Lung Diseases. *New England Journal of Medicine*, 381, 1718-1727.
- Flozak, A. S., A. P. Lam, S. Russell, M. Jain, O. N. Peled, K. A. Sheppard, R. Beri, G. M. Mutlu, G. R. Budinger & C. J. Gottardi (2010) Beta-catenin/T-cell factor signaling is activated during lung injury and promotes the survival and migration of alveolar epithelial cells. *J Biol Chem*, 285, 3157-67.
- Fujiwara, A., Y. Shintani, S. Funaki, T. Kawamura, T. Kimura, M. Minami & M. Okumura (2017) Pirfenidone plays a biphasic role in inhibition of epithelial-mesenchymal transition in non-small cell lung cancer. *Lung Cancer*, 106, 8-16.
- Gan, Y., E. L. Herzog & R. H. Gomer (2011) Pirfenidone treatment of idiopathic pulmonary fibrosis. *Ther Clin Risk Manag*, 7, 39-47.
- George, P. M. & A. U. Wells (2017) Pirfenidone for the treatment of idiopathic pulmonary fibrosis. *Expert Rev Clin Pharmacol*, 10, 483-491.
- Giri, S. N., S. Leonard, X. Shi, S. B. Margolin & V. Vallyathan (1999) Effects of pirfenidone on the generation of reactive oxygen species in vitro. *J Environ Pathol Toxicol Oncol*, 18, 169-77.

- Gurujeyalakshmi, G., M. A. Hollinger & S. N. Giri (1999) Pirfenidone inhibits PDGF isoforms in bleomycin hamster model of lung fibrosis at the translational level. *Am J Physiol*, 276, L311-8.
- Hambly, N. & M. Kolb (2016) Pathways to Precision Medicine in Idiopathic Pulmonary Fibrosis. Time to Relax? 194, 1315-1317.
- Hagimoto, N., K. Kuwano, I. Inoshima, M. Yoshimi, N. Nakamura, M. Fujita, T. Maeyama & N. Hara (2002) TGF-beta 1 as an enhancer of Fas-mediated apoptosis of lung epithelial cells. *J Immunol*, 168, 6470-8.
- Harada, T., K. Watanabe, K. Nabeshima, M. Hamasaki & H. Iwasaki (2013) Prognostic significance of fibroblastic foci in usual interstitial pneumonia and non-specific interstitial pneumonia. *Respirology*, 18, 278-83.
- Helling, B. A. & I. V. Yang (2015) Epigenetics in lung fibrosis: from pathobiology to treatment perspective. *Curr Opin Pulm Med*, 21, 454-62.
- Hilberg, F., G. J. Roth, M. Krssak, S. Kautschitsch, W. Sommergruber, U. Tontsch-Grunt, P. Garin-Chesa, G. Bader, A. Zoepfel, J. Quant, A. Heckel & W. J. Rettig (2008a) BIBF 1120: triple angiokinase inhibitor with sustained receptor blockade and good antitumor efficacy. *Cancer Res*, 68, 4774-82.
- Hill, C., M. G. Jones, D. E. Davies & Y. Wang (2019) Epithelial-mesenchymal transition contributes to pulmonary fibrosis via aberrant epithelial/fibroblastic cross-talk. *J Lung Health Dis*, 3, 31-35.
- Hisatomi, K., H. Mukae, N. Sakamoto, Y. Ishimatsu, T. Kakugawa, S. Hara, H. Fujita, S. Nakamichi, H. Oku, Y. Urata, H. Kubota, K. Nagata & S. Kohno (2012) Pirfenidone inhibits TGF-beta1-induced over-expression of collagen type I and heat shock protein 47 in A549 cells. *BMC Pulm Med*, 12, 24.
- Hostettler, K. E., J. Zhong, E. Papakonstantinou, G. Karakiulakis, M. Tamm, P. Seidel, Q. Sun, J. Mandal, D. Lardinois, C. Lambers & M. Roth (2014) Anti-fibrotic effects of nintedanib in lung fibroblasts derived from patients with idiopathic pulmonary fibrosis. *Respir Res*, 15, 157.
- Huang, R. Y., K. T. Kuay, T. Z. Tan, M. Asad, H. M. Tang, A. H. Ng, J. Ye, V. Y. Chung & J. P. Thiery (2015) Functional relevance of a six mesenchymal gene signature in epithelial-mesenchymal transition (EMT) reversal by the triple angiokinase inhibitor, nintedanib (BIBF1120). *Oncotarget*, 6, 22098-113.
- Iyer, S. N., G. Gurujeyalakshmi & S. N. Giri (1999a) Effects of pirfenidone on procollagen gene expression at the transcriptional level in bleomycin hamster model of lung fibrosis. *J Pharmacol Exp Ther*, 289, 211-8.
- (1999b) Effects of pirfenidone on transforming growth factor-beta gene expression at the transcriptional level in bleomycin hamster model of lung fibrosis. *J Pharmacol Exp Ther*, 291, 367-73.
- Izumi, S., M. Ikura & S. Hirano (2012) Prednisone, azathioprine, and N-acetylcysteine for pulmonary fibrosis. *N Engl J Med*, 367, 870; author reply 870-1.
- Jenkins, R. G., B. B. Moore, R. C. Chambers, O. Eickelberg, M. Konigshoff, M. Kolb, G. J. Laurent, C. B. Nanthakumar, M. A. Olman, A. Pardo, M. Selman, D. Sheppard, P. J. Sime, A. M. Tager, A. L. Tatler, V. J. Thannickal & E. S. White (2017) An Official American Thoracic Society Workshop Report: Use of Animal Models for the Preclinical Assessment of Potential Therapies for Pulmonary Fibrosis. *Am J Respir Cell Mol Biol*, 56, 667-679.
- Jolly, M. K., M. Boareto, B. Huang, D. Jia, M. Lu, E. Ben-Jacob, J. N. Onuchic & H. Levine (2015) Implications of the Hybrid Epithelial/Mesenchymal Phenotype in Metastasis. *Front Oncol*, 5, 155.
- Jolly, M. K., C. Ward, M. S. Eapen, S. Myers, O. Hallgren, H. Levine & S. S. Sohal (2018) Epithelial-mesenchymal transition, a spectrum of states: Role in lung development, homeostasis, and disease. *Dev Dyn*, 247, 346-358.
- Jones, M. G., A. Fabre, P. Schneider, F. Cinetto, G. Sgalla, M. Mavrogordato, S. Jogai, A. Alzetani, B. G. Marshall, K. M. O'Reilly, J. A. Warner, P. M. Lackie, D. E. Davies, D. M. Hansell, A. G. Nicholson, I.

- Sinclair, K. K. Brown & L. Richeldi (2016) Three-dimensional characterization of fibroblast foci in idiopathic pulmonary fibrosis. *JCI Insight*, 1.
- Kamio, K., J. Usuki, A. Azuma, K. Matsuda, T. Ishii, M. Inomata, H. Hayashi, N. Kokuho, K. Fujita, Y. Saito, T. Miya & A. Gemma (2015) Nintedanib modulates surfactant protein-D expression in A549 human lung epithelial cells via the c-Jun N-terminal kinase-activator protein-1 pathway. *Pulm Pharmacol Ther*, 32, 29-36.
- Kim, K. K., M. C. Kugler, P. J. Wolters, L. Robillard, M. G. Galvez, A. N. Brumwell, D. Sheppard & H. A. Chapman (2006) Alveolar epithelial cell mesenchymal transition develops in vivo during pulmonary fibrosis and is regulated by the extracellular matrix. *Proc Natl Acad Sci U S A*, 103, 13180-5.
- Kendall, R. T. & C. A. Feghali-Bostwick (2014) Fibroblasts in fibrosis: novel roles and mediators. *Front Pharmacol*, 5, 123.
- King, T. E., Jr., W. Z. Bradford, S. Castro-Bernardini, E. A. Fagan, I. Glaspole, M. K. Glassberg, E. Gorina, P. M. Hopkins, D. Kardatzke, L. Lancaster, D. J. Lederer, S. D. Nathan, C. A. Pereira, S. A. Sahn, R. Sussman, J. J. Swigris & P. W. Noble (2014) A phase 3 trial of pirfenidone in patients with idiopathic pulmonary fibrosis. *N Engl J Med*, 370, 2083-92.
- King, T. E., Jr., A. Pardo & M. Selman (2011) Idiopathic pulmonary fibrosis. *Lancet*, 378, 1949-61.
- King, T. E., Jr., M. I. Schwarz, K. Brown, J. A. Tooze, T. V. Colby, J. A. Waldron, Jr., A. Flint, W. Thurlbeck & R. M. Cherniack (2001) Idiopathic pulmonary fibrosis: relationship between histopathologic features and mortality. *Am J Respir Crit Care Med*, 164, 1025-32.
- Klee, S., M. Lehmann, D. E. Wagner, H. A. Baarsma & M. Konigshoff (2016) WISP1 mediates IL-6-dependent proliferation in primary human lung fibroblasts. *Sci Rep*, 6, 20547.
- Kliment, C. R. & T. D. Oury (2010) Oxidative stress, extracellular matrix targets, and idiopathic pulmonary fibrosis. *Free Radic Biol Med*, 49, 707-17.
- Knuppel, L., Y. Ishikawa, M. Aichler, K. Heinzemann, R. Hatz, J. Behr, A. Walch, H. P. Bachinger, O. Eickelberg & C. A. Staab-Weijnitz (2017) A Novel Antifibrotic Mechanism of Nintedanib and Pirfenidone. Inhibition of Collagen Fibril Assembly. *Am J Respir Cell Mol Biol*, 57, 77-90.
- Konigshoff, M., N. Balsara, E. M. Pfaff, M. Kramer, I. Chrobak, W. Seeger & O. Eickelberg (2008) Functional Wnt signaling is increased in idiopathic pulmonary fibrosis. *PLoS One*, 3, e2142.
- Königshoff, M. & P. Bonniaud (2014) Live and Let Die: Targeting Alveolar Epithelial Cell Proliferation in Pulmonary Fibrosis. 190, 1339-1341.
- Konigshoff, M., M. Kramer, N. Balsara, J. Wilhelm, O. V. Amarie, A. Jahn, F. Rose, L. Fink, W. Seeger, L. Schaefer, A. Gunther & O. Eickelberg (2009) WNT1-inducible signaling protein-1 mediates pulmonary fibrosis in mice and is upregulated in humans with idiopathic pulmonary fibrosis. *J Clin Invest*, 119, 772-87.
- Korfei, M., S. Skwarna, I. Henneke, B. MacKenzie, O. Klymenko, S. Saito, C. Ruppert, D. von der Beck, P. Mahavadi, W. Klepetko, S. Bellusci, B. Crestani, S. S. Pullamsetti, L. Fink, W. Seeger, O. H. Kramer & A. Guenther (2015) Aberrant expression and activity of histone deacetylases in sporadic idiopathic pulmonary fibrosis. *Thorax*, 70, 1022-32.
- Kugler, M. C., A. L. Joyner, C. A. Loomis & J. S. Munger (2015) Sonic Hedgehog Signaling in the Lung. From Development to Disease. 52, 1-13.
- Kurimoto, R., T. Ebata, S. Iwasawa, T. Ishiwata, Y. Tada, K. Tatsumi & Y. Takiguchi (2017) Pirfenidone may revert the epithelial-to-mesenchymal transition in human lung adenocarcinoma. *Oncol Lett*, 14, 944-950.
- Kwapiszewska, G., A. Gungl, J. Wilhelm, L. M. Marsh, H. Thekkekara Puthenparampil, K. Sinn, M. Didiasova, W. Klepetko, D. Kosanovic, R. T. Schermuly, L. Wujak, B. Weiss, L. Schaefer, M. Schneider, M. Kreuter, A. Olschewski, W. Seeger, H. Olschewski & M. Wygrecka (2018) Transcriptome profiling reveals the complexity of pirfenidone effects in idiopathic pulmonary fibrosis. *Eur Respir J*, 52.

- Lehmann, M., L. Buhl, H. N. Alsafadi, S. Klee, S. Hermann, K. Mutze, C. Ota, M. Lindner, J. Behr, A. Hilgendorff, D. E. Wagner & M. Konigshoff (2018) Differential effects of Nintedanib and Pirfenidone on lung alveolar epithelial cell function in ex vivo murine and human lung tissue cultures of pulmonary fibrosis. *Respir Res*, 19, 175.
- Lehmann, M., M. Korfei, K. Mutze, S. Klee, W. Skronska-Wasek, H. N. Alsafadi, C. Ota, R. Costa, H. B. Schiller, M. Lindner, D. E. Wagner, A. Gunther & M. Konigshoff (2017) Senolytic drugs target alveolar epithelial cell function and attenuate experimental lung fibrosis ex vivo. *Eur Respir J*, 50.
- Lehtonen, S. T., A. Veijola, H. Karvonen, E. Lappi-Blanco, R. Sormunen, S. Korpela, U. Zagai, M. C. Skold & R. Kaarteenaho (2016) Pirfenidone and nintedanib modulate properties of fibroblasts and myofibroblasts in idiopathic pulmonary fibrosis. *Respir Res*, 17, 14.
- Ley, B., H. R. Collard & T. E. King, Jr. (2011) Clinical course and prediction of survival in idiopathic pulmonary fibrosis. *Am J Respir Crit Care Med*, 183, 431-40.
- Li, Y., D. Jiang, J. Liang, E. B. Meltzer, A. Gray, R. Miura, L. Wogensen, Y. Yamaguchi & P. W. Noble (2011) Severe lung fibrosis requires an invasive fibroblast phenotype regulated by hyaluronan and CD44. *J Exp Med*, 208, 1459-71.
- Liang, J., Y. Zhang, T. Xie, N. Liu, H. Chen, Y. Geng, A. Kurkciyan, J. M. Mena, B. R. Stripp, D. Jiang & P. W. Noble (2016) Hyaluronan and TLR4 promote surfactant-protein-C-positive alveolar progenitor cell renewal and prevent severe pulmonary fibrosis in mice. *Nat Med*, 22, 1285-1293.
- Liebler, J. M., C. N. Marconett, N. Juul, H. Wang, Y. Liu, P. Flodby, I. A. Laird-Offringa, P. Minoo & B. Zhou (2016) Combinations of differentiation markers distinguish subpopulations of alveolar epithelial cells in adult lung. *Am J Physiol Lung Cell Mol Physiol*, 310, L114-20.
- Liu, G., A. Friggeri, Y. Yang, J. Milosevic, Q. Ding, V. J. Thannickal, N. Kaminski & E. Abraham (2010) miR-21 mediates fibrogenic activation of pulmonary fibroblasts and lung fibrosis. *J Exp Med*, 207, 1589-97.
- Liu, L., M. C. Kugler, C. A. Loomis, R. Samdani, Z. Zhao, G. J. Chen, J. P. Brandt, I. Brownell, A. L. Joyner, W. N. Rom & J. S. Munger (2013) Hedgehog signaling in neonatal and adult lung. *Am J Respir Cell Mol Biol*, 48, 703-10.
- Liu, Y., F. Lu, L. Kang, Z. Wang & Y. Wang (2017) Pirfenidone attenuates bleomycin-induced pulmonary fibrosis in mice by regulating Nrf2/Bach1 equilibrium. *BMC Pulmonary Medicine*, 17, 63.
- Lopez-Otin, C., M. A. Blasco, L. Partridge, M. Serrano & G. Kroemer (2013) The hallmarks of aging. *Cell*, 153, 1194-217.
- Lovisa, S., M. Zeisberg & R. Kalluri (2016) Partial Epithelial-to-Mesenchymal Transition and Other New Mechanisms of Kidney Fibrosis. *Trends Endocrinol Metab*, 27, 681-695.
- Macias-Barragan, J., A. Caligiuri, J. Garcia-Banuelos, M. Parola, M. Pinzani & J. Armendariz-Borunda (2014) [Effects of alpha lipoic acid and pirfenidone on liver cells antioxidant modulation against oxidative damage]. *Rev Med Chil*, 142, 1553-64.
- Magnini, D., G. Montemurro, B. Iovene, L. Tagliaboschi, R. E. Gerardi, E. Lo Greco, T. Bruni, A. Fabbrizzi, F. Lombardi & L. Richeldi (2017) Idiopathic Pulmonary Fibrosis: Molecular Endotypes of Fibrosis Stratifying Existing and Emerging Therapies. *Respiration*, 93, 379-395.
- Marinković, A., F. Liu & D. J. Tschumperlin (2013) Matrices of physiologic stiffness potentially inactivate idiopathic pulmonary fibrosis fibroblasts. *Am J Respir Cell Mol Biol*, 48, 422-30.
- Martinez, F. J., H. R. Collard, A. Pardo, G. Raghu, L. Richeldi, M. Selman, J. J. Swigris, H. Taniguchi & A. U. Wells (2017) Idiopathic pulmonary fibrosis. *Nat Rev Dis Primers*, 3, 17074.
- Mercer, P. F., H. V. Woodcock, J. D. Eley, M. Plate, M. G. Sulikowski, P. F. Durrenberger, L. Franklin, C. B. Nanthakumar, Y. Man, F. Genovese, R. J. McNulty, S. Yang, T. M. Maher, A. G. Nicholson, A. D. Blanchard, R. P. Marshall, P. T. Lukey & R. C. Chambers (2016) Exploration of a potent PI3 kinase/mTOR inhibitor as a novel anti-fibrotic agent in IPF. *Thorax*, 71, 701-11.

- Minagawa, S., J. Araya, T. Numata, S. Nojiri, H. Hara, Y. Yumino, M. Kawaishi, M. Odaka, T. Morikawa, S. L. Nishimura, K. Nakayama & K. Kuwano (2011) Accelerated epithelial cell senescence in IPF and the inhibitory role of SIRT6 in TGF-beta-induced senescence of human bronchial epithelial cells. *Am J Physiol Lung Cell Mol Physiol*, 300, L391-401.
- Misra, H. P. & C. Rabideau (2000) Pirfenidone inhibits NADPH-dependent microsomal lipid peroxidation and scavenges hydroxyl radicals. *Mol Cell Biochem*, 204, 119-26.
- Mitani, Y., K. Sato, Y. Muramoto, T. Karakawa, M. Kitamado, T. Iwanaga, T. Nabeshima, K. Maruyama, K. Nakagawa, K. Ishida & K. Sasamoto (2008) Superoxide scavenging activity of pirfenidone-iron complex. *Biochem Biophys Res Commun*, 372, 19-23.
- Moeller, A., K. Ask, D. Warburton, J. Gauldie & M. Kolb (2008) The bleomycin animal model: a useful tool to investigate treatment options for idiopathic pulmonary fibrosis? *Int J Biochem Cell Biol*, 40, 362-82.
- Moshaj, E. F., L. Wémeau-Stervinou, N. Cigna, S. Brayer, J. M. Sommé, B. Crestani & A. A. Mailleux (2014) Targeting the Hedgehog–Glioma-Associated Oncogene Homolog Pathway Inhibits Bleomycin-Induced Lung Fibrosis in Mice. 51, 11-25.
- Mouded, M., D. A. Culver, M. J. Hamblin, J. A. Golden, S. Veeraraghavan, R. I. Enelow, L. H. Lancaster, H. J. Goldberg, A. E. Frost, L. C. Ginns, B. J. Maroni, D. Sheppard, N. Kaminski, I. O. Rosas, M. Arjomandi, A. Prasse, C. Stebbins, G. Zhao, G. Song, M. Arefayene, R. C. d. Souza, S. M. Violette, D. C. Gallagher & K. F. Gibson. Randomized, Double-Blind, Placebo-Controlled, Multiple Dose, Dose-Escalation Study of BG00011 (Formerly STX-100) in Patients with Idiopathic Pulmonary Fibrosis (IPF). In *D14. ILD: CLINICAL RESEARCH*, A7785-A7785.
- Munger, J. S., X. Huang, H. Kawakatsu, M. J. Griffiths, S. L. Dalton, J. Wu, J. F. Pittet, N. Kaminski, C. Garat, M. A. Matthay, D. B. Rifkin & D. Sheppard (1999) The integrin alpha v beta 6 binds and activates latent TGF beta 1: a mechanism for regulating pulmonary inflammation and fibrosis. *Cell*, 96, 319-28.
- Mutze, K., S. Vierkotten, J. Milosevic, O. Eickelberg & M. Konigshoff (2015) Enolase 1 (ENO1) and protein disulfide-isomerase associated 3 (PDIA3) regulate Wnt/beta-catenin-driven trans-differentiation of murine alveolar epithelial cells. *Dis Model Mech*, 8, 877-90.
- Nakayama, S., H. Mukae, N. Sakamoto, T. Kakugawa, S. Yoshioka, H. Soda, H. Oku, Y. Urata, T. Kondo, H. Kubota, K. Nagata & S. Kohno (2008) Pirfenidone inhibits the expression of HSP47 in TGF-beta1-stimulated human lung fibroblasts. *Life Sci*, 82, 210-7.
- Nakazato, H., H. Oku, S. Yamane, Y. Tsuruta & R. Suzuki (2002) A novel anti-fibrotic agent pirfenidone suppresses tumor necrosis factor-alpha at the translational level. *Eur J Pharmacol*, 446, 177-85.
- Nathan, S. D., C. Albera, W. Z. Bradford, U. Costabel, I. Glaspole, M. K. Glassberg, D. R. Kardatzke, M. Daigl, K. U. Kirchgaessler, L. H. Lancaster, D. J. Lederer, C. A. Pereira, J. J. Swigris, D. Valeyre & P. W. Noble (2017) Effect of pirfenidone on mortality: pooled analyses and meta-analyses of clinical trials in idiopathic pulmonary fibrosis. *Lancet Respir Med*, 5, 33-41.
- Neuhaus, V., D. Schaudien, T. Golovina, U. A. Temann, C. Thompson, T. Lippmann, C. Bersch, O. Pfennig, D. Jonigk, P. Braubach, H. G. Fieguth, G. Warnecke, V. Yusibov, K. Sewald & A. Braun (2017) Assessment of long-term cultivated human precision-cut lung slices as an ex vivo system for evaluation of chronic cytotoxicity and functionality. *J Occup Med Toxicol*, 12, 13.
- Noble, P. W., C. Albera, W. Z. Bradford, U. Costabel, M. K. Glassberg, D. Kardatzke, T. E. King, Jr., L. Lancaster, S. A. Sahn, J. Szwarcberg, D. Valeyre & R. M. du Bois (2011) Pirfenidone in patients with idiopathic pulmonary fibrosis (CAPACITY): two randomised trials. *Lancet*, 377, 1760-9.
- Noth, I., K. J. Anstrom, S. B. Calvert, J. de Andrade, K. R. Flaherty, C. Glazer, R. J. Kaner & M. A. Olman (2012) A placebo-controlled randomized trial of warfarin in idiopathic pulmonary fibrosis. *Am J Respir Crit Care Med*, 186, 88-95.

- Noth, I., Y. Zhang, S. F. Ma, C. Flores, M. Barber, Y. Huang, S. M. Broderick, M. S. Wade, P. Hysi, J. Scurba, T. J. Richards, B. M. Juan-Guardela, R. Vij, M. K. Han, F. J. Martinez, K. Kossen, S. D. Seiwert, J. D. Christie, D. Nicolae, N. Kaminski & J. G. N. Garcia (2013) Genetic variants associated with idiopathic pulmonary fibrosis susceptibility and mortality: a genome-wide association study. *Lancet Respir Med*, 1, 309-317.
- Ogura, T., H. Taniguchi, A. Azuma, Y. Inoue, Y. Kondoh, Y. Hasegawa, M. Bando, S. Abe, Y. Mochizuki, K. Chida, M. Kluglich, T. Fujimoto, K. Okazaki, Y. Tadayasu, W. Sakamoto & Y. Sugiyama (2015) Safety and pharmacokinetics of nintedanib and pirfenidone in idiopathic pulmonary fibrosis. *Eur Respir J*, 45, 1382-92.
- Oku, H., H. Nakazato, T. Horikawa, Y. Tsuruta & R. Suzuki (2002) Pirfenidone suppresses tumor necrosis factor-alpha, enhances interleukin-10 and protects mice from endotoxic shock. *Eur J Pharmacol*, 446, 167-76.
- Oku, H., T. Shimizu, T. Kawabata, M. Nagira, I. Hikita, A. Ueyama, S. Matsushima, M. Torii & A. Arimura (2008) Antifibrotic action of pirfenidone and prednisolone: different effects on pulmonary cytokines and growth factors in bleomycin-induced murine pulmonary fibrosis. *Eur J Pharmacol*, 590, 400-8.
- Oldham, J. M., S. F. Ma, F. J. Martinez, K. J. Anstrom, G. Raghu, D. A. Schwartz, E. Valenzi, L. Witt, C. Lee, R. Vij, Y. Huang, M. E. Streck & I. Noth (2015) TOLLIP, MUC5B, and the Response to N-Acetylcysteine among Individuals with Idiopathic Pulmonary Fibrosis. *Am J Respir Crit Care Med*, 192, 1475-82.
- Ota, C., J. P. Ng-Blichfeldt, M. Korfei, H. N. Alsafadi, M. Lehmann, W. Skronska-Wasek, M. D. S. M, A. Guenther, D. E. Wagner & M. Konigshoff (2018) Dynamic expression of HOPX in alveolar epithelial cells reflects injury and repair during the progression of pulmonary fibrosis. *Sci Rep*, 8, 12983.
- Pandit, K. V., D. Corcoran, H. Yousef, M. Yarlagadda, A. Tzouveleakis, K. F. Gibson, K. Konishi, S. A. Yousem, M. Singh, D. Handley, T. Richards, M. Selman, S. C. Watkins, A. Pardo, A. Ben-Yehudah, D. Bouros, O. Eickelberg, P. Ray, P. V. Benos & N. Kaminski (2010) Inhibition and role of let-7d in idiopathic pulmonary fibrosis. *Am J Respir Crit Care Med*, 182, 220-9.
- Parker, M. W., D. Rossi, M. Peterson, K. Smith, K. Sikstrom, E. S. White, J. E. Connett, C. A. Henke, O. Larsson & P. B. Bitterman (2014) Fibrotic extracellular matrix activates a profibrotic positive feedback loop. *J Clin Invest*, 124, 1622-35.
- Peljto, A. L., Y. Zhang, T. E. Fingerlin, S. F. Ma, J. G. Garcia, T. J. Richards, L. J. Silveira, K. O. Lindell, M. P. Steele, J. E. Loyd, K. F. Gibson, M. A. Seibold, K. K. Brown, J. L. Talbert, C. Markin, K. Kossen, S. D. Seiwert, E. Murphy, I. Noth, M. I. Schwarz, N. Kaminski & D. A. Schwartz (2013) Association between the MUC5B promoter polymorphism and survival in patients with idiopathic pulmonary fibrosis. *Jama*, 309, 2232-9.
- Perry, C. J. & A. J. Lawrence (2017) Hurdles in Basic Science Translation. *Front Pharmacol*, 8, 478.
- Richeldi, L., H. R. Collard & M. G. Jones (2017) Idiopathic pulmonary fibrosis. *Lancet*, 389, 1941-1952.
- Rock, J. R., C. E. Barkauskas, M. J. Counce, Y. Xue, J. R. Harris, J. Liang, P. W. Noble & B. L. Hogan (2011) Multiple stromal populations contribute to pulmonary fibrosis without evidence for epithelial to mesenchymal transition. *Proc Natl Acad Sci U S A*, 108, E1475-83.
- Raghu, G., J. Behr, K. K. Brown, J. J. Egan, S. M. Kawut, K. R. Flaherty, F. J. Martinez, S. D. Nathan, A. U. Wells, H. R. Collard, U. Costabel, L. Richeldi, J. de Andrade, N. Khalil, L. D. Morrison, D. J. Lederer, L. Shao, X. Li, P. S. Pedersen, A. B. Montgomery, J. W. Chien & T. G. O'Riordan (2013) Treatment of idiopathic pulmonary fibrosis with ambrisentan: a parallel, randomized trial. *Ann Intern Med*, 158, 641-9.
- Raghu, G., H. R. Collard, J. J. Egan, F. J. Martinez, J. Behr, K. K. Brown, T. V. Colby, J. F. Cordier, K. R. Flaherty, J. A. Lasky, D. A. Lynch, J. H. Ryu, J. J. Swigris, A. U. Wells, J. Ancochea, D. Bouros, C. Carvalho, U. Costabel, M. Ebina, D. M. Hansell, T. Johkoh, D. S. Kim, T. E. King, Jr., Y. Kondoh, J. Myers, N. L. Muller, A. G. Nicholson, L. Richeldi, M. Selman, R. F. Dudden, B. S. Griss, S. L. Protzko & H. J.

- Schunemann (2011) An official ATS/ERS/JRS/ALAT statement: idiopathic pulmonary fibrosis: evidence-based guidelines for diagnosis and management. *Am J Respir Crit Care Med*, 183, 788-824.
- Ramos, C., M. Montano, J. Garcia-Alvarez, V. Ruiz, B. D. Uhal, M. Selman & A. Pardo (2001) Fibroblasts from idiopathic pulmonary fibrosis and normal lungs differ in growth rate, apoptosis, and tissue inhibitor of metalloproteinases expression. *Am J Respir Cell Mol Biol*, 24, 591-8.
- Rangarajan, S., A. Kurundkar, D. Kurundkar, K. Bernard, Y. Y. Sanders, Q. Ding, V. B. Antony, J. Zhang, J. Zmijewski & V. J. Thannickal (2016) Novel Mechanisms for the Antifibrotic Action of Nintedanib. *Am J Respir Cell Mol Biol*, 54, 51-9.
- Renzone, E. A. (2004) Neovascularization in idiopathic pulmonary fibrosis: too much or too little? *Am J Respir Crit Care Med*, 169, 1179-80.
- Richeldi, L., H. R. Collard & M. G. Jones (2017) Idiopathic pulmonary fibrosis. *Lancet*, 389, 1941-1952.
- Richeldi, L., U. Costabel, M. Selman, D. S. Kim, D. M. Hansell, A. G. Nicholson, K. K. Brown, K. R. Flaherty, P. W. Noble, G. Raghu, M. Brun, A. Gupta, N. Juhel, M. Kluglich & R. M. du Bois (2011) Efficacy of a tyrosine kinase inhibitor in idiopathic pulmonary fibrosis. *N Engl J Med*, 365, 1079-87.
- Richeldi, L., R. M. du Bois, G. Raghu, A. Azuma, K. K. Brown, U. Costabel, V. Cottin, K. R. Flaherty, D. M. Hansell, Y. Inoue, D. S. Kim, M. Kolb, A. G. Nicholson, P. W. Noble, M. Selman, H. Taniguchi, M. Brun, F. Le Maulf, M. Girard, S. Stowasser, R. Schlenker-Herceg, B. Disse & H. R. Collard (2014) Efficacy and safety of nintedanib in idiopathic pulmonary fibrosis. *N Engl J Med*, 370, 2071-82.
- Richeldi, L., M. Kreuter, M. Selman, B. Crestani, A. M. Kirsten, W. A. Wuyts, Z. Xu, K. Bernois, S. Stowasser, M. Quaresma & U. Costabel (2018) Long-term treatment of patients with idiopathic pulmonary fibrosis with nintedanib: results from the TOMORROW trial and its open-label extension. *Thorax*, 73, 581-583.
- Rock, J. R., C. E. Barkauskas, M. J. Counce, Y. Xue, J. R. Harris, J. Liang, P. W. Noble & B. L. Hogan (2011) Multiple stromal populations contribute to pulmonary fibrosis without evidence for epithelial to mesenchymal transition. *Proc Natl Acad Sci U S A*, 108, E1475-83.
- Rosas, I. O., T. J. Richards, K. Konishi, Y. Zhang, K. Gibson, A. E. Lokshin, K. O. Lindell, J. Cisneros, S. D. Macdonald, A. Pardo, F. Sciruba, J. Dauber, M. Selman, B. R. Gochuico & N. Kaminski (2008) MMP1 and MMP7 as potential peripheral blood biomarkers in idiopathic pulmonary fibrosis. *PLoS Med*, 5, e93.
- Roth, G. J., R. Binder, F. Colbatzky, C. Dallinger, R. Schlenker-Herceg, F. Hilberg, S. L. Wollin & R. Kaiser (2015) Nintedanib: from discovery to the clinic. *J Med Chem*, 58, 1053-63.
- Roth, G. J., A. Heckel, F. Colbatzky, S. Handschuh, J. Kley, T. Lehmann-Lintz, R. Lotz, U. Tontsch-Grunt, R. Walter & F. Hilberg (2009) Design, synthesis, and evaluation of indolinones as triple angiokinase inhibitors and the discovery of a highly specific 6-methoxycarbonyl-substituted indolinone (BIBF 1120). *J Med Chem*, 52, 4466-80.
- Rubino, C. M., S. M. Bhavnani, P. G. Ambrose, A. Forrest & J. S. Loutit (2009) Effect of food and antacids on the pharmacokinetics of pirfenidone in older healthy adults. *Pulm Pharmacol Ther*, 22, 279-85.
- Salton, F., M. C. Volpe & M. Confalonieri (2019) Epithelial-Mesenchymal Transition in the Pathogenesis of Idiopathic Pulmonary Fibrosis. *Medicina (Kaunas)*, 55.
- Sato, S., S. Shinohara, S. Hayashi, S. Morizumi, S. Abe, H. Okazaki, Y. Chen, H. Goto, Y. Aono, H. Ogawa, K. Koyama, H. Nishimura, H. Kawano, Y. Toyoda, H. Uehara & Y. Nishioka (2017) Anti-fibrotic efficacy of nintedanib in pulmonary fibrosis via the inhibition of fibrocyte activity. *Respir Res*, 18, 172.
- Schaefer, C. J., D. W. Ruhmundt, L. Pan, S. D. Seiwert & K. Kossen (2011) Antifibrotic activities of pirfenidone in animal models. *Eur Respir Rev*, 20, 85-97.
- Schuster, N. & K. Kriegstein (2002) Mechanisms of TGF-beta-mediated apoptosis. *Cell Tissue Res*, 307, 1-14.

- Selman, M., T. E. King & A. Pardo (2001) Idiopathic pulmonary fibrosis: prevailing and evolving hypotheses about its pathogenesis and implications for therapy. *Ann Intern Med*, 134, 136-51.
- Selman, M. & A. Pardo (2002) Idiopathic pulmonary fibrosis: an epithelial/fibroblastic cross-talk disorder. *Respir Res*, 3, 3.
- (2006) Role of epithelial cells in idiopathic pulmonary fibrosis: from innocent targets to serial killers. *Proc Am Thorac Soc*, 3, 364-72.
- (2012) Alveolar epithelial cell disintegrity and subsequent activation: a key process in pulmonary fibrosis. *Am J Respir Crit Care Med*, 186, 119-21.
- (2014) Revealing the pathogenic and aging-related mechanisms of the enigmatic idiopathic pulmonary fibrosis. an integral model. *Am J Respir Crit Care Med*, 189, 1161-72.
- (2020) The leading role of epithelial cells in the pathogenesis of idiopathic pulmonary fibrosis. *Cell Signal*, 66, 109482.
- Selman, M., A. Pardo & N. Kaminski (2008) Idiopathic pulmonary fibrosis: aberrant recapitulation of developmental programs? *PLoS Med*, 5, e62.
- Selman, M., G. Carrillo, A. Estrada, M. Mejia, C. Becerril, J. Cisneros, M. Gaxiola, R. Pérez-Padilla, C. Navarro, T. Richards, J. Dauber, T. E. King, Jr., A. Pardo & N. Kaminski (2007) Accelerated Variant of Idiopathic Pulmonary Fibrosis: Clinical Behavior and Gene Expression Pattern. *PLOS ONE*, 2, e482.
- Shi, S., J. Wu, H. Chen, H. Chen, J. Wu & F. Zeng (2007) Single- and multiple-dose pharmacokinetics of pirfenidone, an antifibrotic agent, in healthy Chinese volunteers. *J Clin Pharmacol*, 47, 1268-76.
- Shi, Y. & J. Massague (2003) Mechanisms of TGF-beta signaling from cell membrane to the nucleus. *Cell*, 113, 685-700.
- Shin, J. M., J. H. Park, I. H. Park & H. M. Lee (2015) Pirfenidone inhibits transforming growth factor beta1-induced extracellular matrix production in nasal polyp-derived fibroblasts. *Am J Rhinol Allergy*, 29, 408-13.
- Siegel, P. M. & J. Massague (2003) Cytostatic and apoptotic actions of TGF-beta in homeostasis and cancer. *Nat Rev Cancer*, 3, 807-21.
- Sisson, T. H., M. Mendez, K. Choi, N. Subbotina, A. Courey, A. Cunningham, A. Dave, J. F. Engelhardt, X. Liu, E. S. White, V. J. Thannickal, B. B. Moore, P. J. Christensen & R. H. Simon (2010) Targeted injury of type II alveolar epithelial cells induces pulmonary fibrosis. *Am J Respir Crit Care Med*, 181, 254-63.
- Spagnolo, P. & V. Cottin (2017) Genetics of idiopathic pulmonary fibrosis: from mechanistic pathways to personalised medicine. *J Med Genet*, 54, 93-99.
- Stewart, G. A., G. F. Hoyne, S. A. Ahmad, E. Jarman, W. A. Wallace, D. J. Harrison, C. Haslett, J. R. Lamb & S. E. Howie (2003) Expression of the developmental Sonic hedgehog (Shh) signalling pathway is up-regulated in chronic lung fibrosis and the Shh receptor patched 1 is present in circulating T lymphocytes. *J Pathol*, 199, 488-95.
- Stuart, B. D., J. S. Lee, J. Kozlitina, I. Noth, M. S. Devine, C. S. Glazer, F. Torres, V. Kaza, C. E. Girod, K. D. Jones, B. M. Elicker, S. F. Ma, R. Vij, H. R. Collard, P. J. Wolters & C. K. Garcia (2014) Effect of telomere length on survival in patients with idiopathic pulmonary fibrosis: an observational cohort study with independent validation. *Lancet Respir Med*, 2, 557-65.
- Surolia, R., F. J. Li, Z. Wang, H. Li, G. Liu, Y. Zhou, T. Luckhardt, S. Bae, R. M. Liu, S. Rangarajan, J. de Andrade, V. J. Thannickal & V. B. Antony (2017) 3D pulmospheres serve as a personalized and predictive multicellular model for assessment of antifibrotic drugs. *JCI Insight*, 2, e91377.
- Takizawa, H., M. Satoh, H. Okazaki, G. Matsuzaki, N. Suzuki, A. Ishii, M. Suko, H. Okudaira, Y. Morita & K. Ito (1997) Increased IL-6 and IL-8 in bronchoalveolar lavage fluids (BALF) from patients with sarcoidosis: correlation with the clinical parameters. *Clin Exp Immunol*, 107, 175-81.

- Taniguchi, H., M. Ebina, Y. Kondoh, T. Ogura, A. Azuma, M. Suga, Y. Taguchi, H. Takahashi, K. Nakata, A. Sato, M. Takeuchi, G. Raghu, S. Kudoh & T. Nukiwa (2010) Pirfenidone in idiopathic pulmonary fibrosis. *Eur Respir J*, 35, 821-9.
- Tanjore, H., X. C. Xu, V. V. Polosukhin, A. L. Degryse, B. Li, W. Han, T. P. Sherrill, D. Plieth, E. G. Neilson, T. S. Blackwell & W. E. Lawson (2009) Contribution of Epithelial-derived Fibroblasts to Bleomycin-induced Lung Fibrosis. *American Journal of Respiratory and Critical Care Medicine*, 180, 657-665.
- Tatler, A. L., J. Barnes, A. Habgood, A. Goodwin, R. J. McAnulty & G. Jenkins (2016) Caffeine inhibits TGFbeta activation in epithelial cells, interrupts fibroblast responses to TGFbeta, and reduces established fibrosis in ex vivo precision-cut lung slices. *Thorax*, 71, 565-7.
- Thannickal, V. J. (2013) Mechanistic links between aging and lung fibrosis. *Biogerontology*, 14, 609-15.
- Togami, K., Y. Kanehira & H. Tada (2015) Pharmacokinetic evaluation of tissue distribution of pirfenidone and its metabolites for idiopathic pulmonary fibrosis therapy. *Biopharm Drug Dispos*, 36, 205-15.
- Tsuchiya, H., M. Kaibori, H. Yanagida, N. Yokoigawa, A. H. Kwon, T. Okumura & Y. Kamiyama (2004) Pirfenidone prevents endotoxin-induced liver injury after partial hepatectomy in rats. *J Hepatol*, 40, 94-101.
- Uhal, B. D. (2003) Epithelial apoptosis in the initiation of lung fibrosis. *European Respiratory Journal*, 22, 7s-9s.
- Uhl, F. 2015. Determination of lung regeneration using an ex vivo tissue slice model. Ludwig-Maximilians-Universität München.
- Uhl, F. E., S. Vierkotten, D. E. Wagner, G. Burgstaller, R. Costa, I. Koch, M. Lindner, S. Meiners, O. Eickelberg & M. Königshoff (2015) Preclinical validation and imaging of Wnt-induced repair in human 3D lung tissue cultures. *Eur Respir J*, 46, 1150-66.
- Ulsamer, A., Y. Wei, K. K. Kim, K. Tan, S. Wheeler, Y. Xi, R. S. Thies & H. A. Chapman (2012) Axin pathway activity regulates in vivo pY654-beta-catenin accumulation and pulmonary fibrosis. *J Biol Chem*, 287, 5164-72.
- Umachandran, M., J. Howarth & C. Ioannides (2004) Metabolic and structural viability of precision-cut rat lung slices in culture. *Xenobiotica*, 34, 771-80.
- Vancheri, C., M. Kreuter, L. Richeldi, C. J. Ryerson, D. Valeyre, J. C. Grutters, S. Wiebe, W. Stansen, M. Quaresma, S. Stowasser & W. A. Wuyts (2018) Nintedanib with Add-on Pirfenidone in Idiopathic Pulmonary Fibrosis. Results of the INJOURNEY Trial. 197, 356-363.
- Varga, J. & B. Pasche (2008) Antitransforming growth factor-beta therapy in fibrosis: recent progress and implications for systemic sclerosis. *Curr Opin Rheumatol*, 20, 720-8.
- Visner, G. A., F. Liu, P. Bizargity, H. Liu, K. Liu, J. Yang, L. Wang & W. W. Hancock (2009) Pirfenidone inhibits T-cell activation, proliferation, cytokine and chemokine production, and host alloresponses. *Transplantation*, 88, 330-8.
- Waghray, M., Z. Cui, J. C. Horowitz, I. M. Subramanian, F. J. Martinez, G. B. Toews & V. J. Thannickal (2005) Hydrogen peroxide is a diffusible paracrine signal for the induction of epithelial cell death by activated myofibroblasts. *Faseb j*, 19, 854-6.
- Warshamana, G. S., M. Corti & A. R. Brody (2001) TNF-alpha, PDGF, and TGF-beta(1) expression by primary mouse bronchiolar-alveolar epithelial and mesenchymal cells: tnf-alpha induces TGF-beta(1). *Exp Mol Pathol*, 71, 13-33.
- Weng, T., J. M. Poth, H. Karmouty-Quintana, L. J. Garcia-Morales, E. Melicoff, F. Luo, N. Y. Chen, C. M. Evans, R. R. Bunge, B. A. Bruckner, M. Loebe, K. A. Volcik, H. K. Eltzschig & M. R. Blackburn (2014) Hypoxia-induced deoxycytidine kinase contributes to epithelial proliferation in pulmonary fibrosis. *Am J Respir Crit Care Med*, 190, 1402-12.
- Westra, I. M., D. Oosterhuis, G. M. Groothuis & P. Olinga (2014) Precision-cut liver slices as a model for the early onset of liver fibrosis to test antifibrotic drugs. *Toxicol Appl Pharmacol*, 274, 328-38.

- Willis, B. C., J. M. Liebler, K. Luby-Phelps, A. G. Nicholson, E. D. Crandall, R. M. du Bois & Z. Borok (2005) Induction of epithelial-mesenchymal transition in alveolar epithelial cells by transforming growth factor-beta1: potential role in idiopathic pulmonary fibrosis. *Am J Pathol*, 166, 1321-32.
- Wind, S., U. Schmid, M. Freiwald, K. Marzin, R. Lotz, T. Ebner, P. Stopfer & C. Dallinger (2019) Clinical Pharmacokinetics and Pharmacodynamics of Nintedanib. *Clin Pharmacokinet*.
- Wollin, L. (2015) Interpretation of data from studies of effects of nintedanib on surfactant protein-D expression in human lung epithelial cells. *Pulm Pharmacol Ther*, 33, 15-6.
- Wollin, L., J. H. W. Distler, E. F. Redente, D. W. H. Riches, S. Stowasser, R. Schlenker-Herceg, T. M. Maher & M. Kolb (2019a) Potential of nintedanib in treatment of progressive fibrosing interstitial lung diseases. *European Respiratory Journal*, 54, 1900161.
- Wollin, L., J. H. W. Distler, E. F. Redente, D. W. H. Riches, S. Stowasser, R. Schlenker-Herceg, T. M. Maher & M. Kolb (2019b) Potential of Nintedanib in Treatment of Progressive Fibrosing Interstitial Lung Diseases. 1900161.
- Wollin, L., I. Maillet, V. Quesniaux, A. Holweg & B. Ryffel (2014) Antifibrotic and anti-inflammatory activity of the tyrosine kinase inhibitor nintedanib in experimental models of lung fibrosis. *J Pharmacol Exp Ther*, 349, 209-20.
- Wollin, L., E. Wex, A. Pautsch, G. Schnapp, K. E. Hostettler, S. Stowasser & M. Kolb (2015) Mode of action of nintedanib in the treatment of idiopathic pulmonary fibrosis. *Eur Respir J*, 45, 1434-45.
- Wolters, P. J., H. R. Collard & K. D. Jones (2014) Pathogenesis of idiopathic pulmonary fibrosis. *Annu Rev Pathol*, 9, 157-79.
- Xu, J., S. Lamouille & R. Derynck (2009) TGF-beta-induced epithelial to mesenchymal transition. *Cell Res*, 19, 156-72.
- Xu, Y. D., J. Hua, A. Mui, R. O'Connor, G. Grotendorst & N. Khalil (2003) Release of biologically active TGF-beta1 by alveolar epithelial cells results in pulmonary fibrosis. *Am J Physiol Lung Cell Mol Physiol*, 285, L527-39.
- Yanagi, S., H. Tsubouchi, A. Miura, N. Matsumoto & M. Nakazato (2015) Breakdown of Epithelial Barrier Integrity and Overdrive Activation of Alveolar Epithelial Cells in the Pathogenesis of Acute Respiratory Distress Syndrome and Lung Fibrosis. *Biomed Res Int*, 2015, 573210.
- Yang, I. V., T. E. Fingerlin, C. M. Evans, M. I. Schwarz & D. A. Schwartz (2015) MUC5B and Idiopathic Pulmonary Fibrosis. *Ann Am Thorac Soc*, 12 Suppl 2, S193-9.
- Yang, I. V., B. S. Pedersen, E. Rabinovich, C. E. Hennessy, E. J. Davidson, E. Murphy, B. J. Guardela, J. R. Tedrow, Y. Zhang, M. K. Singh, M. Correll, M. I. Schwarz, M. Geraci, F. C. Sciruba, J. Quackenbush, A. Spira, N. Kaminski & D. A. Schwartz (2014) Relationship of DNA methylation and gene expression in idiopathic pulmonary fibrosis. *Am J Respir Crit Care Med*, 190, 1263-72.
- Yang, I. V. & D. A. Schwartz (2015) Epigenetics of idiopathic pulmonary fibrosis. *Transl Res*, 165, 48-60.
- Yao, C., X. Guan, G. Carraro, T. Parimon, X. Liu, G. Huang, H. J. Soukiasian, G. David, S. S. Weigt, J. A. Belperio, P. Chen, D. Jiang, P. W. Noble & B. R. Stripp (2019) Senescence of alveolar stem cells drives progressive pulmonary fibrosis. *bioRxiv*, 820175.
- Yu, H., M. Konigshoff, A. Jayachandran, D. Handley, W. Seeger, N. Kaminski & O. Eickelberg (2008) Transgelin is a direct target of TGF-beta/Smad3-dependent epithelial cell migration in lung fibrosis. *Faseb j*, 22, 1778-89.
- Zhang, L., Y. Wang, G. Wu, W. Xiong, W. Gu & C. Y. Wang (2018) Macrophages: friend or foe in idiopathic pulmonary fibrosis? *Respir Res*, 19, 170.
- Zhou, Y., X. Huang, L. Hecker, D. Kurundkar, A. Kurundkar, H. Liu, T. H. Jin, L. Desai, K. Bernard & V. J. Thannickal (2013) Inhibition of mechanosensitive signaling in myofibroblasts ameliorates experimental pulmonary fibrosis. *J Clin Invest*, 123, 1096-108.
- Zscheppang, K., J. Berg, S. Hedtrich, L. Verheyen, D. E. Wagner, N. Suttorp, S. Hippenstiel & A. C. Hocke (2018) Human Pulmonary 3D Models For Translational Research. *Biotechnol J*, 13.

8.2 List of Figures

Figure 1: UIP pattern in HRCT	4
Figure 2: An integral model of genetic and environmental factors contributing to alveolar epithelial cell disintegration in the aged lung.	7
Figure 3: FVC outcomes from all Pirfenidone phase-III trials.	14
Figure 4: Long-term results of the TOMORROW study.	18
Figure 5: Primary murine alveolar epithelial type II cell isolation.	31
Figure 6: Generation of ex-vivo 3D-lung tissue cultures.	33
Figure 7: Induction of fibrotic marker expression in ex-vivo murine 3D-LTCs upon TGF- β treatment.	38
Figure 8: Maintenance of fibrotic phenotype of 3D-LTCs during cultivation.	40
Figure 9: Effect of Nintedanib and Pirfenidone on fibrotic marker expression in TGF- β treated 3D-LTCs.	41
Figure 10: Effect of Nintedanib and Pirfenidone on fibrotic marker expression in fibrotic 3D-LTCs.	42
Figure 11: Double treatment with Nintedanib and Pirfenidone in fibrotic 3D-LTCs.	43
Figure 12: Effect of Nintedanib and Pirfenidone on proSP-C protein expression in TGF- β treated 3D-LTCs.	44
Figure 13: Effect of Nintedanib and Pirfenidone on epithelial cell function in TGF- β 1 treated 3D-LTCs.	44
Figure 14: Effect of Nintedanib and Pirfenidone on proSP-C protein expression in fibrotic 3D-LTCs.	45
Figure 15: Effect of Nintedanib and Pirfenidone on epithelial cell function in fibrotic 3D-LTCs.	45
Figure 16: Induction of fibrotic marker expression in pmAT II upon TGF- β treatment.	46
Figure 17: Effect of Nintedanib and Pirfenidone on fibrotic marker expression in TGF- β treated pmAT II cells.	47
Figure 18: Effect of Nintedanib and Pirfenidone on inflammatory marker IL-6 secretion in TGF- β treated pmAT II cells.	47
Figure 19: pmAT II derived from Bleomycin treated mice retain their pro-fibrotic phenotype in culture.	48
	91

Figure 20: Effect of Nintedanib and Pirfenidone on fibrotic marker expression in fibrotic pmAT II cells.	48
Figure 21: TGF- β treatment affecting epithelial cell marker expression in pmAT II cell monoculture.	49
Figure 22: Effect of Nintedanib and Pirfenidone on epithelial cell marker gene expression in TGF- β treated pmAT II cells.	49
Figure 23: Effect of Nintedanib and Pirfenidone on epithelial cell marker protein expression in TGF- β treated pmAT II cells.	50
Figure 24: Effect of Nintedanib and Pirfenidone on Wisp1 secretion in TGF- β treated pmAT II cells.	50
Figure 25: Epithelial cell injury is retained in fibrotic primary murine (pm) AT II cells during culture.	51
Figure 26: Effect of Nintedanib and Pirfenidone on epithelial cell marker expression in fibrotic pmAT II cells.	51
Figure 27: Induction of fibrotic marker expression in ex-vivo human 3D-LTCs upon TGF- β treatment.	52
Figure 28: <i>Ex-vivo</i> effect of Nintedanib and Pirfenidone on fibrotic gene expression in TGF- β treated human 3D-LTCs.	53
Figure 29: Treatment scheme with fibrotic cocktail (FC) or control cocktail (CC) and Nintedanib (1 μ M) or Pirfenidone (500 μ M) and subsequent downstream analysis.	53
Figure 30: Fibrotic cocktail induces fibrotic marker gene and protein expression in human 3D-LTCs <i>ex-vivo</i> .	54
Figure 31: <i>Ex-vivo</i> effect of Nintedanib and Pirfenidone on fibrotic cocktail induced “early fibrosis like changes” in human 3D-LTCs.	54
Figure 32: Effect of TGF- β on epithelial cell marker expression in human 3D-LTCs.	55
Figure 33: <i>Ex-vivo</i> effect of Nintedanib and Pirfenidone on epithelial cell function in TGF- β treated human 3D-LTCs.	56
Figure 34: <i>Ex-vivo</i> effect of Nintedanib and Pirfenidone on epithelial cell phenotype marker in fibrotic cocktail (FC) treated human 3D-LTCs.	57
Figure 35: <i>Ex-vivo</i> effect of Nintedanib on epithelial cell marker protein expression in fibrotic cocktail (FC) treated human 3D-LTCs.	58
Supplemental Figure 1: Dose dependent effect of Nintedanib and Pirfenidone on murine 3D-LTC metabolic activity.	72

Supplemental Figure 2: Maintenance of control and fibrotic 3D-LTCs in culture.	72
Supplemental Figure 3: Effect of Nintedanib and Pirfenidone on fibrotic marker expression in control 3D-LTCs.	73
Supplemental Figure 4: Effect of Nintedanib and Pirfenidone on fibrotic marker expression in PBS treated 3D-LTCs.	73
Supplemental Figure 5: Effect of Nintedanib and Pirfenidone on epithelial cell function in control 3D-LTCS.	74
Supplemental Figure 6: Effect of Nintedanib and Pirfenidone on epithelial cell function in PBS treated 3D-LTCs.	74
Supplemental Figure 7: Effect of Nintedanib and Pirfenidone on control pmAT II cells.	75
Supplemental Figure 8: Effect of Nintedanib and Pirfenidone on pmAT II cells derived from PBS treated mice.	75
Supplemental Figure 9: Effect of Nintedanib and Pirfenidone on epithelial cell function in control pmAT II cells.	76
Supplemental Figure 10: Effect of Nintedanib and Pirfenidone on pmAT II cells derived from PBS treated mice.	76
Supplemental Figure 11: <i>Ex-vivo</i> effect of Nintedanib and Pirfenidone on fibrotic gene expression in control human 3D-LTCs.	78
Supplemental Figure 12: Metabolic activity of human 3D-LTCs cultured with CC/FC and Pirfenidone and Nintedanib.	77
Supplemental Figure 13. <i>Ex-vivo</i> effect of Nintedanib and Pirfenidone on epithelial cell function in control human 3D-LTCs.	77

8.3 List of Tables

Table 1: Laboratory Equipment	22
Table 2: Software	23
Table 3: Chemicals and reagents	23
Table 4: Consumables	25
Table 5: Buffers, solutions and media	26
Table 6: Kits	27
Table 7: Primary Antibodies for immunofluorescence	27
Table 8: Primary Antibodies for Western Blot	27
Table 9: Secondary Antibodies for immunofluorescence	28
Table 10: Secondary Antibody for Western Blot, HRP linked	28
Table 11: Antibodies used for FACS analysis (primary and secondary)	28
Table 12: Murine quantitative PCR primers	29
Table 13: Human quantitative PCR Primers	29
Table 14: Mastermix for cDNA Synthesis	34
Table 15: qPCR Mastermix	35
Table 16: LC480 Light cycler reaction program	35

9. ACKNOWLEDGEMENTS

First of all, I am deeply thankful to my supervisor Melanie Königshoff for giving me the opportunity to join her lab as a MD student. Her constant support, patience and friendliness is the basis for this thesis to be written. Above all, her enthusiasm and profound knowledge about pulmonary science has consistently been a source of inspiration for this work.

I am especially thankful to Mareike Lehmann! She accompanied me through all up and downs during this thesis. Her scientific input and guidance in the day-to-day lab work had been truly helpful. Without her this work wouldn't have been published.

I wish to thank Stephan Klee for helping me with his technical and scientific expertise every day.

Thanks to Maria Magdalena Stein for being such a patient teacher regarding all technical lab work.

I also would like to thank all present and former lab members for making my time in the CPC so memorable: Aina, Ana, Carlo, Chiharu, Daniela, Darcy, Florian, Hani, Hendrik, Hoeke, JP, Kathrin, Martina, Nadine, QJ, Rabea, Rita, and Wiola.

Finally, I want to thank my family and friends for supporting me throughout the last years. I couldn't have done it without them.

10. APPENDIX

10.1 Abstracts and publications

10.1.1 Abstracts

May 2017: *“Effects of Nintedanib and Pirfenidone on Alveolar Epithelial Cells in 2D and 3D Lung Cultures”*, ATS International Conference, Washington, presented by Dr. Mareike Lehmann

March 2017: *“Antifibrotic effects of Nintedanib and Pirfenidone on alveolar epithelial cells in 2D and 3D culture”*, LSC International Conference, Lisbon

Feb. 2017: *“Antifibrotic effects of Nintedanib and Pirfenidone on alveolar epithelial cells in 2D and 3D culture”*, DZL Meeting, Munich

Oct. 2016: *“Anti-Fibrotic Effects of Nintedanib and Pirfenidone in 2D- versus 3D-Culture”*, Munich-Pittsburg Lung Conference, Pittsburg, presented by Dr. Mareike Lehmann

Sept. 2016: *“LATE-BREAKING ABSTRACT: Anti-fibrotic effects of nintedanib and pirfenidone in 2D versus 3D lung cultures”*, ERS International Conference, London, selected for oral presentation, presented by Dr. Mareike Lehmann

Feb. 2016: *“Epithelial Cell Responses To Anti-fibrotic Drugs Pirfenidone and Nintedanib”*, AIR Symposium, Mainz

10.1.2 Publications

Lehmann M*, Buhl L*, Alsafadi H, Klee S, Hermann S, Mutze K, Ota C, Lindner M, Behr J, Hilgendorff, Wagner DE and Königshoff M (*contributed equally) *“Differential effects of Nintedanib and Pirfenidone on lung alveolar epithelial cell function in ex vivo murine and human lung tissue cultures of pulmonary fibrosis”*; Respiratory Research, Sept. 2018

10.2 Eidesstattliche Erklärung

Hiermit erkläre ich, Lara Buhl, an Eides statt, dass ich die vorliegende Dissertation mit dem Thema

*„Anti-fibrotic effects of Nintedanib and Pirfenidone on alveolar epithelial cell function in ex-vivo
3D- Lung Tissue Cultures“*

selbstständig verfasst, mich außer der angegebenen keiner weiteren Hilfsmittel bedient und alle Erkenntnisse, die aus dem Schrifttum ganz oder annähernd übernommen sind, als solche kenntlich gemacht und nach ihrer Herkunft unter Bezeichnung der Fundstelle einzeln nachgewiesen habe.

Ich erkläre des Weiteren, dass die hier vorgelegte Dissertation nicht in gleicher oder in ähnlicher Form bei einer anderen Stelle zur Erlangung eines akademischen Grades eingereicht wurde.

München, den 02. Dezember 2020

Lara Buhl